63-3-5

INTERIM SCIENTIFIC REPORT NO. 1

CONTRACT AF 33(657)-10567

SUPERCONDUCTING MAGNET RESEARCH AND APPLICATION TO MHD POWER GENERATORS

PERIOD COVERED:

FEBRUARY 1, 1963 TO APRIL 30, 1963

MAY 10, 1963

405 829

SUBMITTED BY:

Westinghouse Electric Corporation
Astronuclear Laboratory
Pittsburgh 36, Pennsylvania

Westinghouse Electric Corporation

Astronuclear Laboratory Box 10864, Pittsburgh 36, Pa.
Tel/phone: 466-6800

May 20, 1963

Aeronautical Systems Division
Attention: ASRPP-20/P. J. Hutchison/22208
Wright-Patterson Air Force Base
Ohio

Gentlemen:

Attached is the First Quarterly Technical Progress Report covering the period February 1 to April 30, 1963, for Contract AF 33(657)-10567, "Superconducting Magnet Research and Application to MHD Power Generators."

Distribution of these reports has been made in accordance with the distribution list transmitted by your letter of April 6, 1963, and amended May 13, 1963.

Any question regarding the attached report may be directed to Mr. S. L. Chiazza at the Westinghouse Dayton Office located at 1306 Farr Drive, or to me.

Very truly yours,

E. A. Stroup
DOD Marketing
Astronuclear Laboratory

/dvc

Interim Scientific Report No. 1

Contract AF 33(657)-10567

Superconducting Magnet Research and Application to MHD Power Generators

Period Covered:

February 1, 1963 to April 30, 1963

May 10, 1963

Westinghouse Astronuclear Laboratory
P. O. Box 10864
Pittsburgh 36, Pennsylvania

The work covered by this report was accomplished under Air Force Contract AF 33(657)-10567, but this report is being published and distributed prior to Air Force review. The publication of this report, therefore, does not constitute approval by the Air Force of the findings of conclusions contained herein. It is published for exchange and stimulation of ideas.

TABLE OF CONTENTS

Contributors: W. A. Stewart, T. C. Tsu, H. W. Szymanowski, D. T. Beecher, R. E. Kothmann, R. R. Akers.

I. INTRODUCTION

Contract AF 33(657)-10567 provides for an investigation of the recently developed superconducting magnets and their application to MHD power generators for space use. The work will include theoretical analysis of an MHD generator with particular emphasis on the magnetic field requirements and a study of the problems of superconducting magnet design to fulfill these requirements.

To attain this end, models of a superconducting magnet, cooling equipment and an MHD generator will be analyzed. The total power system including a reactor heat source and radiator will then be optimized on a power to weight basis to find the optimum magnetic field. With this completed, a comparison will then be made between superconducting magnets and conventional magnets to illustrate the advantages or disadvantages of both.

II. MHD POWER GENERATOR

A. General Considerations

The purpose of the MHD generator model for this study is to provide an estimate of the magnetic field requirements which must be satisfied by superconducting magnets for space power generation. Particular areas of study are: heat transfer and wall friction as they are affected by magnetic fields; insulation requirements to reduce the heat conducted to the superconducting magnet from the hot plasma or high temperature walls; effects due to high fields such as ion slip, losses such as end losses, and joule heating; and the flux homogeneity required in the channel to prevent circulating currents and other effects.

A power unit to fulfill this requirement will need to have an electrical output of at least 1 MW, be representative of the state of the art in materials and technology and have a reasonable operating efficiency. It must be realized that MHD units are competing with a much more advanced state of the art in turbine-generator power systems. Therefore sizable advantages of these units must be shown to make their development economically feasible.

Investigators[1] have shown that the Rankine cycle is superior to the Brayton cycle for space power generation. This is largely due to the radiator size which results from the requirement of heat rejection from a gas at a relatively low temperature characteristic of the Brayton cycle. Selecting a Rankine cycle fluid with known thermodynamic and electrical properties leads to many serious problems and compromises. Rankine cycle fluid requirements are discussed by Keenan[2] and possible fluids to fulfill these requirements are outlined by Tsu[3].

To date most of the plasma diagnostic work has been performed on either combustion systems or on gas systems seeded with an alkali vapor. Electrically the alkali vapors are advisable due to the low ionization potential and the knowledge of their electrical and thermodynamic properties. However, thermodynamically other metal and salt vapors may be more desirable.

Lithium appears to be the best fluid because of its low molecular weight but more important, its vapor pressure allows reasonable operation in the temperature range of 1400 to 2200° K which is the range of interest for this application. It is still advisable to use cesium as a seeding agent to obtain reasonable conductivities and maximum power densities. Power density will be maximized later in this report for varying seeding ratios. It will still be necessary to assume some degree of non-thermal ionization either from an electron bombardment ionization scheme or from some other source.

B. MHD Generator Model

Models are available in the literature for various MHD generator configurations. The one selected was a constant Mach number solution by Swift-Hook[4, 5] since this analysis includes both heat-transfer and frictional effects which are among the major losses in an MHD generator. The solution is based upon maximum electrical power extraction per unit length and describes a segmented electrode Faraday generator operating at constant magnetic field and with a constant loading parameter (E_y/uB). It is basically applicable to the lithium vapor

MHD power generator since for this case the mobility is rather low and with reasonable magnetic fields the Hall parameters $\mu_e B$ will be in the range of 1 to 20.

Figures 1 and 2 show the ranges of applicability of solutions based on continuous electrode Faraday and Hall MHD generators compared to the segmented electrode Faraday generators.

The walls of a duct containing a condensable vapor near saturation conditions must be maintained at a very high temperature to prevent condensation which would cause short circuits. This can be accomplished by suitable insulation and heating due to the stagnation temperature of the boundary layer, in general this temperature will be 100 to 200° K above the static temperature of the gas stream. Neglecting heat transfer and including frictional effects causes the solution to deviate from the small perturbations assumed by Swift-Hook but also leads to a more definable solution. It will be derived in this report beyond the point where it deviates from the solution in reference 5.

The momentum and energy equations respectively appear as equations 7 and 8 in reference 5:

$$\rho u \frac{du}{dx} + \frac{dp}{dx} + jB + \frac{N_s}{A} = 0 \qquad (1)$$

$$\rho u \frac{d}{dx}\left(C_p T + \frac{u^2}{2}\right) + jE + \frac{H_s}{A} = 0 \qquad (2)$$

where $\frac{N_s}{A}$ is the frictional force per unit volume and $\frac{H_s}{A}$ is convective heat loss per unit volume which will be assumed negligible for this case.

In an ionized fluid the frictional effects are a function of the applied magnetic field, however, after examining several of the solutions giving frictional coefficients as function

of magnetic field, it was determined that the frictional coefficient assumed by Swift-Hook is a reasonable assumption and gives comparative results for the assumed turbulent flow, it is:

$$f = \frac{0.046}{Rey^{1/5}} \tag{3}$$

where for square ducts he gives:

$$Rey = \frac{\rho u A^{1/2}}{\mu} \tag{4}$$

therefore:

$$N = 1/2\ f \rho u^2 \tag{5}$$

Now using the equation of state, the Mach number equation and Ohm's law current equation:

$$j = \sigma (u B - E_y) \tag{6}$$

and solving equations 1 and 2 simultaneously leads to:

$$\frac{1}{T}\frac{dT}{dx} = \eta' \left(\frac{\gamma - 1}{\gamma}\right) \frac{1}{p}\frac{dp}{dx} + \eta' M^2 (\gamma - 1)\frac{f}{2}\left(\frac{s}{A}\right) \tag{7}$$

where

$$\eta' = K \left[1 + \frac{(1 - K)(\gamma - 1) M^2}{2}\right]^{-1} \tag{8}$$

and

$$K = \frac{E_y}{u B} \tag{9}$$

which is the customary loading parameter.

Now integration results in:

$$\frac{T}{T_1} = \left(\frac{p}{p_1}\right)^{\eta' \frac{(\gamma - 1)}{\gamma}} + \int_o^x \eta' M^2 (\gamma - 1) \frac{f}{2} \left(\frac{s}{A}\right) dx \tag{10}$$

he sets:

$$\ln a = \int_o^x \eta' M^2 (\gamma - 1) \frac{f}{2} \left(\frac{s}{A}\right) dx \tag{11}$$

giving:

$$\frac{p}{p_1} = \frac{t^{\beta}}{a} \tag{12}$$

where

$$t = \frac{T}{T_1} \tag{13}$$

and

$$\beta = \frac{\gamma}{(\gamma - 1)\eta'} \tag{14}$$

and other thermodynamic properties are given as:

$$\frac{\rho}{\rho_1} = \frac{t^{\beta - 1}}{a} \tag{15}$$

$$\frac{u}{u_1} = t^{1/2} \tag{16}$$

$$\frac{A}{A_1} = a\, t^{1/2-\beta} \tag{17}$$

It remains to find these variables as a function of the independent parameter x which can be found using the energy equation. This results in, after some degree of manipulation,

$$\frac{dt}{dx} = \left(\frac{\sigma}{\sigma_1}\right)\left(\frac{u}{u_1}\right)\left(\frac{\rho_1}{\rho}\right)\frac{1}{x_o} \tag{18}$$

where

$$x_o = \frac{P w_1}{K(1-K)\,\sigma_i\, u_1^{\,2}\, B^2} \tag{19}$$

Total inlet power per unit area is designated by:

$$P_{w_1} = \rho_1\, u_1\, C_p\, T_{o_1} \tag{20}$$

The power law approximation for conductivity holds reasonably well for this case also:

$$\frac{\sigma}{\sigma_i} = \left(\frac{T}{T_1}\right)^{y}\left(\frac{p}{p_1}\right)^{-z} \tag{21}$$

where

$$y = \left[\frac{d(\ln \sigma)}{d(\ln T)}\right]_{p\ =\ \text{constant}} \tag{22}$$

and

$$z = -\left[\frac{d(\ln \sigma)}{d(\ln p)}\right]_{T\ =\ \text{constant}} \tag{23}$$

Equation (17) becomes by substituting the variables as f (α, t):

$$\frac{dt}{dx} = -\frac{\alpha^{z+1}}{x_o} t^{(1-w)} \tag{24}$$

where

$$w = (z+1)\beta - y - 0.5 \tag{25}$$

To this point the solution was taken from Swift-Hook, the only difference being the neglecting of the heat transfer term in each of the equations. To solve this for the frictional case, the coefficient α can be re-written as f (α, t) by substitution of the variables in that form into equation 11.

$$\ln \alpha = \int_o^x -\tau\, \alpha^{-0.4}\, t^{\frac{2\beta - 1 + n}{5}}\, dx \tag{26}$$

where

$$\tau = \frac{-2\eta' f_1 M^2 (\gamma - 1)}{A_1^{1/2}} \tag{27}$$

We have assumed that viscosity is represented as by Swift-Hook:

$$\mu = m T^n \tag{28}$$

where

$$m = 1.09 \times 10^{-6} \tag{29}$$

and

$$n = 0.44 \tag{30}$$

for the case of cesium seeded lithium in the 1600 to 2000° K temperature range.

Differentiating equation (26) gives:

$$\frac{d\,a}{d\,x} = -\tau a^{0.6}\ t\ \frac{2\beta - 0.56}{5} \tag{31}$$

dividing (24) by (31) and separating variables gives:

$$\tau x_o \int_1^t t\ \frac{2\ -0.56-5+5\,w}{5}\ d\,t = \int_1^a a^{0.4+z}\ d\,a \tag{32}$$

which integrates to:

$$a = \left[1 + \xi\,(t^{\psi} - 1)\right]^{\frac{1}{1.4+z}} \tag{33}$$

where

$$\xi = \frac{\tau x_o\ (1.4+z)}{\psi} \tag{34}$$

$$\psi = \frac{2\beta - 0.56 + 5\,w}{5} \tag{35}$$

substituting (33) into (24):

$$\left[1 + \xi\,(t^{\psi} - 1)\right]^{-\left(\frac{1+z}{1.4+z}\right)}\ t^{(w-1)}\ d\,t = -\frac{d\,x}{x_o} \tag{36}$$

which is the form of the incomplete beta function [5]. This function is written as:

$$B_y\,(l,\,q) = \int_o^y y^{(l-1)}\ (1-y)^{(q-1)}\ d\,y \tag{37}$$

This form is obtained by use of the substitution:

$$t^{\psi} = \left(1 - \frac{1}{\xi}\right)\ y \tag{38}$$

where y is the new variable, equation (36) becomes:

$$\int_o^{y_2} (1-y)^{(q-1)}{}_y\,(1-1)\,dy - \int_o^{y_1} (1-y)^{(q-1)}{}_y\,(1-1)\,dy$$
$$= -\phi\int_o^x dx = -\phi x \tag{39}$$

and

$$\phi = \frac{\psi}{x_o}\,(-\xi)\,\frac{w}{\psi}\,(1-\xi)^{\left(\frac{1+z}{1.4+z} - \frac{w}{\phi}\right)}$$

where

$$q = 1 - \frac{1+z}{1.4+z} \tag{40}$$

and

$$l = \frac{w}{\psi} \tag{41}$$

In general, the tables for the incomplete beta function are compiled over increments too large for use and the values for l and q can occur outside of the tables. Therefore, a rapidly convergent series seems the best method of representation. The most rapidly convergent series representation is:

$$B_y(l, q) = \sum_{n=o}^{\infty} \binom{q-1}{n} (-1)^n \frac{y^{n+1}}{n+1} \tag{42}$$

where $\binom{q-1}{n}$ represents the binomial coefficient.

To obtain an idea of efficiency for this machine we will use the turbine or isentropic efficiency.

$$\eta_s = \frac{\text{Actual enthalpy drop}}{\text{Isentropic enthalpy drop}} \tag{43}$$

which results in:

$$\eta_s = \frac{1 - t}{1 - \frac{t^{1/\left(\frac{\gamma - 1}{\gamma}\right)}}{a}} \tag{44}$$

this leaves the only undefined parameter as the Hall voltage:

$$E_x = \mu_e \upsilon B^2 (K - 1) \tag{45}$$

Power output as a function of temperature ratio for the case of negligible heat transfer is:

$$\frac{d W_e}{d x} = j E A = \rho \upsilon A \frac{d}{d x} \left(C_p T + \frac{\upsilon^2}{2}\right) \tag{46}$$

integrating:

$$W_e = Q_1 \eta \tag{47}$$

where Q_1 is the total inlet convective enthalpy:

$$Q_1 = \rho_1 \upsilon_1 A_1 C_p T_{o_1} = P_{w_1} A_1 \tag{48}$$

and

$$\eta = 1 - t \tag{49}$$

Power output can now be determined as a function of length by equation (39).

C. Gas Properties

With the duct parameters determined it remains to define the gas properties and the operating conditions of the generator. To obtain the maximum power density for the machine it is necessary to determine an optimum seeding ratio. For a segmented Faraday generator the power density per unit volume can be written, over the range of interest, as:

$$\frac{P}{Vol.} = \sigma u^2 B^2 K (1 - K) \tag{50}$$

Now assuming the gas will have only a small degree of ionization conductivity can be written for the electron-neutral collision processes as:

$$\sigma = n_e \mu_e e \tag{51}$$

Electron collision cross section data for lithium vapors is obtained from reference 6 and it is assumed that for reasonable cesium seeding rates the mobility is unaffected by the addition of cesium. Figure 3 shows electron mobility as a function of gas temperature.

The two parameters of equation (50) which will determine power density and are a function of seeding ratio are conductivity and velocity. Conductivity will increase with increased cesium concentration and velocity will decrease due to the increasing molecular weight. Therefore equation (50) will reach a maximum. To determine this maximum we can write each of these variables as a function of seeding ratio:

$$u^2 \approx \frac{1 + \epsilon}{Mol_{li} + Mol_{cs}\epsilon} \tag{52}$$

and

$$\sigma \approx \left[\frac{1}{1+\epsilon}\right]^{1/2}\left[\left(\frac{\epsilon}{\exp \frac{I_{cs} e}{kT}}\right)^{1/2} + \left(\frac{1}{\exp \frac{I_{li} e}{kT}}\right)^{1/2}\right] \tag{53}$$

by virtue of the changing electron density based on the Saha equation. We can see that this expression is a weak function of temperature.

Substituting these expressions into (46) results in:

$$P' \approx \frac{1+\epsilon}{Mol_{li} + Mol_{cs}\,\epsilon} \left[\frac{\epsilon^{1/2}}{\exp \frac{I_{cs} e}{2kT}} + \frac{1}{\exp \frac{I_{li} e}{2kT}} \right] \tag{54}$$

This expression is represented by figure 4 for the minimum operating temperature of the generator and results in a rather flat curve with a maximum near 0.07 which will be used for future calculations.

Knowing the gas mixture, the average molecular weight, specific heat, viscosity, and conductivity can now be calculated. The data for these properties were obtained from reference 8. Equilibrium values were assumed near the upper operating temperature since the gas will have reached an equilibrium passing through the reactor heat source and will be semi-frozen on passing at high velocity through the generator. Conductivity is given as figures 5 and 6 and viscosity as figure 7.

D. Operating Conditions

When operating with a condensing vapor MHD power generation cycle, numerous considerations must be made. First and foremost, it is advisable to operate as near saturation conditions as possible to obtain the maximum Carnot efficiency. The upper temperature limit is set by the material considerations of the reactor and a minimum temperature is set by the radiating temperature of the radiator. The Carnot efficiency is reduced by a factor of 0.58 if the maximum temperature is reduced only from 2000° K to 1900° K as is illustrated by figure 8.

Choosing the inlet conditions to be very near saturated vapor at 2000° K gives a pressure of 9.2 atm and the conductivity becomes very low (0.45 mho/m). It becomes very obvious that for a lithium vapor cycle some means of non-thermal ionization must be developed

and considered. An electron temperature of 0.5 volts would seem reasonable and results in a conductivity of 10 mho/m. Based on this conductivity Table I below shows the other conditions and to calculate duct length as a function of varying magnetic fields and for three different inlet velocities corresponding to Mach numbers of 0.9, 1.275, 2.0. Tables II, III, and IV, show the conditions and parameters which are unique to each case.

TABLE I

Mol	= 17.8	T_1	= 2000° K
C_p	= 3,893 $\frac{\text{joules}}{\text{kg°K}}$	P_1	= 9.2 atm
R	= 466.8 $\frac{\text{joules}}{\text{kg°K}}$	ρ_1	= 0.99614 $\frac{\text{kg}}{\text{m}^3}$
γ	= 1.14	K	= 0.75
t	= 0.8	σ_1	= 10
η	= 0.2		

TABLE II

M = 2.0

u_1	= 2,063 m/sec	η'	= 0.70093
T_{o_1}	= 2,547° K	β	= 11.617
P_{w_1}	= 20.377×10^9 watts/m^2	w	= 5.3255
A_1	= 2.4537×10^{-4} m^2	ψ	= 9.860
Rey_1	= 1.0452×10^6	I	= 0.54011
f_1	= 2.90×10^{-3}	q	= 0.21053
τ_1	= 0.1453		

TABLE III

M = 1.275

u_1	=	1,3153 m/sec	η'	=	0.70093
T_{o_1}	=	2,222° K	β	=	11.617
P_{w_1}	=	11.334×10^9 watts/m^2	w	=	4.649
A_1	=	4.4116×10^{-4} m^2	ψ	=	9.0034
Rey_1	=	1.0452×10^6	I	=	0.5163
f_1	=	2.90×10^{-3}	q	=	0.21053
τ_1	=	- 0.14533			

TABLE IV

M = 0.9

u_1	=	928.4 m/sec	η'	=	0.7395
T_{o_1}	=	2111° K	β	=	11.011
P_{w_1}	=	7.599×10^9	w	=	4.416
A_1	=	6.579×10^{-4}	ψ	=	8.7089
Rey_1	=	0.7698×10^6	I	=	0.50712
f_1	=	3.06×10^{-3}	q	=	0.21053
τ_1	=	0.0200			

These were calculated for magnetic fields ranging from 4 webers/m^2 to 32 webers/m^2 which covers the full range of present or future operating areas. The higher magnetic field is definitely out of reach of any known superconducting material, however, it was used as a limiting point in the analysis. Figures 9 and 10 show the length and isentropic efficiencies as a function of magnetic field for the three cases. The advantages of high magnetic fields are obvious, however the increase both in length and efficiency becomes smaller per unit increase in magnetic field above 14 webers/m^2. Therefore in the optimization based upon weight considerations it appears the optimum value of magnetic field will be near this value.

A typical set of inlet and outlet parameters have been calculated and are shown as Table V to illustrate currents, voltages, and thermodynamic properties.

TABLE V

$M = 1.275$ $\qquad B = 12.5 \ \frac{\text{webers}}{m^2}$

x, 2.86 meters

T_1	$= 2000^\circ$ K	T_2	$= 1600$
P_1	$= 9.2$ atm	P_2	$= 0.69$ atm
ρ_1	$= 0.99614$ kg/m^3	ρ_2	$= 9.295 \times 10^{-2}$ kg/m^3
u_1	$= 1,315$ m/sec	u_2	$= 1,176$ m/sec
A_1	$= 4.41 \times 10^{-4}$ m^2	A_2	$= 49.57 \times 10^{-4}$ m^2
i_{y_1}	$= 4.11 \times 10^4$ amp/m^2	i_{y_2}	$= 1.01 \times 10^4$ amp/m^2
E_{y_1}	$= 1.23 \times 10^4$ volt/m	E_{y_2}	$= 1.10 \times 10^4$ volt/m
E_{x_1}	$= 4.52 \times 10^2$ volt/m	E_{x_2}	$= 50.53 \times 10^2$ volt/m
β_{e_1}	$= 0.110$	β_{e_2}	$= 1.375$
σ_1	$=$ 10 mho/m	σ_2	$= 2.74$ mho/m

E. Effects of Strong Magnetic Field on the MHD Process

A strong magnetic field is expected to affect the MHD process in four respects:

1. The "Hall" effect.
2. Tensor conductivity.
3. Hydrodynamic effects (wall friction and heat transfer coefficients; turbulence, stability, and transition from laminar to turbulent flow).
4. Ion slip.

These items were discussed in our original proposal to PR-141108 dated October 25, 1963, which led to the present contract. In that discussion we cited 31 references and indicated that "Hall" effect and tensor conductivity were well enough understood and, therefore, no further work was proposed. Hydrodynamic effects have been studied extensively as evidenced by the large number of publications available in the literature. In spite of massive effort, our knowledge is still not as complete as one could wish for. In particular, information is relatively scarce regarding magnetic effects on stability, turbulent boundary layer, and transition from laminar to turbulent flow. This is primarily a reflection of the state of fluid dynamics. Even without magnetic effects, problems in the areas mentioned have to be solved more or less empirically to meet the needs of individual situations. In our judgement, large research efforts spent on hydrodynamic effects might yield only small returns, if at all. For this reason, we did not propose to spend much time working in this area.

The remaining area, "Ion Slip", is where we shall concentrate our main effort. Very little published information is available on this subject. Nevertheless, the effects of ion slip are believed to be important when magnetic fields become very strong. This problem should be understood if strong fields are to be effectively utilized in MHD machines.

Since electron mobility in an MHD gas is much larger than ion mobility, the electric current produced in an MHD generator under a weak magnetic field is almost entirely electronic. As the field increases in strength there is a gradual transition from electron

current to ion current. In the limit, as the field becomes infinitely strong there can be no current whatever. All electrons and ions spin in infinitesimal circles. They are effectively arrested. As the magnetic field increases from zero to infinity, we expect that the power output of an MHD generator will first increase, then level off at a plateau, then decrease, and finally become zero.

In the usual arrangement of MHD generators, an ionized gas flows from a non-magnetic region to a magnetic region. As the gas crosses the magnetic field, the continuity of ion flow requires that the ion concentration must change. This situation is easy to understand if one considers the limiting case of an infinitely strong field. As soon as ions enter the magnetic region, they are forced to spin in infinitesimal circles. Thus, while the neutrals are free to move through the magnetic region, the ions are arrested. Therfore, the ion concentration inside the field cannot be the same as that outside.

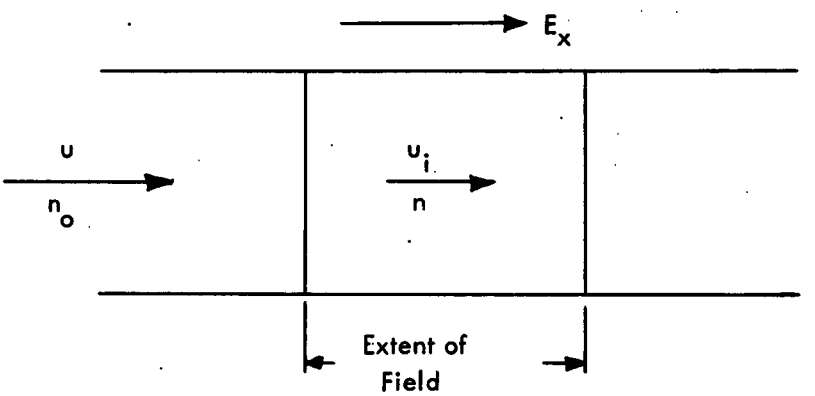

Continuity of Ion Flow

Consider the flow of an ionized gas through a duct with an electric field E_x as shown. Let the ion density be n_o and the gas velocity be u outside the field. The ion velocity is assumed equal to the gas velocity due to frequent collisions. If the ion velocity inside the field region is u_i, then continuity of ion flow requires

$$n_o u = n u_i \tag{55}$$

where n is ion density in the field region. If the ion mobility is μ_i, then by definition,

$$u_i = u + \mu_i E_x \tag{56}$$

combining (55) and (56) gives:

$$\frac{n_o}{n} = 1 + \frac{\mu_i E_x}{u} \tag{57}$$

Ordinarily the quantity $\mu_i E_x$ is small compared to u; and the difference between n and n_o is insignificant.

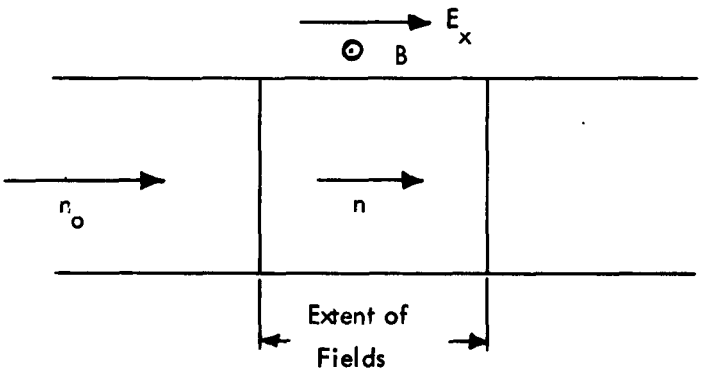

Continuity of Ion Flow with Magnetic Field

If in addition to the electric field E_x there is also a magnetic field B, then, as will be shown later, the ion drift velocity becomes:

$$v_{ix} = \frac{u\beta_i}{1+\beta_i^2} \left[\frac{E_x}{uB} - \beta_i \right] \tag{58}$$

where $\beta_i \equiv \mu_i B$. Since continuity of ion flow requires

$$n_o u = n \mu_i = n (u + v_{ix}) , \tag{59}$$

we obtain from (58) and (59)

$$\frac{n_o}{n} = 1 + \frac{\beta_i}{1+\beta_i^2} \left[\frac{E_x}{uB} - \beta_i \right] \tag{60}$$

As the magnetic field becomes very strong, B becomes very large. $E_x / uB \to 0$ and $\beta_i^2 \gg 1$. Under those conditions $n_o / n \to 0$. Hence in a very strong magnetic field the ion density could be much larger than that outside the field region.

1. Hall Effect on Ions

Consider a moving gas containing singly charged ions. Let $\bar{E}'$ be the electric field with respect to the moving gas; $\bar{B}$, the magnetic flux density; and $\bar{v}_i$, the ion drift velocity. Then the force acting on each ion (charge + e) is

$$\bar{F}_i = e \left(\bar{E}' + \bar{v}_i \times \bar{B} \right) \tag{61}$$

If the ion mobility is μ_i, the drift velocity v_i is given by

$$v_i = \frac{\mu_i}{e} \bar{F}_i = \mu_i \left(\bar{E}' + \bar{v}_i \times \bar{B} \right) \tag{62}$$

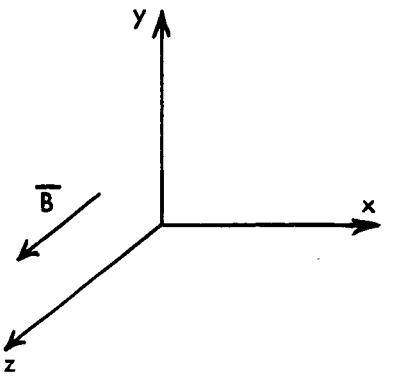

Coordinate System

If we select our coordinate system such that $\bar{B}$ acts in the z - direction, then the components of equation (62) are:

$$v_{ix} = \mu_i \, (E'_x + v_{iy} B) \tag{63}$$

$$v_{iy} = \mu_i \, (E'_y - v_{ix} B) \tag{64}$$

Solving (63) and (64) for v_{ix} and v_{iy}, we obtain:

$$v_{ix} = \frac{\mu_i}{1+\beta_i^2} \, (E'_x + \beta_i \, E'_y) \tag{65}$$

$$v_{iy} = \frac{\mu_i}{1+\beta_i^2} \, (E'_y - \beta_i \, E'_x) \tag{66}$$

where $\beta_i = \mu_i B$, as before.

Now since the ion current

$$j_i = n_i \, e \, v_i \, , \tag{67}$$

we have

$$j_{ix} = \frac{n_i \, e \, \mu_i}{1 + \beta_i^2} \left(E'_x + \beta_i \, E'_y \right) \tag{68}$$

$$j_{iy} = \frac{n_i \, e \, \mu_i}{1 + \beta_i^2} \left(E'_y - \beta_i \, E'_x \right) \tag{69}$$

By following through a similar procedure, it may be shown that the electron current components are:

$$j_{ex} = \frac{n_e \, e \, \mu_e}{1 + \beta_e^2} \left(E'_x - \beta_e \, E'_y \right) \tag{70}$$

$$j_{ey} = \frac{n_e \, e \, \mu_e}{1 + \beta_e^2} \left(E'_y + \beta_e \, E'_x \right) \tag{71}$$

where μ_e is the electron mobility and $\beta_e \equiv \mu_e \, B$.

Combining equations (68) with (70), and (69) with (71), we obtain the total electric currents:

$$j_x = j_{ix} + j_{ex} = \left(\frac{\sigma_i}{1 + \beta_i^2} + \frac{\sigma_e}{1 + \beta_e^2} \right) E'_x + \left(\frac{\sigma_i \, \beta_i}{1 + \beta_i^2} - \frac{\sigma_e \, \beta_e}{1 + \beta_e^2} \right) E'_y \tag{72}$$

$$j_y = j_{iy} + j_{ey} = \left(\frac{\sigma_i}{1 + \beta_i^2} + \frac{\sigma_e}{1 + \beta_e^2} \right) E'_y + \left(\frac{\sigma_i \beta_i}{1 + \beta_i^2} - \frac{\sigma_e \, \beta_e}{1 + \beta_e^2} \right) E'_x \tag{73}$$

where $\sigma_i = n_i \, e \, \mu_i$ is the ionic conductivity and $\sigma_e = n_e \, e \, \mu_e$ is the electronic conductivity. Let

$$M \equiv \frac{\sigma_i}{1+\beta_i^2} + \frac{\sigma_e}{1+\beta_e^2} \tag{74}$$

$$N \equiv \frac{\sigma_i \, \beta_i}{1+\beta_i^2} - \frac{\sigma_e \, \beta_e}{1+\beta_e^2} \tag{75}$$

then we have

$$j_x = M E_x' + N E_y' \tag{76}$$

$$j_y = M E_y' - N E_x' \tag{77}$$

These equations are general. In the work to follow we shall apply them to the special cases of "Hall" type and segmented-electrode type MHD generators.

F. The Effects of a Non-Uniform Magnetic Field

The magnetic field created by a coil winding, whether made of normal conductors or superconductors, cannot be absolutely uniform. In general, the cost of the magnet increases sharply as one strives for a high degree of uniformity. On the other hand, a non-uniform field penalizes the performance of an MHD generator. The practical problem facing a designer, therefore, is to balance the magnet cost on the one hand and the generator performance on the other hand. In this study we attempt to get some quantitative information to help the designer make his judgement.

1. Past Work

The problem of flux non-uniformity is of course an old one. What particularly concerns us here, however, is the effect of non-uniform flux on the MHD process.

Sonnerup[9] has treated theoretically the steady, laminar flow of a viscous, compressible, and slightly ionized gas through a magnetic field. Although he allows an arbitrary variation of the field in the flow direction, his formal solution ends with an expression for the gas temperature. He does not specifically discuss the effects of a non-uniform field. Ehlers[10] analyzed the special case of axisymmetric flow of a conducting gas through a cylindrical channel, where the non-uniformity in magnetic field arises from a tangentially circulating current. Sakurai and Naito[11] investigated a more general case where a non-uniform field is generated by a system of electric currents and magnetic dipoles. They obtained solutions for the variation of velocity and pressure inside a two-dimensional channel, but their solutions are restricted to incompressible flow.

The effect of a non-uniform magnetic field is to some extent similar to that of a non-uniform velocity profile. In this respect the work of Yeh and Sutton[12] is of interest.

Although in the present study we are primarily interested in magnetic fields which are non-uniform in space, a brief mention should also be made of fields which vary with time. Some fundamental work on the motion of a charged particle in a slowly increasing magnetic field has been done by Braer[13]. The application of a traveling magnetic field to accelerate a plasma has been studied fairly extensively. Some representative publications are those of Meyer[14], Light[15], and Smotrich, Janes, and Bratenahl[16].

2. Model and Approach

The question that we are particularly interested in here is the effect on MHD generator performance of a non-uniform magnetic field. The literature already cited, although helpful, is not directly applicable. Before a meaningful analysis can be made, let us first examine the nature of non-uniformity produced by a typical

electro-magnet. Figures 11, 12, and 13, taken from reference (17), show the flux density variation throughout the working volume of a rectangular MHD duct. Figure 11 shows the variation in the flow direction. Figures 12 and 13 show, respectively, the variations in the horizontal and vertical directions (normal to flow). An examination of these figures reveals that the largest variation occurs in the flow direction. Furthermore, almost all of this variation takes place in the first quarter and last quarter of the duct length. The field is quite uniform in the center portion of the duct. For the purpose of our analysis to follow, therefore, we will adopt a model as shown in Figure 14. Between 0 and L/4, the flux density increases from $\alpha' B_o$ to B_o, where α' is some number less than unity. Between L/4 and (3/4) L, $B = B_o$ = constant. Between (3/4) L and L, B decreases from B_o to αB_o. From 0 to L/4 the variation of B may be represented by the equation:

$$\frac{B}{B_o} = \frac{1 - \alpha'}{.0311} \sin\left(\frac{x}{L} - \frac{1}{4} + \frac{\pi}{2}\right) + \frac{\alpha' - .9689}{.0311} \tag{78}$$

Equation (78) will be used in our analysis to be reported next quarter. We plan to vary the degree of non-uniformity by changing the number α'. If $\alpha' = 1$, equation (78) reduces to $B/B_o = 1$.

III. SUPERCONDUCTING MAGNET

Refrigeration Requirements for Various Optimized Methods of Cooling Cryogenic Electrical Current Leads, Conduction and Radiation Transfer Paths. (W. A. Stewart)

A. INTRODUCTION

In cryogenic systems, and in particular the superconducting magnet cryogenic electrical systems, heat is transferred from an ambient high temperature region, through vacuum insulation by radiation and conduction in support structure and is transferred by conduction and generated by Joule heat loss in electrical leads carrying current. A superconductor must be maintained near 4.2° K, the standard vaporization temperature for helium. Although the usual cryogenic techniques result in rather small heat fluxes, because refrigerator coefficients of performance are small ($< T_o / T_a - T_o$, where a refers to rejection and o refrigeration temperatures) a much larger refrigeration work rate or power, W, is required. Nearly 1000 watt of heat at 4.2° K. Heat that is rejected therefore is practically equal to W.

The particular superconducting magnet system under study is to provide a high field across a long, large, varying section MHD duct which is part of a nuclear-MHD space power system. The one important subsystem comprises (1) MHD duct insulation, (2) cryogenic insulation, (3) magnet winding, (4) magnet force supports, (5) refrigeration apparatus and (6) heat rejection radiators. The weights of refrigeration apparatus, the penalty to weight of the power used for refrigeration and heat rejection radiators are proportional to W. Refrigeration power studies are reported here for various configurations of cooling which will minimize that power. Although the analytic work presented here does not relate to the details of constructed systems which will accomplish the many different methods, separate studies are being made to find the relative practicality and details for implementing the theoretical methods derived in this work. It is sufficient to

say that the methods can be used in ways that are now practised by we or others in cryogenic systems and modifications are feasible. The purpose of the study, moreover, is to obtain comparisons of methods which will lead to best or optimum (for weight and reliability) magnet systems.

It is assumed that an MHD magnet may require provision for current charging in the space application. Therefore facility for cooling electrical leads which deliver the large amount of magnetic energy will be required. This is notwithstanding the fact that persistent mode operation eliminates the need for leads when steady state is attained after a long time for charging.

B. TECHNICAL DISCUSSION

Cooling of (1) electrical leads, (2) conduction paths and (3) radiation paths are studied analytically and in detail for varying or constant electrical resistivity, thermal conductivity and ratio of actual COP (coefficient of refrigerator performance) to Carnot COP, η , in part C . When some heat flux is removed at a temperature above the lowest temperature, T_o , refrigeration has a higher COP and total work, W, is reduced. This technique is exploited by (a) optimum staged cooling all along a heat transfer path, (b) vapor cooling to remove the same heat in each temperature increment along a heat transfer path and (c) two stage cooling at an intermediate temperature, T_1 , between the high, T_a , and low, T_o . In addition (d) cooling can be applied just at the cold end, T_o . All of the methods, a, b, c, d are applied to path types 1, 2, 3 in the analysis and further optimization of length-area ratio, l/A, T_1 , etc. found.

1. Electrical Leads

McFee, in reference 18, examined cooling of an electrical lead at T_o and found optimum l/A. Part C, Section 3, Case A essentially reproduces this result. Kothmann and Stewart, in reference 19, examined vapor cooling and the results are contained in Part C, Section 2, Case A. Sobol and McNichol, reference 21, later gave experimental

verification of their analysis of this case. Tsu, in reference 22, examined optimum cooling but did not analyze by a variational approach. He achieved about a 40% improvement over the McFee result.

The results of the present analysis considering the model electrical lead shown in Figure 15, are shown in Figure 17 for constant properties, and in Figure 18 for properly varying resistivity. It may be noted in Figure 18 that the optimum case is really slightly poorer than for vapor cooling. This is the result of the limiting restriction in the problem where calculus of variations is used that, a given heat flux or, alternatively, T' (o) is taken. The parameter f relates heat flux at the bottom of the lead to the cooling along the lead. Figure 17 shows the strong influence of this parameter.

Smith, in reference 20, used McFee's approach and found that for varying properties and cooling at T_o, the minimum refrigeration work would be 40 watts per ampere in the lead if COP is 0.001 from 4.2 to 300° K. Figure 18 shows that a 10.7 reduction is possible so that only 3.64 watts per ampere might be required.

2. Conduction and Radiation Paths

Analysis of cooling of conduction and radiation paths is contained in Part C, Sections 4 through 8. Results are shown ploted in Figures 19 and 24. Again, as seen in Figures 19, 21, and 24 for small values of T_d/T_o, the restriction imposed by the natural boundary condition of the variational problem makes the "optimum" work more than work with vapor cooling.

No complete conclusions will be drawn except those that are self evident from the curves. Substantial reductions in work and system weight are possible when using an optimum method rather than cooling only at T_o. Optimum two stage cooling is nearly as effective as vapor cooling. In general, vapor cooling is also near optimum cooling except for radiation exchange. With radiation, the high order transfer coefficient variation with temperature, makes optimum cooling much better than any other method.

C. ANALYTICAL DISCUSSION

1. Optimum Cooling of an Electrical Conductor

One dimensional heat flow in a conductor such as shown in figure 16, with current, i, electrical resistivity, ρ, and thermal conductivity, k, is governed by equation 79 .

$$\frac{d}{dx}\left(k A \frac{dT}{dx}\right) + \frac{i^2 \rho}{A} - \phi = 0 \tag{79}$$

The heat, $\phi\, dx$, is removed from the length element, dx, at temperature T by refrigeration and is rejected at the ambient or radiation temperature, T_a. Therefore refrigeration work for ϕ, using equation 79 is:

$$W_\phi = \int_o^l \frac{1}{\eta} \frac{T_a - T(x)}{T(x)} \phi(x)\, dx = \int_o^l \frac{1}{\eta}\left(\frac{T_a}{T} - 1\right)\left[\frac{d}{dx}\left(kA\frac{dT}{dx}\right) + \frac{i^2\rho}{A}\right] dx \tag{80}$$

The variational problem to find T and hence ϕ which minimizes W has the following form, Euler equation and natural boundary conditions:

$$\left.\begin{aligned} &\delta W = \delta \int_o F(x, T, T', T'')\, dx = 0 \\ &\frac{d^2}{dx^2}\left(\frac{\partial F}{\partial T''}\right) - \frac{d}{dx}\left(\frac{\partial F}{\partial T'}\right) + \frac{d}{dx}\left(\frac{\partial F}{\partial T}\right) = 0 \\ &\left\{\left[\frac{d}{dx}\left(\frac{\partial F}{\partial T''}\right) - \frac{\partial F}{\partial T'}\right]\delta T\right\}_o^l = 0, \quad \left[\frac{\partial F}{\partial T''}\,\delta T'\right]_o^l = 0 \end{aligned}\right\} \tag{81}$$

F is the integrand of equation 80. Both natural boundary conditions are satisfied since T is to be fixed at $x = 0$ and l, $\partial F/\partial T''$ is equal $\frac{1}{\eta}\left(\frac{T_a}{T} - 1\right) kA = 0$ at $x = l$,

$T = T_a$ and dT/dx or heat flux may be considered fixed at $x = 0$. When η is constant, the Euler equation becomes:

$$T'' - \frac{T'^2}{T} + \frac{(kA)' T'}{(kA)} + \frac{i^2 \rho}{2(kA)A} - \left(\frac{T_a}{T} - 1\right) \frac{T^2}{2T_a (kA)} \left[T'' \frac{\partial (kA)}{\partial T} + T' \frac{\partial (kA)'}{\partial T} + i^2 \frac{\partial (\rho/A)}{\partial T}\right] = 0 \qquad (82)$$

The partial differentiations are taken when kA or ρ/A are explicit functions of T. Most materials of interest as electrical leads (having a small ρk product) also have nearly constant thermal conductivity. Then introducing dimensionless temperature, $\theta = T/T_a$, and parameter $\gamma = i^2 \rho_a / 2\,(kA)\, AT_a$, while A cannot be an explicit function of T, reduces equation 82 to:

$$\theta'' - \frac{\theta'^2}{\theta} + \gamma \frac{\rho}{\rho_a} - (\theta - \theta^2)\, \gamma \frac{\partial (\rho/\rho_a)}{\partial \theta} = 0 \qquad (83)$$

Two cases are of interest and for which the non-linear Euler equation possesses analytical solutions. These are for resistivity constant and for resistivity varying linearly with absolute temperature.

Case A - Resistivity Constant

The equation and boundary conditions are:

$$\theta'' = \frac{\theta'^2}{\theta} - \gamma, \quad \theta(0) = \theta_o, \theta(1) = 1 \qquad (84)$$

Reference 23 gives the first integration of this equation as:

$$\theta'^2 = 2\gamma\theta \pm \gamma a \theta^2 \qquad (85)$$

Either the positive or negative sign may be taken, depending on the constant of integration which is $\gamma\,\alpha$. When the positive sign is taken final integration and the boundary conditions give:

$$\sqrt{\alpha\gamma}\,x = \sin^{-1}(\alpha\theta - 1) - \sin^{-1}(\alpha\theta_o - 1) \tag{86}$$

$$\sqrt{\alpha\gamma}\,l = \sin^{-1}(\alpha - 1) - \sin^{-1}(\alpha\theta_o - 1) \tag{87}$$

The total refrigeration work, including that due to the heat flux $(k\,A)\,T'(0)$ and W_ϕ is found as:

$$W = \frac{kAT_a}{\eta}\left\{\int_o^l \left(\frac{1}{\theta} - 1\right)(\theta'' + 2\gamma)\frac{dx}{d\theta}\cdot d\theta + \left(\frac{1}{\theta_o} - 1\right)\theta'(o)\right\}$$

$$= \frac{kAT_a\sqrt{\gamma}}{\eta}\left\{4\sqrt{\frac{2}{\theta_o} - \alpha} - 4\sqrt{2-\alpha} - \frac{(2+\alpha)}{\sqrt{\alpha}}\left[\sin^{-1}(\alpha-1) - \sin^{-1}(\alpha\theta_o - 1)\right]\right\}$$

$$= \frac{i}{\eta}\sqrt{\rho_a k T_a}\;\frac{1}{2}\left\{4\sqrt{2r-\alpha} - 4\sqrt{2-\alpha} - \frac{(2+\alpha)}{\sqrt{\alpha}}\left[\sin^{-1}(\alpha-1) - \sin^{-1}\left(\frac{\alpha}{r} - 1\right)\right]\right\} \tag{88}$$

Here r is the ratio $T_a/T_o = 1/\theta_o$. The optimum value of l for minimum W can be found alternatively by setting the derivative of equation 88 with respect to α equal to zero and solving for α. That optimum α is 2, and optimum l is found from 87. Then:

$$W_{opt.} = \frac{i}{\eta}\sqrt{\rho_a k T_a}\left\{4\sqrt{r-1} - \pi + 2\sin^{-1}\left(\frac{2}{r} - 1\right)\right\} \tag{89}$$

$$\frac{i\,l}{A}_{opt.} = \sqrt{\frac{kT_a}{\rho_a}}\left\{\frac{\pi}{2} - \sin^{-1}\left(\frac{2}{r} - 1\right)\right\} \tag{90}$$

$$\phi^*_{opt.} = \frac{\phi \Delta x}{\Delta T} = i\sqrt{\frac{\rho_a k}{T_a}}\left\{\frac{(3 - a\theta)}{2\sqrt{\theta - \frac{a}{2}\theta^2}}\right\} = i\sqrt{\frac{\rho_a k}{T_a}}\,\frac{(3 - 2\theta)}{2\sqrt{\theta - \theta^2}} \tag{91}$$

When the negative sign in equation 85 is used the solutions corresponding to equations 86, 88, 89 , 90 , and 91 are:

$$\sqrt{a\gamma}\,x = \ln\left[\frac{\sqrt{2a\theta + a^2\theta^2} + a\theta + 1}{\sqrt{2a\theta_o + a^2\theta_o^2} + a\theta_o + 1}\right] \tag{86 a}$$

$$W = \frac{i}{\eta}\sqrt{\rho_a kT_a}\,\frac{1}{\sqrt{2}}\left\{4\sqrt{2r + a} - 4\sqrt{2 + a} - \frac{(2-a)}{\sqrt{a}}\ln\left[\frac{\sqrt{2a + a^2} + a + 1}{\sqrt{2\frac{a}{r} + \frac{a^2}{r^2}} + \frac{a}{r} + 1}\right]\right\} \tag{88a}$$

$$\frac{i\,l}{A} = \sqrt{\frac{kT_a}{\rho_a}}\left\{\sqrt{\frac{2}{a}}\ln\left[\frac{\sqrt{2a + a^2} + a + 1}{\sqrt{2\frac{a}{r} + \frac{a^2}{r^2}} + \frac{a}{r} + 1}\right]\right\} \tag{90a}$$

$$\phi^* = \frac{\phi \Delta x}{\Delta T} = i\sqrt{\frac{\rho_a k}{T_a}}\left\{\frac{3 + a\theta}{2\sqrt{\theta + \frac{a}{2}\theta^2}}\right\} \tag{91a}$$

Case B - Varying Resistivity $\rho = \rho_a (T / T_a)$

Equation 83 becomes now:

$$\theta'' = \frac{\theta'^2}{\theta} - \gamma \theta^2, \quad \theta(o) = \theta_o, \quad \theta(1) = 1 \tag{92}$$

Reference 23 gives the first integration of this equation as:

$$\theta'^2 = \frac{2\gamma}{\beta} \theta^2 - 2\gamma \theta^3 \tag{93}$$

The constant of integration is $2\gamma/\beta$ and is positive. Integration of equation 93 and the boundary conditions give:

$$\sqrt{\frac{\gamma}{2\beta}}\, x = \ln \left[\sqrt{\frac{\theta}{\theta_o}} \, \frac{(1 + \sqrt{1 - \beta\theta_o})}{(1 + \sqrt{1 - \beta\theta})} \right] \tag{94}$$

$$\sqrt{\frac{\gamma}{2\beta}}\, l = \ln \left[\sqrt{\frac{1}{\theta_o}} \, \frac{(1 + \sqrt{1 - \beta\theta_o})}{(1 + \sqrt{1 - \beta})} \right] \tag{95}$$

The total refrigeration work, found in the same manner as in equation 88 is:

$$W = \frac{1}{\eta} \sqrt{\rho_a k T_a} \, \frac{2}{\sqrt{\beta}} \left\{ 2\sqrt{1-\beta} - 2\sqrt{1 - \frac{\beta}{r}} + (1+\beta) \ln \left[\sqrt{r} \, \frac{(1 + \sqrt{1 - \frac{\beta}{r}})}{(1 + \sqrt{1-\beta})} \right] \right\} \tag{96}$$

Optimizing W to find β, which again is equivalent to finding optimum l, results in an optimum β of 1.

$$W_{opt.} = \frac{1}{\eta} \sqrt{\rho_a k T_a} \left\{ 4 \ln \left[\sqrt{r} + \sqrt{r-1} \right] - 4 \, \frac{\sqrt{r-1}}{\sqrt{r}} \right\} \tag{97}$$

$$\frac{i\,l}{A}\ \text{opt.} = \sqrt{\frac{k_a T_a}{\rho_a}} \left\{ 2 \ln \left[\sqrt{r} + \sqrt{r-1} \right] \right\} \tag{98}$$

$$\phi^*\ \text{opt.} = \frac{\phi\,\Delta x}{\Delta T} = i \sqrt{\frac{\rho_a \cdot k}{T_a}} \left\{ \frac{\theta - \frac{3}{2}\,\theta^2 + 1}{\theta \sqrt{1-\theta}} \right\} \tag{99}$$

2. Vapor Cooling of an Electrical Conductor

When a lead is cooled by a stream of vapor flowing along the conductor from cold to warm end and convection heat transfer coefficients are high, then vapor temperature and lead temperatures are the same at any location, x. Furthermore, since vapor specific heat C_p is independent of temperature, ϕ^*, is constant. That means that the same cooling or heat removal occurs between equal temperature increments all along the lead. Since ϕ (heat removed per unit length) is equal ϕ^* (heat removed per unit temperature change) times $d T/d x$, equation 79 may be written as:

$$\frac{d}{dx}\left(kA \frac{d T}{d x}\right) + \frac{i^2 \rho}{A} - \phi^* \frac{d T}{d x} = 0 \tag{100}$$

Again two solutions are of interest, either constant or linearly varying resistivity and constant conductivity, k, and area A.

Case A - Resistivity Constant

When $\phi^* = kAD$, a constant, equation 100 and boundary conditions become:

$$\theta'' = D\,\theta' = -2\gamma, \quad \theta(o) = \theta_o, \ \theta(l) = 1 \tag{101}$$

The solution of this equation is:

$$\Theta = \frac{(1 - \Theta_o - \frac{2\gamma l}{D}) e^{dx} - (1 - \Theta_o e^{Dl} - \frac{2\gamma l}{D})}{e^{Dl} - 1} + \frac{2\gamma x}{D} \qquad (102)$$

Total refrigeration work, including that due to a heat flux at the cold end of the lead is:

$$W = \int_o^l \frac{1}{\eta} \left(\frac{T_a - T}{T}\right) \phi \, dx = \frac{1}{\eta} \left(\frac{T_a - T_o}{T_o}\right) kAT'(o)$$

$$= \frac{kAT_a}{\eta} \left\{ \int_{\Theta_o}^{1} \left(\frac{1}{\Theta} - 1\right) D \, d\Theta + \left(\frac{1}{\Theta_o} - 1\right) \Theta'(o) \right\}$$

$$= \frac{kAT_a D}{\eta} \left\{ \ln r - \left(1 - \frac{1}{r}\right) + (r - 1) \left[\frac{1 - \frac{1}{r} - \frac{2\gamma l}{D}}{e^{Dl} - 1} + \frac{2\gamma}{D^2} \right] \right\} \qquad (103)$$

Using equation 103, W may be minimized with respect to l. The resulting equation for optimum l is:

$$\frac{2\gamma}{D^2} + \frac{D\left(1 - \frac{1}{r} - \frac{2\gamma l}{D}\right)}{1 - e^{-Dl}} = 0 \qquad (104)$$

Assuming that Dl is large, e^{-Dl} is negligible compared with one. Then

$$Dl_{opt.} = 1 + \frac{D^2}{2\gamma}\left(1 - \frac{1}{r}\right) \qquad (105)$$

When vapor cooling is used, there is often a unique relation between the heat transferred to evaporating refrigerant and the vapor cooling parameter D. For a flow rate, $\dot{m}$,

caused by heat flux kAT' (o):

$$D = \frac{\phi^*}{kA} = \frac{\dot{m} C_p}{kA} = \frac{(kAT'(o) / h_{fg})\ C_p}{kA}$$

$$= \frac{T_o C_p\ \Theta'(o)}{h_{fg}\ \Theta_o} = \frac{\Theta'(o)}{f \Theta_o} \qquad (106)$$

Here f is a factor, near 1 for helium, defined as heat of vaporization, h_{fg}, divided by $C_p T_o$. An equation using the optimum result, equation 105, and equation 102 in equation 106 gives:

$$\frac{D^2}{2\gamma} = \frac{r}{f}\left[1 - e^{-\left[1 + \frac{D^2}{2\gamma}\left(1 - \frac{1}{r}\right)\right]}\right] \qquad (107)$$

Equation 107 is satisfied for $D^2/2\gamma$ nearly equal r/f, which is generally larger than one. Then, equation 105 shows that optimum D l is larger than two. This conclusion justifies neglecting e^{-Dl} in equation 104.

The results may finally be written making use of equations 106 and 107 in equations 103 and 105.

$$W = \frac{i}{\eta}\sqrt{k \rho_a T_a}\left\{\sqrt{\frac{rg}{r}}\left[\ln r - (1 - f)\left(1 - \frac{1}{r}\right)\right]\right\} \qquad (108)$$

$$\frac{i}{A}\Big|_{\text{opt.}} = \sqrt{\frac{kT_a}{\rho_a}}\left\{\sqrt{\frac{f}{rg}}\left[1 + \frac{(r-1)}{f}\, g\right]\right\} \qquad (109)$$

$$\phi^* = i\sqrt{\frac{\rho_a k}{T_a}}\sqrt{\frac{r g}{f}} \qquad (110)$$

where $g = 1 - e^{-\left(1 + \frac{r-1}{f}\right)} \simeq 1$

An optimum f, equivalent to providing refrigeration at just T_o and also vapor cooling so that f is variable, can be found from equation 108. When g equals 1.

$$f_{opt.} = \frac{\ln r}{\left(1 - \frac{1}{r}\right)} - 1 \tag{111}$$

$$W_{opt.} = \frac{i}{\eta} \sqrt{k \rho_a T_a} \left\{ 2 \sqrt{(r-1)\left[\ln r - \left(1 - \frac{1}{r}\right)\right]} \right\} \tag{112}$$

Case B - Resistivity Variable, $\rho = \rho_a (T/T_a)$

When $\phi^* = 2kAd$, a constant, equation 100 and boundary conditions become:

$$\Theta'' - 2d\Theta' + 2\gamma\Theta = 0, \quad \Theta(o) = \Theta_o, \quad \Theta(l) = 1 \tag{113}$$

The solution of equation 113 is:

$$\Theta = e^{dx}\left[\Theta_o e^{ax} - (\Theta_o e^{a} - e^{-dl}) \frac{\sinh ax}{\sinh al}\right]$$

$$= \frac{e^{dx}\left[\Theta_o \sin \beta (l - x) + e^{-dl} \sin \beta x\right]}{\sin \beta l} \tag{114}$$

where: $a = \sqrt{d^2 - 2\gamma}$, $\beta = \sqrt{2\gamma - d^2}$.

The total refrigeration work, considering that $d = \Theta(o) / 2 f \Theta_o$, is:

$$W = \frac{2 k A T_a}{\eta} \left\{ \ln r - (1 - f)\left(1 - \frac{1}{r}\right) \right\} d \tag{115}$$

To minimize W it is necessary to minimize d with respect to l. Using the equation for d as:

$$d = \frac{\Theta'(o)}{2f\Theta_o} = \frac{d\Theta_o + \alpha\left[\Theta_o - \frac{(\Theta_o e^{\alpha l} - e^{-dl})}{\sinh \alpha l}\right]}{2f\Theta_o} \tag{116}$$

From equation 116 these alternative conditions are found:

$$(2\gamma - 1) = \sqrt{1 - \frac{2\gamma}{d^2}}\left[\frac{re^{-(dl)} - \cosh\sqrt{1 - \frac{2\gamma}{d^2}}\,(dl)}{\sinh\sqrt{1 - \frac{2\gamma}{d^2}}\,(dl)}\right] \tag{117}$$

$$(2f - 1) = \sqrt{\frac{2\gamma}{d^2} - 1}\left[\frac{re^{-(dl)} - \cos\sqrt{\frac{2\gamma}{d^2} - 1}\,(dl)}{\sin\sqrt{\frac{2\gamma}{d^2} - 1}\,(dl)}\right] \tag{118}$$

If d^2 is greater than but near 2γ, equation 117 reduces to:

$$(2f - 1) = \frac{1}{(dl)}\left[re^{-(dl)} - 1\right] \tag{119}$$

Since it is possible to satisfy equation 119, and solve it for (dl), d may be as small as $\sqrt{2\gamma}$. The second condition, equation 118, therefore should be used to find dl which minimizes d or maximizes $2\gamma/d^2$ in equation 118. An alternative is to find maximum $\sqrt{(2\gamma/d^2) - 1} = p$ optimizing dl. Equation 118 can be solved for r and the variation of it set equal to zero for p and dl varying. Then dp/d (dl) is set equal zero from that expression to find an optimizing condition. This results in an equation for pdl in terms of p. When f = 1, dl = lnr and p may be found from the original equation 118 by a graphical solution of the transcendental function.

●

3. Cooling an Electrical Lead at One End

An electrical lead that is cooled only at x equal zero is described by equation 79 except that the advantages in staged cooling are not used and ϕ is zero. Again two cases are of interest, constant or linearly varying resistivity with constant conductivity and area.

Case A - Resistivity Constant

Equation 79 and its boundary conditions become:

$$\Theta'' + 2\gamma = 0 , \quad \Theta(o) = \Theta_o , \quad \Theta(l) = 1 \tag{120}$$

The solution of equation 120 is:

$$\Theta = \Theta_o + \left[\frac{(1 - \Theta_o)}{l} + \gamma l\right] x - \gamma x^2 \tag{121}$$

The refrigeration work required to remove the flux of heat at $x = 0$, T_o to T_a is:

$$W = \frac{kA}{\eta}\left(\frac{T_a - T_o}{T_o}\right) T'(o) \tag{122}$$

To minimize W it is only necessary to minimize $\Theta'(o)$ with respect to l.

$$\Theta'(o) = \frac{1 - \Theta_o}{l} + \gamma l \tag{123}$$

From this the optimum length to area ratio and refrigeration work are:

$$\frac{i l_{opt}}{A} = \sqrt{\frac{2k(T_a - T_o)}{\rho_a}} = \sqrt{\frac{2kT_a}{\rho_a}}\sqrt{\frac{r-1}{r}} \tag{124}$$

$$W_{opt.} = \frac{i}{\eta} \sqrt{\rho_a k T_a} \left(\sqrt{2} \frac{(r-1)}{\sqrt{r}}^{3/2} \right) \tag{125}$$

Case B - Varying Resistivity $\rho = \rho_a (T/T_a)$

Equation 79 and its boundary conditions become:

$$\Theta'' + 2\gamma\Theta = 0, \quad \Theta(o) = \Theta_o, \quad \Theta(1) = 1 \tag{126}$$

The solution of equation 126 is:

$$\Theta = \frac{\Theta_o \sin \sqrt{2\gamma}\,(1-x) + \sin \sqrt{2\gamma}\, x}{\sin \sqrt{2\gamma}\, 1} \tag{127}$$

The refrigeration work required, that given by equation 122 , can be minimized with respect to l. Then:

$$\frac{i\,l}{A}_{opt.} = \sqrt{\frac{k\,T_a}{\rho_a}} \cos^{-1} \frac{1}{r} \tag{128}$$

$$W_{opt.} = \frac{i}{\eta} \sqrt{k\,\rho_a\,T_a} \left\{ \frac{(r-1)}{r} \sqrt{r^2 - 1} \right\} \tag{129}$$

4. Optimum Cooling of a Conduction Path

One dimensional heat flow in a conduction path is shown schematically in Figure . The heat, $\phi^*\,dT$, is removed at temperature T by refrigeration and rejected at ambient T_a. Heat flux Q flows toward the cold end at the section x with temperature T. Total refrigeration work is:

$$W = \int_{T_o}^{T_a} \frac{1}{\eta} \left(\frac{T_a}{T} - 1 \right) \phi^*(T)\,dT + \frac{1}{\eta} \left(\frac{T_a}{T_o} - 1 \right) Q_o \tag{130}$$

Heat transfer can be described in two ways:

$$dx = \frac{k A \, dT}{Q(T)} \tag{131}$$

$$dQ = \phi^* \, dT \tag{132}$$

Equation 131 establishes a constraint for the minimization of W. The integral of equation 131 is:

$$I = \int_{T_o}^{T_a} \frac{k A \, dT}{Q(T)} \tag{133}$$

Using equation 132 in equation 130 and introducing the Lagrange multiplier, λ, the problem is to minimize:

$$I = \int_{T_o}^{T_a} \left[\frac{1}{\eta(T)} \left(\frac{T_a}{T} - 1 \right) \frac{dQ}{dT} + \frac{Q_o}{\eta(T_o) T_o} + \lambda \frac{k A}{Q(T)} \right] dT \tag{134}$$

The integral has the form

$$I = \int_{T_o}^{T_a} \left[f_2(T) \frac{dQ}{dT} + \lambda \frac{f_1(T)}{Q} + C_1 \right] dT \tag{135}$$

The Euler equation is:

$$\frac{d f_2(T)}{dT} + \frac{\lambda f_1(T)}{Q^2} = 0 \tag{136}$$

Consequently:

$$Q^2 = \frac{\lambda k A \eta T^2}{T_a T} \tag{137}$$

The Lagrange multiplier is evaluated by using equation 137 in equation 133. The result from Q is:

$$Q = \sqrt{\frac{k A \eta}{T T_a}}\, T \int_{T_o}^{T_a} \sqrt{\frac{k A \eta}{T T_a}}\, \frac{dT}{T} \tag{138}$$

Refrigeration work can be found as:

$$W = \int_{T_o}^{T_a} \sqrt{\frac{kAT_a}{T\eta}}\, \frac{dT}{T} \left[\int_{T_o}^{T_a} \frac{1}{\eta} \left(\frac{T_a}{T_o} - 1 \right) \frac{d}{dT} \left(\sqrt{\frac{kAT_a}{T\eta}}\, T \right) dT + \sqrt{\frac{kAT_a}{T\eta}} \Bigg|_{T = T_o} \left(1 - \frac{T_o}{T_a} \right) \right] \tag{139}$$

Two cases are of interest, that for variable thermal conductivity, k, (actually, k A) and variable efficiency, η, and that for constant k and η.

Case A - Variable Conductivity, $kA = k_a A (T/T_a)^n$, and Efficiency, $\eta = \eta_a (T/T_a)^m$

When the conductivity and efficiency functions are used in equations 138 and 139 the results are:

$$W = \frac{k_a A T_a}{\eta_a l} \left\{ \frac{(2n + 2 - p)}{p^2 (p + 2)} \left[1 - \frac{1}{r^{p/2}} \right] \left[4 - \frac{(4 - p^2)}{r^{p/2}} - \frac{p^2}{r^{\frac{p+2}{2}}} \right] \right\} \quad (140)$$

where $p = n - m \neq 0$, $r = T_a / T_o$

$$\phi^* = \frac{k_a A}{l} \left\{ \frac{(2n + 2 - p)}{p} \left[1 - \frac{1}{r^{p/2}} \right] \Theta^{(n+m)/2} \right\} \quad (141)$$

Solution of equation 131 for for resulting temperature distribution with Q given by equation 138 and the property variations is:

$$\Theta = \left[\frac{1}{r^{p/2}} \left(1 - \frac{x}{l} \right) + \frac{x}{l} \right]^{2/p} \quad (142)$$

Case B - Constant Conductivity and Refrigerator Efficiency

Application of equations 138 and 139 gives:

$$W = \frac{k_a A T_a}{\eta_a l} \left[\ln r \right]^2 \quad (143)$$

$$\phi^* = \frac{k_a A}{T_a} \left[\ln r \right] \quad (144)$$

The resulting temperature distribution is:

$$\Theta = \left(\frac{1}{r} \right)^{1 - \frac{x}{l}} \quad (145)$$

Note that since ϕ^* is constant, vapor cooling is also optimum cooling.

5. Vapor Cooling of a Conduction Path

When vapor cooling is used ϕ^* is a constant. Recalling equation 106 where f was introduced, equation 130 may be written

$$W = \phi^* \left[\int_{T_o}^{T_a} \frac{1}{\eta} \left(\frac{T_a}{T} - 1 \right) dT + \frac{f}{\eta(o)} (T_a - T_o) \right] \tag{146}$$

Equation 132 may be used to find Q as:

$$Q = Q_o + \phi^* (T - T_o) = \phi^* \left[T - (1 - f) T_a \right] \tag{147}$$

Then equation 131 when integrated evaluates ϕ^* as:

$$\phi^* = \frac{1}{I} \int_{T_o}^{T_a} \frac{k A dT}{\left[T - (1 - f) T_a \right]} \tag{148}$$

When properties are variable, it may be seen that k variations appear only in ϕ^* and η variations only in the integral of equation 146 for W. Several useful results may be obtained.

Case A - Refrigeration Efficiency Variable $\eta = \eta_a (T / T_a)^m$

Refrigeration work from equation 146 becomes:

$$W = \frac{T_a}{\eta_a} \phi^* \left[\frac{1}{m(m-1)} + \left(\frac{1}{m} + f \right) r^m - \left(\frac{1}{m-1} + f \right) r^{m-1} \right] \tag{149}$$

There are three useful cases when considering conductivity variation.

Case A-1 - Conductivity Variable, $k = k_a (T / T_a)^n$, $f = 1$

This case corresponds to the use of helium. Equations 148 and 149 give:

$$\phi^* = \frac{k_a A}{l} \left[\frac{1}{n} \left(1 - \frac{1}{r^n} \right) \right] \tag{150}$$

$$W = \frac{k_a A T_a}{\eta_a l} \left\{ \frac{1}{n} \left(1 - \frac{1}{r^n} \right) \left[\frac{1}{m(m-1)} + \frac{m+1}{m} r^m + \frac{m}{m-1} r^{m-1} \right] \right\} \tag{151}$$

Case A-2 - Conductivity Variable, $k = k_a (T / T_a)$

Integration in equation 148 may be performed with f general.

$$\phi^* = \frac{k_a A}{l} \left\{ \left(1 - \frac{1}{r}\right) + (1 - f) \frac{1}{r} \ln \left[\frac{r - (1 - f)}{f} \right] \right\} \tag{152}$$

$$W = \frac{k_a A T_a}{\eta_a l} \left\{ \left(1 - \frac{1}{r}\right) + (1 - f) \frac{1}{r} \ln \left[\frac{r - (1 - f)}{f} \right] \right\} \times$$

$$\left\{ \frac{1}{m(m-1)} + \left(\frac{1}{m} + f \right) r^m - \left(\frac{1}{m-1} + f \right) r^{m-1} \right\} \tag{153}$$

Case A-3 - Conductivity Constant

For this case equations 148 and 149 give:

$$\phi^* = \frac{k_a A}{l} \ln \left(\frac{r - (1 - f)}{f} \right) \tag{154}$$

$$W = \frac{k_a A T_a}{\eta_a l} \left\{ \ln \left[\frac{r - (1-f)}{f} \right] \left[\frac{1}{m(m-1)} + \left(\frac{1}{m} + f \right) r^m - \left(\frac{1}{m-1} + f \right) r^{m-1} \right] \right\} \tag{155}$$

Case B - Refrigeration Efficiency Constant

Refrigeration work from equation 146 becomes:

$$W = \frac{T_a}{\eta_a} \phi^* \left[\ln r - (1 - f)(1 - \frac{1}{r}) \right] \tag{156}$$

Again there are three subcases of interest. Since the same ϕ^*'s as found in subcases A-1, A-2 and A-3 apply, only refrigeration work will be summarized.

Case B-1 - Conductivity Variable, $k = k_a (T/T_a)^n$, $f = 1$

$$W = \frac{k_a A T_a}{\eta_a l} \left[\frac{1}{n} (1 - \frac{1}{r^n}) \ln r \right] \tag{157}$$

Case B-2 - Conductivity Variable, $k = k_a (T/T_a)$

$$W = \frac{k_a A T_a}{\eta_a l} \left\{ (1 - \frac{1}{r}) + (1 - f) \frac{1}{r} \ln \left[\frac{r - (1-f)}{f} \right] \right\} \left\{ \ln r - (1-f)(1 - \frac{1}{r}) \right\} \tag{158}$$

Case B-3 - Conductivity Constant

$$W = \frac{k_a A T_a}{\eta_a l} \left\{ \ln \left[\frac{r - (1 - f)}{f} \right] \left[\ln r - (1 - f)(1 - \frac{1}{r}) \right] \right\} \tag{159}$$

6. Cooling a Conduction Path in Two Stages

A conduction path cooled in two places, a the cold end and somewhere ($x = l_o$) at temperature T_1 is an approximation of optimum cooling. For this problem both the best temperature, T_1, and location of intermediate cooling, l_o, may be found. The general case where k and η are variable as well as that special case $n = 1$ and η constant are of interest.

Case A - Variable Conductivity, $k = k_a (T/T_a)^n$ and Efficiency, $\eta = \eta_a (T/T_a)^m$.

The equation governing heat transfer in length l_o is equation 131.

$$dx = \frac{k_a A}{Q_o T_a^n} T^n \, dT, \quad T(o) = T_o, \quad T(l) = T_1 \tag{160}$$

Integration gives:

$$Q_o = \frac{k_a A T_a}{l_o} \frac{1}{(n+1)} \left[\left(\frac{T_1}{T_a}\right)^{n+1} - \left(\frac{T_o}{T_a}\right)^{n+1} \right] \tag{161}$$

Similarly if the heat flux Q_1 is flowing from T_a to T_1:

$$Q_1 = \frac{k_a A T_a}{l_o} \frac{1}{(n+1)} \left[1 - \left(\frac{T_1}{T_a}\right)^{n+1} \right] \tag{162}$$

The work required by refrigeration of Q_o and $Q_1 - Q_o$, i.e., W_o and W_1 is:

$$W_o = \frac{1}{\eta_a} \left(\frac{T_a}{T_o}\right)^m \left(\frac{T_a}{T_o} - 1\right) Q_o ; \quad W_1 = \frac{1}{\eta_a} \left(\frac{T_a}{T_1}\right)^m \left(\frac{T_a}{T_1} - 1\right) (Q_1 - Q_o) \tag{163}$$

Total work required is $W_o + W_1$ and when $r = T_a / T_o$, $S = T_a / T_1$ and $\lambda = l_1 / l_o$:

$$W = \frac{k_a A T_a}{\eta_a l} \left(\frac{\lambda + 1}{n+1}\right) \left[\frac{(S-1) S^m \left(1 - \frac{1}{S^{n+1}}\right)}{\lambda} + \left(\frac{1}{S^{n+1}} - \frac{1}{r^{n+1}}\right) \cdot \left((r-1) r^m - (S-1) S^m \right) \right] \tag{164}$$

Then also:

$$Q_o = \frac{k_a A T_a}{l}\left(\frac{\lambda+1}{n+1}\right)\left(\frac{1}{S^{n+1}} - \frac{1}{r^{n+1}}\right) \tag{165}$$

$$Q_1 = \frac{k_a A T_a}{l}\left(\frac{\lambda+1}{n+1}\right)\left(\frac{1}{\lambda} + \frac{1}{r^{n+1}} - \frac{(\lambda+1)}{\lambda}\frac{1}{S^{n+1}}\right) \tag{166}$$

The optimum value of λ is found as:

$$\lambda^2_{opt.} = \frac{(S-1)\,S^m\,(1 - \frac{1}{S^{n+1}})}{\left[(r-1)\,r^m - (S-1)\,S^m\right]\left[\frac{1}{S^{n+1}} - \frac{1}{r^{n+1}}\right]} \tag{167}$$

Then minimum work is:

$$W_{opt.} = \frac{k_a A T_a}{\eta_a l}\left(\frac{1}{n+1}\right)\left[\left\{(S-1)S^m\left(1 - \frac{1}{S^{n+1}}\right)\right\}^{1/2} + \left\{\left[(r-1)\,r^m - (S-1)S^m\right]\left[\frac{1}{S^{n+1}} - \frac{1}{r^{n+1}}\right]\right\}^{1/2}\right]^2 \tag{168}$$

For any n and m, numerical trial is the most effective method to find best values of S given r.

Case B - Linearly Varying Conductivity, $k = k_a (T/T_a)$, Efficiency Constant

From equations 167 and 168 for $n = 1$ and $m = 0$.:

$$\lambda_{opt.} = \frac{(S-1)\,r}{(r-s)}\sqrt{\frac{S+1}{r+S}} \tag{169}$$

$$W_{opt.} = \frac{k_a A T_a}{\eta_a l}\left\{\frac{1}{2}\left[\left(\frac{S-1}{S}\right)\sqrt{S+1} + \left(\frac{r-S}{rS}\right)\sqrt{r+S}\right]\right\}^2 \tag{170}$$

Case C - Constant Conductivity and Efficiency

From equations 167 and 168 for $n = 0$ and $m = 0$

$$\lambda_{opt.} = \frac{S-1}{r-S}\sqrt{r} \tag{171}$$

$$W_{opt.} = \frac{k_a A T_a}{\eta_a l}\left[\frac{S-1}{\sqrt{S}} + \frac{r-S}{\sqrt{rS}}\right]^2 \tag{172}$$

The optimum value of S is found from equation 172 as $S = \sqrt{r}$. The refrigeration work is:

$$W_{opt.} = \frac{k_a A T_a}{\eta_a l}\; 4\left[r^{1/4} - \frac{1}{r^{1/4}}\right]^2 \tag{173}$$

7. Cooling a Conduction Path at One End

The refrigeration work required for a conduction path cooled just at T_o is a specialized case in the preceding section where $S = r$. Use of equation 168 then gives:

$$W = \frac{k_a A T_a}{\eta_a l}\left\{\left(\frac{1}{n+1}\right)\left[r^{m+1} - r^{m} - \frac{1}{r^{n-m}} + \frac{1}{r^{n-m+1}}\right]\right\} \tag{174}$$

This result may be used where refrigeration efficiency and thermal conductivity vary ($n \neq 0$, $m \neq 0$), or where one or both these parameters are constant so that $m = 0$ or $n = 0$.

8. Cooling a Multiple Shielded Radiation Path

Heat transfer by radiation between a surface No. 1, and a second surface, No. 2, very near to it is given by:

$$Q = \frac{\sigma A}{\frac{1}{\epsilon_1} + \frac{1}{\epsilon_2} - 1}\left(T_1^4 - T_2^4\right) = \frac{k_r}{(1/N)} A (T_1 - T_2) \tag{175}$$

Equation 175 defines an apparent conductivity k_r. If there are a number, N, of radiation shields between T_a and T_o, then adjacent shields or radiation surfaces have

absolute temperatures that are not very different in magnitude. Because of this, k_r may be written as:

$$k_r = \frac{\sigma_1 (T_1 + T_2)(T_1^2 + T_2^2)}{N\left(\frac{1}{\epsilon_1(T_1)} + \frac{1}{\epsilon_2(T_2)} - 1\right)} = \frac{4\sigma_1 T^3}{N\left(\frac{2}{\epsilon(T)} - 1\right)} \tag{176}$$

Emissivities, ϵ, are made much less than 1, so that a good approximation for k_r is $4\epsilon(T)\sigma_1 T^3/N$. Now it is possible to use k_r in the preceding theory for conduction paths with variable conductivity. Now if $\epsilon/\epsilon_a = (T/T_a)^j$, $n = 3 + j$. For example, with constant ratio, n, of refrigeration efficiency to carnot cycle efficiency and constant emissivity ϵ.

Case A - Optimum Cooling

From equations 140 and 141 with m = 0, n = 3:

$$W = \frac{4\epsilon\sigma A T_a^4}{\eta_a N}\left\{\frac{1}{9}\left[1 - \frac{1}{r^{3/2}}\right]\left[4 + \frac{5}{r^{3/2}} - \frac{9}{r^{5/2}}\right]\right\} \tag{177}$$

$$Q^* = \frac{4\epsilon\sigma A T_a^4}{N}\left\{\frac{5}{3}\left[1 - \frac{1}{r^{3/2}}\right]\Theta^{3/2}\right\} \tag{178}$$

Case B - Vapor Cooling

From equations 148 and 156:

$$W = \frac{T_a}{\eta_a}\,\phi^*\left\{\ln r - (1 - f)\left(1 - \frac{1}{r}\right)\right\} \tag{179}$$

$$\phi^* = \frac{4\epsilon\sigma A T_a^3}{N}\left\{\frac{1}{r^3}\left[\frac{r^3 - 1}{3} + \frac{(1-f)(r^2-1)}{2} + (1 - f)^2(r - 1) + (1 - f)^3 \ln\left(\frac{r - (1 - f)}{f}\right)\right]\right\} \tag{180}$$

Case C - Two Stage Cooling

From equation 168, with λ taken as optimum and interpreted as N_1 / N_o, the number of shields between hot T_a amd cooling at T_1 divided by the number of shields between T_1 and cooling at T_o:

$$W_{opt.} = \frac{4\epsilon\sigma A T_a^4}{\eta_a N}\left(\frac{1}{4}\right)\left\{\left[(S-1)\left(1-\frac{1}{S^4}\right)\right]^{1/2}+\left[(r-S)\left(\frac{1}{S^4}-\frac{1}{r^4}\right)\right]^{1/2}\right\}^2 \qquad (181)$$

It may be shown that optimum S is found from:

$$\frac{r^4 - S^4}{r^4 (r - S)} = \frac{S^4 - 1}{S - 1} \qquad (182)$$

When r is larger than about 3, $S^4 \ll r^4$ and equation 182 may be solved for r when S is optimum.

$$r = S_{opt.} + \frac{S_{opt.}^2}{16}\,\frac{(S_{opt.}^4 - 1)}{(S_{opt.} - 1)} \qquad (183$$

The resulting expression for W in terms of $S_{opt.}$ becomes:

$$W_{opt.} = \frac{4\epsilon\sigma A T_a^4}{\eta_a N}\left\{\frac{1}{48}\,\frac{(S_{opt.}^4 - 1)(5S_{opt.} - 4)^2}{S_{opt.}^4 (S_{opt.} - 1)}\right\} \qquad (184)$$

Case D - Cooling only at T_o

Equation 174 gives:

$$W = \frac{4\epsilon\sigma A T_a^4}{\eta_a N}\left\{\frac{1}{4}\left[r - 1 - \frac{1}{r^4} + \frac{1}{r^5}\right]\right\} \qquad (185)$$

APPENDIX A

References

1. Redding, A. H., et al, "Nuclear MHD Space Power Generation Study", Westinghouse Astronuclear Laboratory Technical Report, WANL-TNR-094, Westinghouse Astronuclear Laboratory, Pittsburgh 36, Pa., March, 1963.

2. Keenan, J. H., "Thermodynamics", John Wiley & Sons, Inc., New York August 1957, pp 193 - 194.

3. Tsu, T. C., "Metal Vapors as Possible Heat-Engine Working Fluids: Their Thermodynamic and Electrical Properties", Westinghouse Research Report, 63-118-266-R1, Westinghouse Research Laboratories, Pittsburgh 35, Pa., February 1, 1963.

4. Swift-Hook, D. T. and Wright, J. K., "The Constant-Mach-Number MHD Generator", Journal of Fluid Mechanics, 15, 1, January 1963, pp 97 - 110.

5. Swift-Hook, D. T., "Wall Effects in an MHD Generator", Symposium on Magnetoplasmadynamics Electrical Power Generation, King's College, University of Durham, Newcastle Upon Tyne, September 6-8, 1962.

6. Erdilye, A., Editor, "Higher Transcendental Functions", Bateman Manuscript Project, California Institute of Technology, McGraw-Hill Book Company, Inc., New York, 1953, pp. 87.

7. Perel, J., Englander, P., Bederion, B., "Measurement of Total Cross Sections for the Scattering of Low Energy Electrons by Lithium, Sodium, and Potassium", Physical Review, 128, 3, November 1, 1962, pp. 1148 - 1154.

8. Weatherford, W. D. Jr., Tyler, J. L., Ku P. M., "Properties of Inorganic Energy-Conversion and Heat-Transfer Fluids for Space Applications", WADD Technical Report 61-96, Astia AD 267541, Aeronautical Systems Division, November 1961.

9. Sonnerup, B. U. Ö., "Theory of Viscous Magnetogasdynamic Flow in Slowly Diverging Two-Dimensional Channels", paper appearing in Plasma Hydromagnetics edited by D. Bershader, pp. 124-136; Stanford University Press, 1962.

10. Ehlers, F. E., "Linearized Magnetogasdynamic Channel Flow with Axial Symmetry", ARS Journal, vol. 31, no. 3, pp. 334 - 342; March 1961.

11. Sakurai, T., and Naito, M., "Steady Two-Dimensional Channel Flow of an Incompressible Perfect Fluid with Small Electric Conductivity in the Presence of Non-Uniform Magnetic Fields", Jour. Phys. Soc. Japan, vol. 17, no. 4, pp. 675 - 681, April 1962.

12. Yeh, H., and Sutton, G. W., "Current Output and Efficiency of MHD Generators with Segmented Electrodes and Non-Uniform Velocity Profiles", paper presented at Symposium on Magnetoplasmadynamic Electrical Power Generation at King's College University of Durham, Newcastle upon Tyne, England; 6-8 September, 1962.

13. Broer, L. J. F., "Motion of a Charged Particle in a Slowly Increasing Magnetic Field", paper appearing in Magneto-Fluid Dynamics, edited by F. M. Frenkiel and W. R. Sears; NAS-NRC Publication 829, pp. 742 - 743, 1960.

14. Meyer, R. X., "Plasma Propulsion by Means of a Traveling Sinusoidal Magnetic Field", paper appearing in Plasma Acceleration, edited by S. W. Kash, pp. 37-46; Stanford Univ. Press, 1960.

15. Light, G. C., "Magnetic Insulation Experiments with a Traveling Magnetic Piston Plasma Accelerator", Proceedings of 4th Symposium on the Engineering Aspects of MHD, pp. 13 - 21; Berkeley, California; 1963.

16. Smotrich, H., Janes, G. S., and Bratenahl, A., "Experimental Studies of a Magnetohydrodynamic C. W. Traveling Wave Accelerator", Proceedings of 4th Symposium on the Engineering Aspects of MHD, pp. 73 - 92; Berkeley, California, 1963.

17. Westinghouse Research Laboratories, "Long Life Closed Loop MHD Research and Development Unit", Interim Scientific Report No. 3, Contract AF 33(657)-8311; December 15, 1962.

18. McFee, R., "Optimum Input Leads for Cryogenic Apparatus", Rev. Sci. Inst., 30, No. 2, 98, (1959)

19. Kothmann, R. E., and Stewart, W. A., "Vapor Cooled Input Leads in Cryogenic Systems", Westinghouse Research Report d62-118-283-R3, (1962).

20. Smith, R. J., "Thermal Analysis of a Superconducting Generator", ASD Technical Documentary Report No. ASD-TDR-62-811, (1962).

21. Sobol, H., and McNichol, J. J., "Evaporation of Helium I Due to Current-Carrying Leads", Rev. Sci. Inst., 33, No. 4, (1962).

22. Tsu, T. C., "Optimum Electrical Connection Between a Normal Conductor and a Superconductor", Westinghouse Research Memo 318-W000-M7, (1961).

23. Ince, E. L., "Ordinary Differential Equations", Dover Publications, Inc., p. 335, (1956).

APPENDIX B

Table of Symbols - Equations 1 through 78

A	Cross-sectional area of duct
B	Magnetic flux density
B_o	Magnetic flux density in central region of duct
C_p	Constant pressure specific heat
e	Electronic charge (1.6×10^{-19} coul)
E	Applied electric field
E'	Electric field relative to gas
f	Frictional coefficient
F	Force acting on an ion, equation 61
H	Convective heat transfer rate
j	Current density
k	Boltzman's constant (1.38×10^{-23} joule/^{o}K)
K	Loading parameter, equation 9
l	Constant, equation 41
m	Constant, equation 29
M	Mach number
M	Constant in equations 74 - 77 only
n	Number density of particles
n	Constant, equation 28 - 30 only
N	Drag at wall, equation 5
N	Constant in equations 74 - 77 only
p	Static pressure
P_{w_1}	Convective power (inlet) per unit area, equation 20
q	Constant, equation 40
Rey	Reynolds number, based on duct width
/A	Hydraulic diameter
s	Duct perimeter

t	Temperature ratio, equation 13
T	Static temperature
T_{o_1}	Total or stagnation temperature (inlet)
u	Velocity
v	Ion drift velocity
w	Constant, equation 25
x_o	Constant, equation 19
x	Distance along axis
y	Variable f(t), equation 38
α	Frictional parameter, equation 11
α'	Magnetic field parameter
β	Constant, equation 14
β_e	Product ($\mu_e B$)
β_i	Product ($\mu_i B$)
γ	Ratio of specific heats
ϵ	Seeding ratio (moles cesium/moles lithium)
η	Ratio of electrical power to total inlet enthalpy, equation 49
η'	Constant, equation 8
η_s	Isentropic or turbine efficiency, equation 44
μ	Viscosity
μ_e	Electron mobility
μ_i	Ion mobility
ξ	Constant, equation 34
ρ	Density
σ	Scalar electronic conductivity
σ_e	Electronic conductivity

σ_i	Ionic conductivity
τ	Constant, equation 27
ϕ	Constant, after equation 39
ψ	Constant, equation 35

Superscripts

—	Designates vector quantities

Subscripts

e	Electron
i	Ion
x	Coordinate, axial direction of flow
y	Coordinate, direction of applied electric field
z	Coordinate, direction of applied magnetic field
1	Specifies inlet conditions
2	Specified outlet conditions

Exponents

y	Conductivity variation with temperature, equation 22
z	Conductivity variation with pressure, equation 23

APPENDIX C

Table of Symbols - Equations 79 through 185

A	Cross section area of lead, conduction path or radiation path
C_p	Specific heat of vapor
D	Cooling parameter for lead with constant resistivity, $= \phi^* / kA$.
d	Cooling parameter for lead with variable resistivity, $= \phi^*/2\,kA$.
F	Integrand of equation 2.
f	Parameter, $= Q_o / T_o \dot{m} C_p = Q_o / \phi^* T_o$.
f_1, f_2	Functions of T
g	Parameter defined after equation 22
h_{fg}	Specific enthalpy change during vaporization
i	Electrical current
j	Exponent of variation of ϵ with T
k	Thermal conductivity
l	Length of conductor or conduction path
l_o, l_1	Lengths of cold and warm parts of two-stage cooled conduction path
m	Exponent of variation of η with T
$\dot{m}$	Mass flow rate of vapor
N	Number of radiation shields
n	Exponent of variation of k with T
p	Parameter, $\sqrt{(2\gamma / d^2) - 1}$, or else difference n - m
Q	Heat flux
r	Ratio of absolute temperatures, T_a / T_o.
S	Ratio of absolute temperatures, T_a / T_1.
T	Absolute temperature
W	Rate of refrigeration work
x	Length coordinate of lead or conduction path measured from the cold end

α, β	Parameters
γ	Parameter, $= i^2 \rho_a / 2(kA)AT_a$.
ϵ	Emissivity
η	Ratio of actual COP to Carnot COP in refrigeration system
Θ	Dimensionless absolute temperature, T/T_a
λ	Lagrange multiplier or else ratio, I_1 / I_o
ρ	Electrical resistivity
σ	Stefan-Boltzmann constant
ϕ	Rate of heat removed per unit length at x and T
ϕ^*	Rate of heat removed per unit temperature change along lead or conduction path at x and T

Subscripts

a	Ambient or condition at which heat is rejected
o	Condition at lowest temperature in the system
opt.	Optimum value or condition
1.	Condition at intermediate cooling temperature

APPENDIX D

Curves and Diagrams

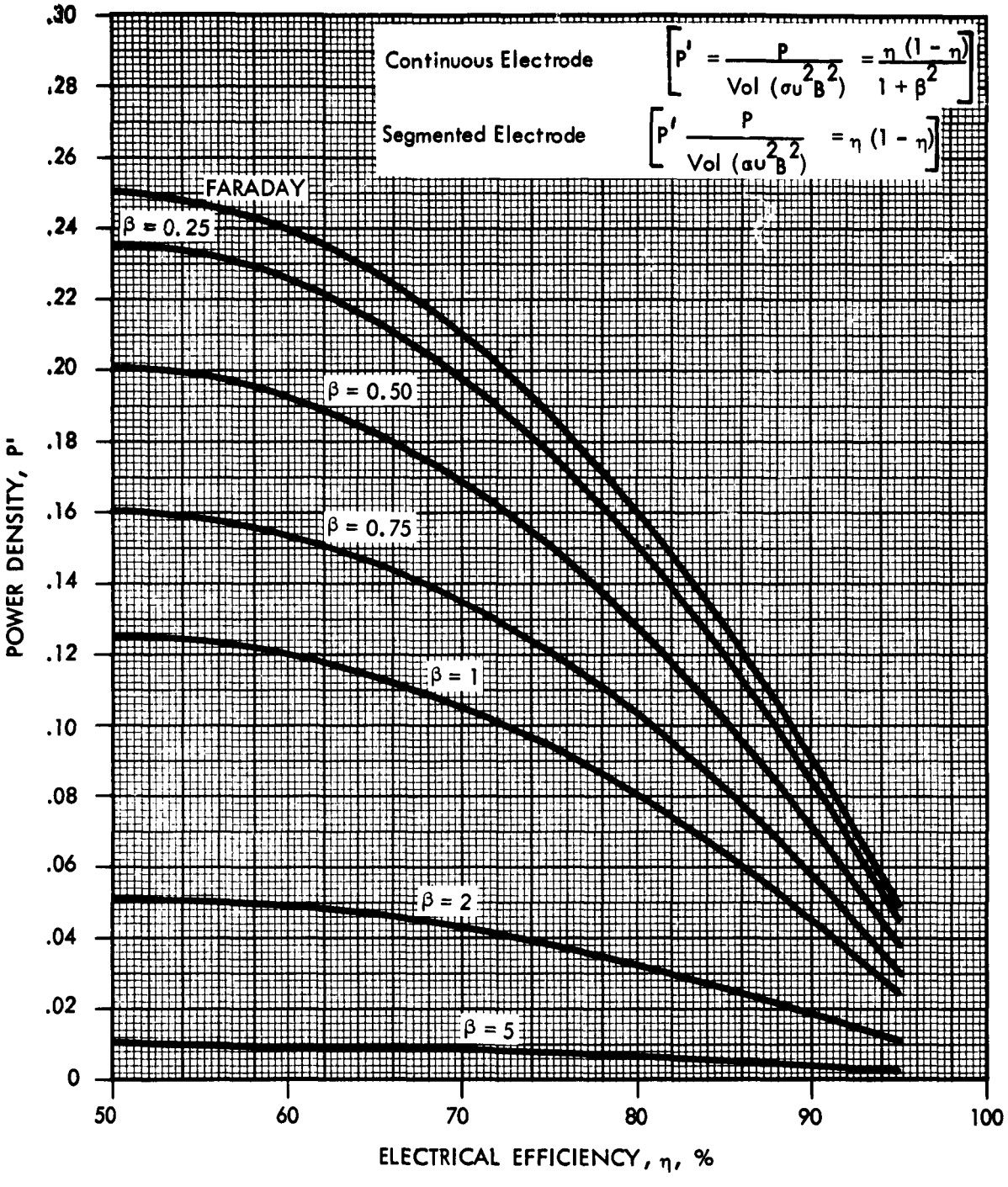

DIMENSIONLESS POWER DENSITY CURVES FOR SEGEMENTED AND CONTINUOUS ELECTRODE FARADAY MHD GENERATOR

FIGURE 1

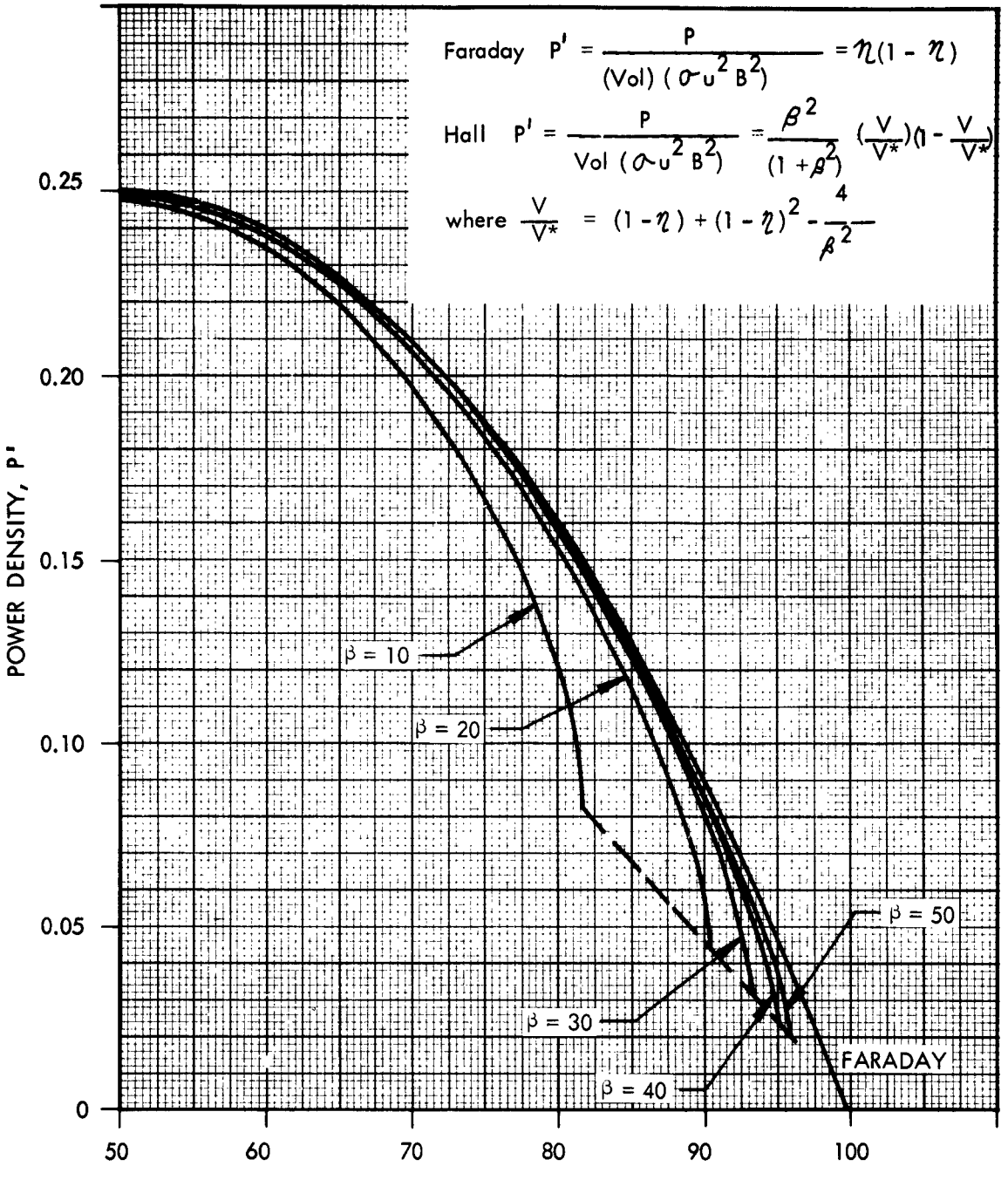

DIMENSIONLESS POWER DENSITY CURVES FOR SEGMENTED FARADAY AND HALL MHD GENERATORS

FIGURE 2

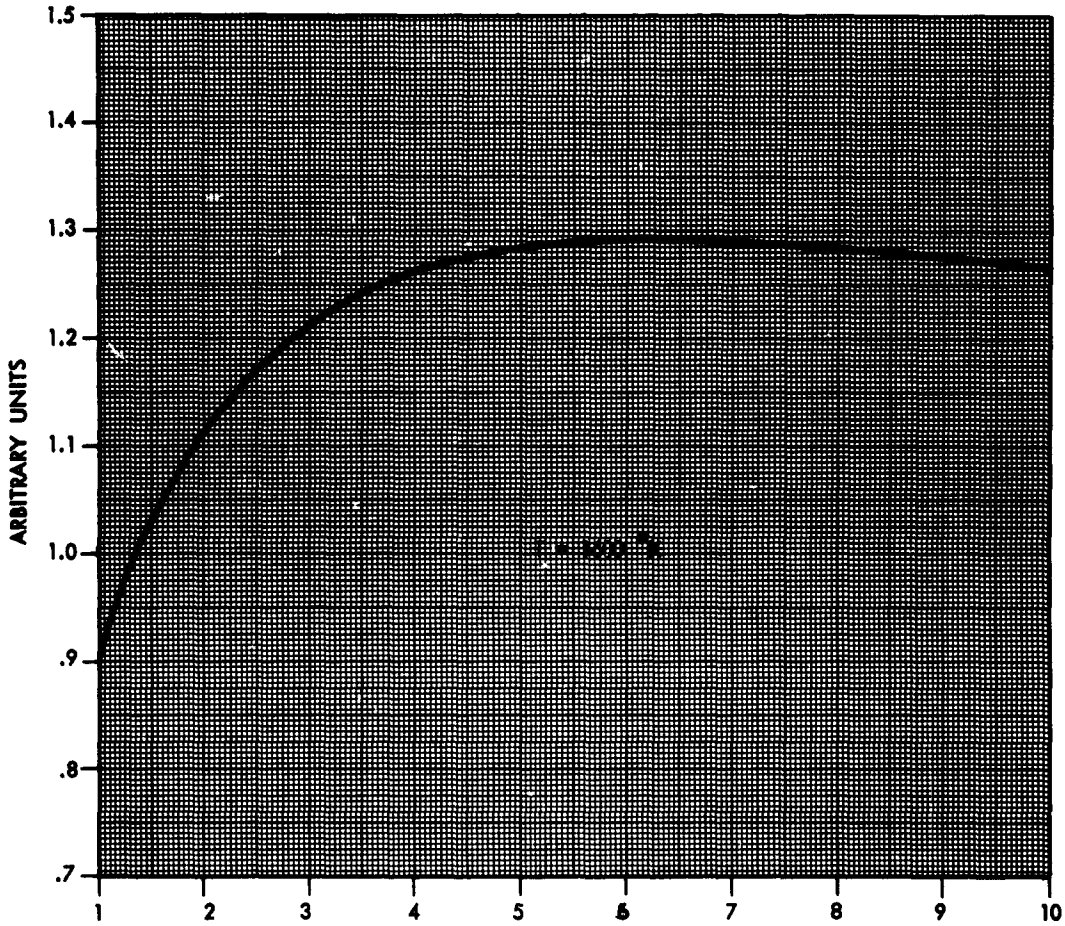

OPTIUM SEEDING RATIO

FIGURE 3

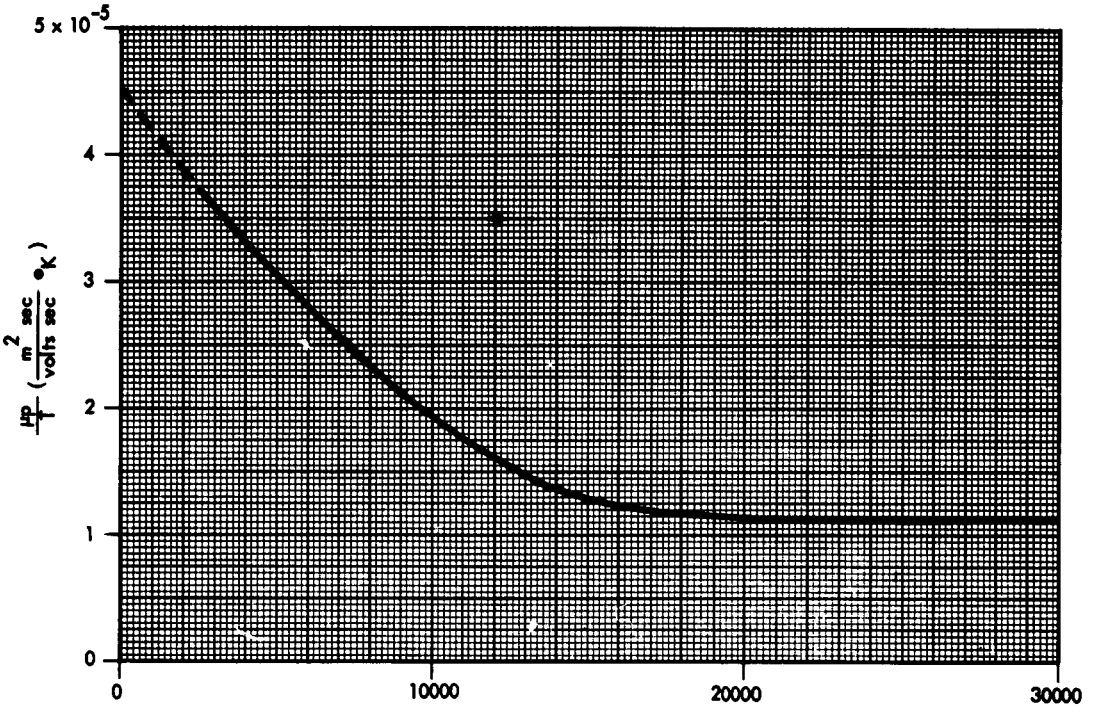

ELECTRON MOBILITY IN LITHIUM VAPOR

FIGURE 4

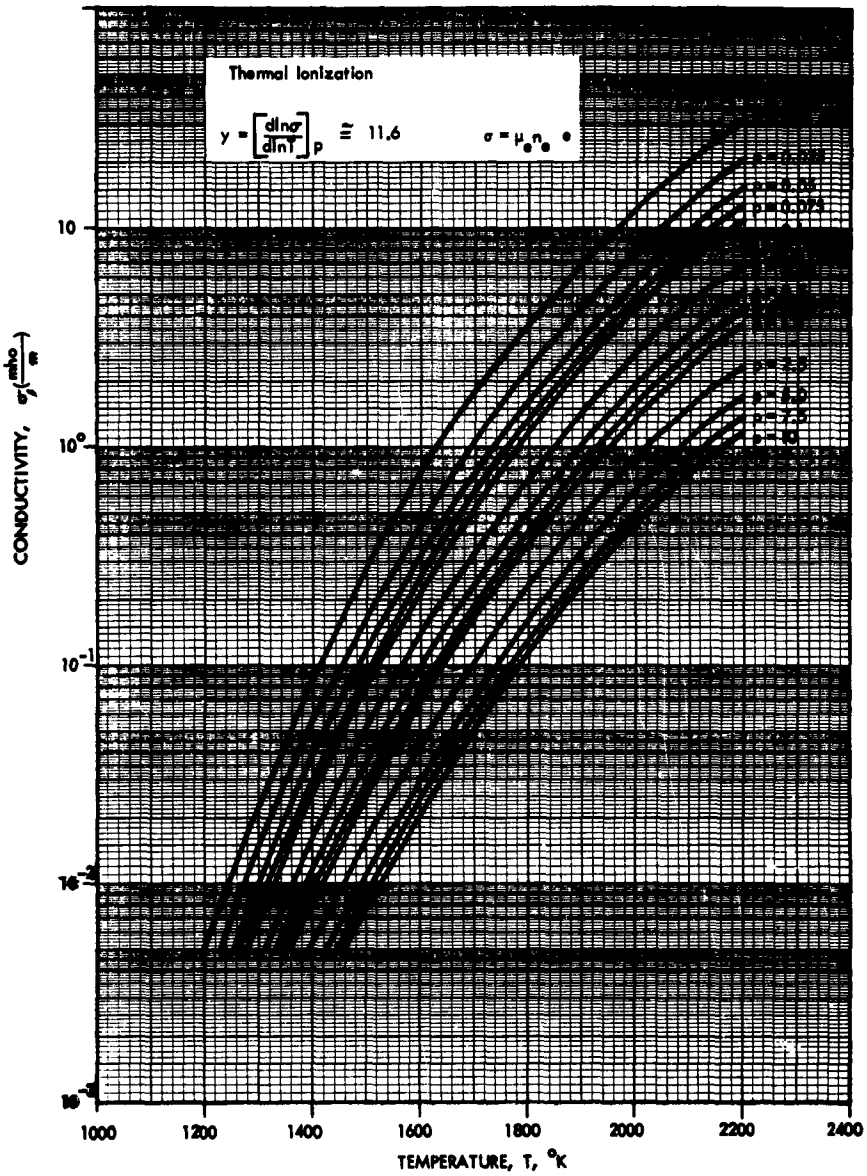

CONDUCTIVITY OF LITHIUM +0,07 CESIUM

FIGURE 5

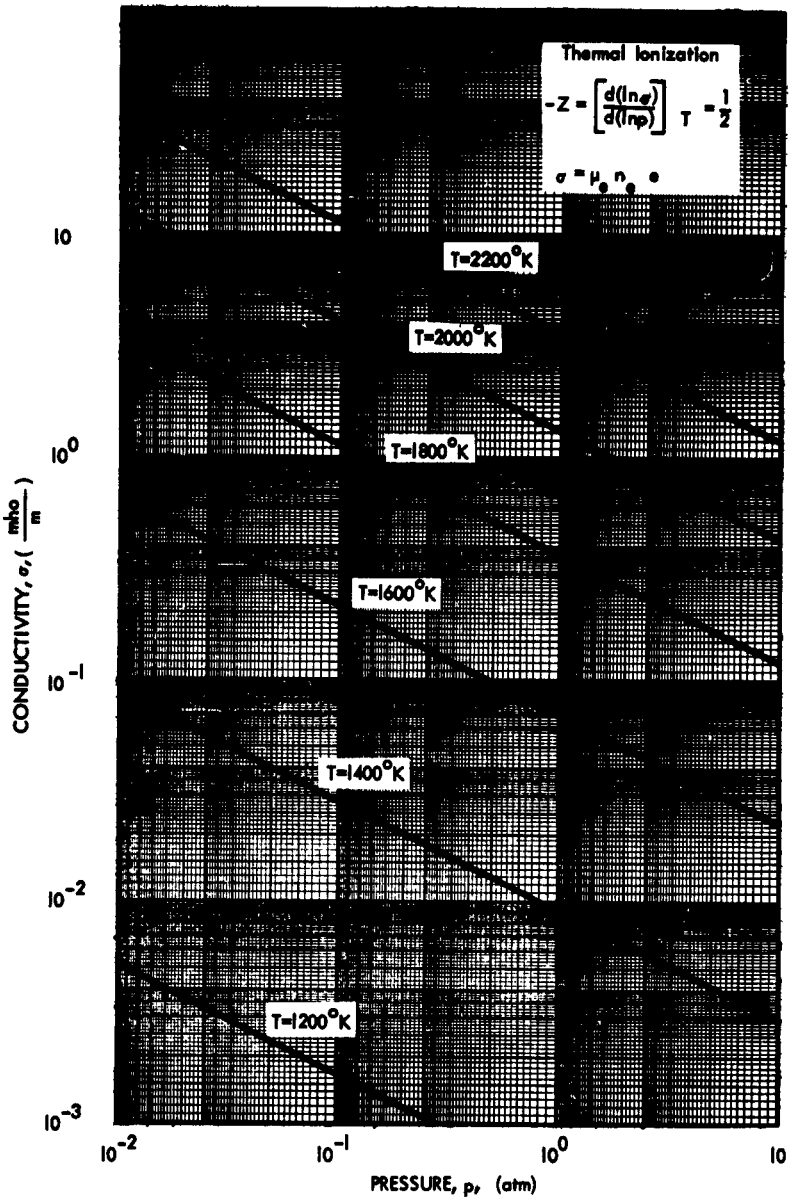

CONDUCTIVITY OF LITHIUM + 0.07 CESIUM

FIGURE 6

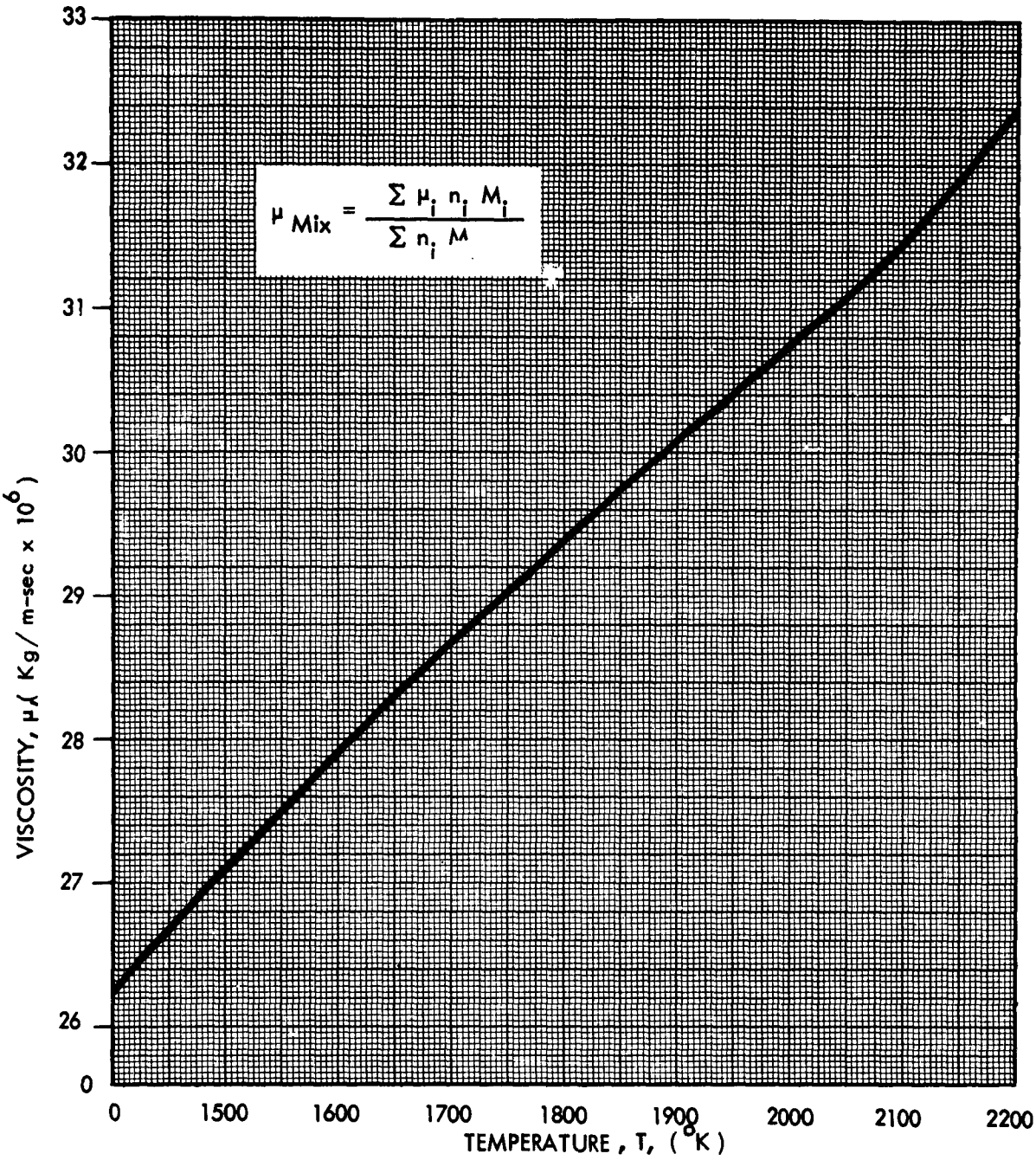

VISCOSITY OF LITHIUM +0.07 CESIUM

FIGURE 7

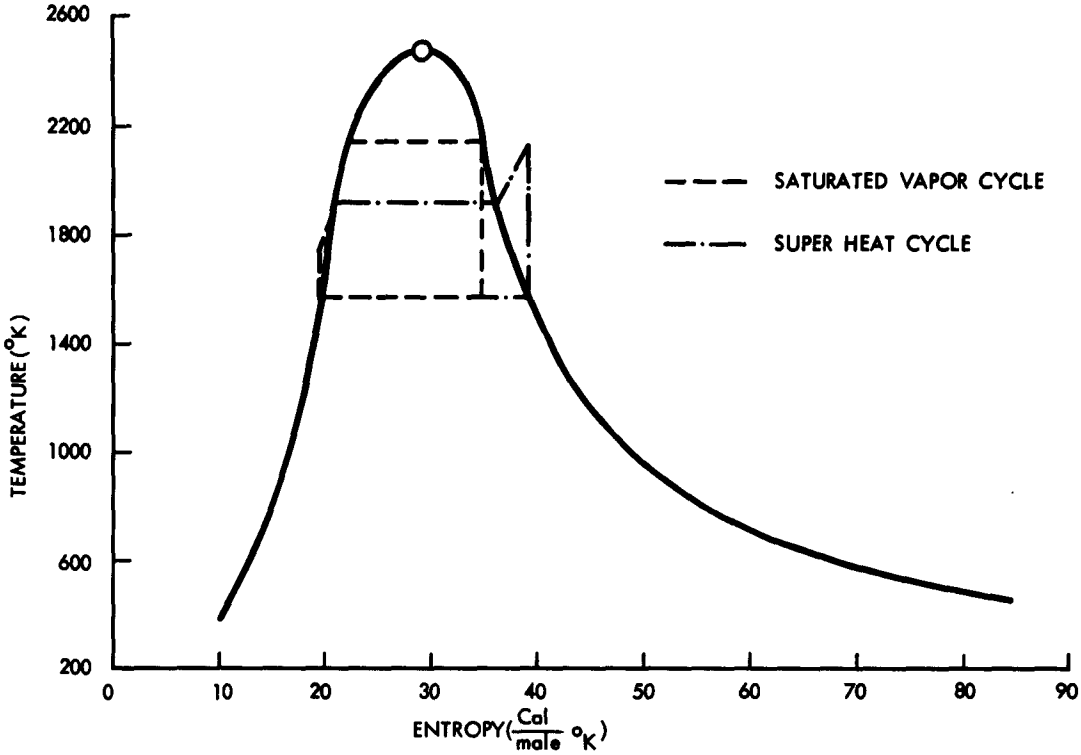

COMPARISON OF GENERATOR CYCLES FOR LITHIUM

FIGURE 8

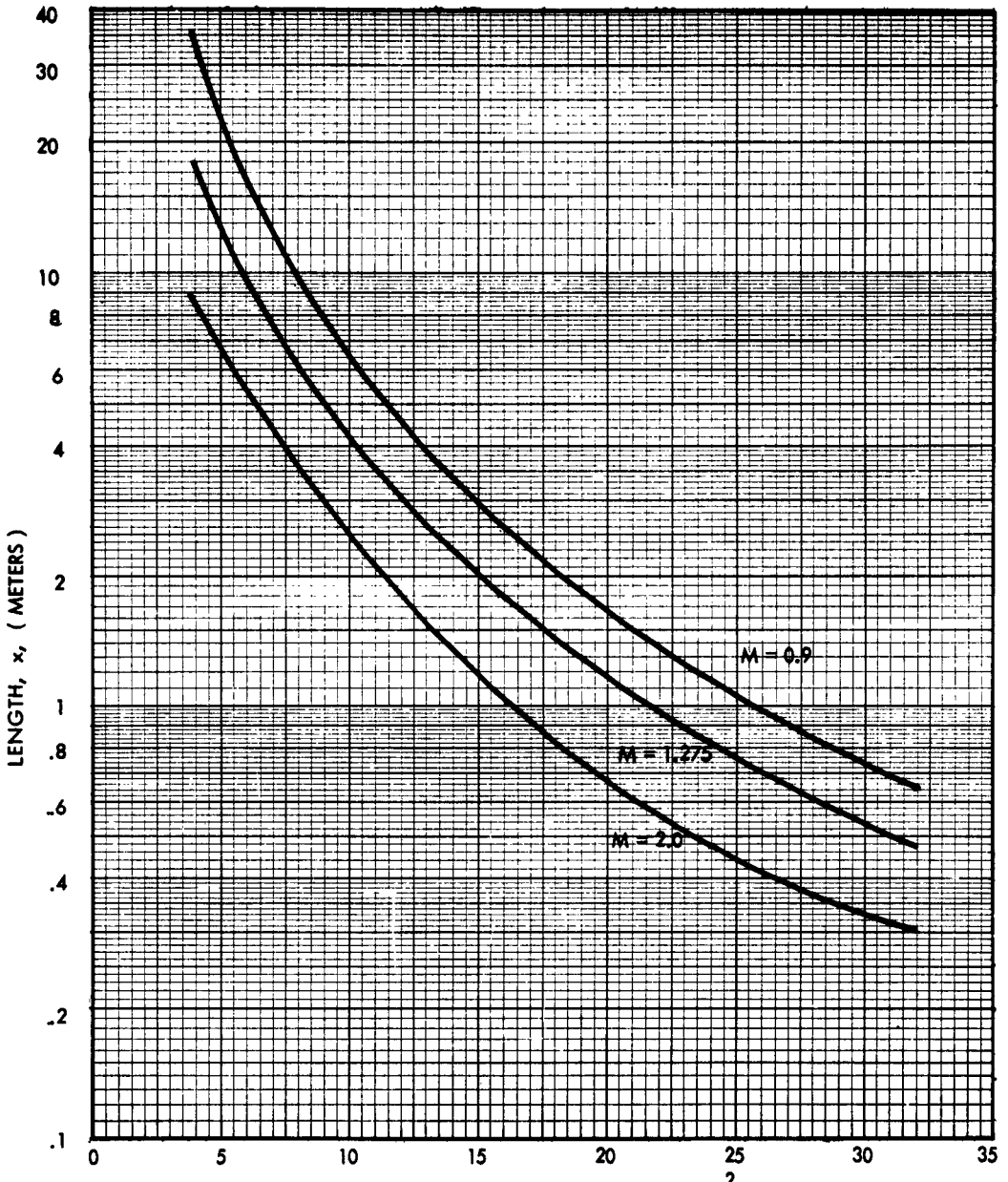

MHD GENERATOR LENGTH
FOR LITHIUM -0.07 CESIUM PLASMA

FIGURE 9

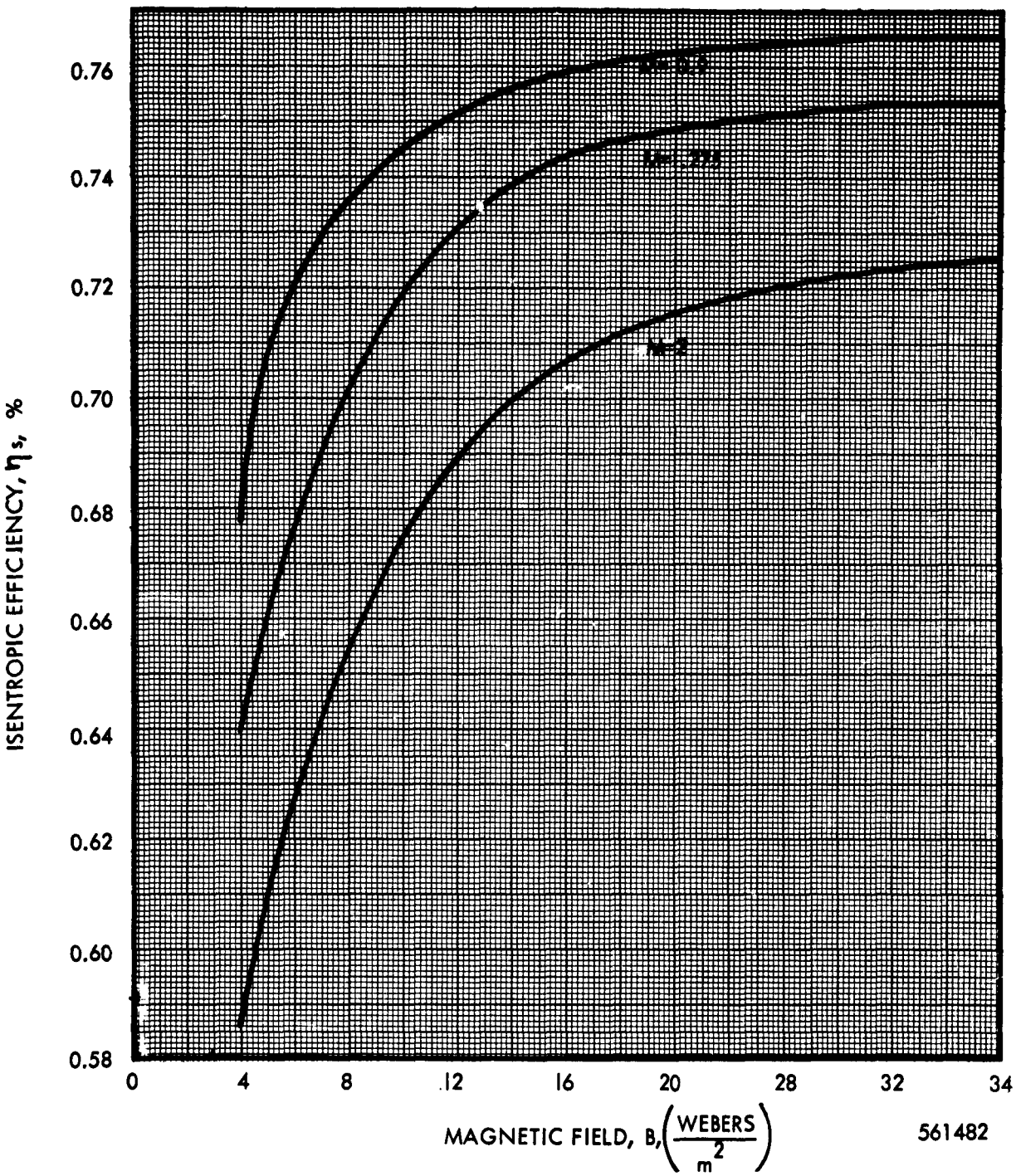

MHD GENERATOR ISENTROPIC EFFICIENCY
FOR LITHIUM - 0.07 CESIUM PLASMA

FIGURE 10

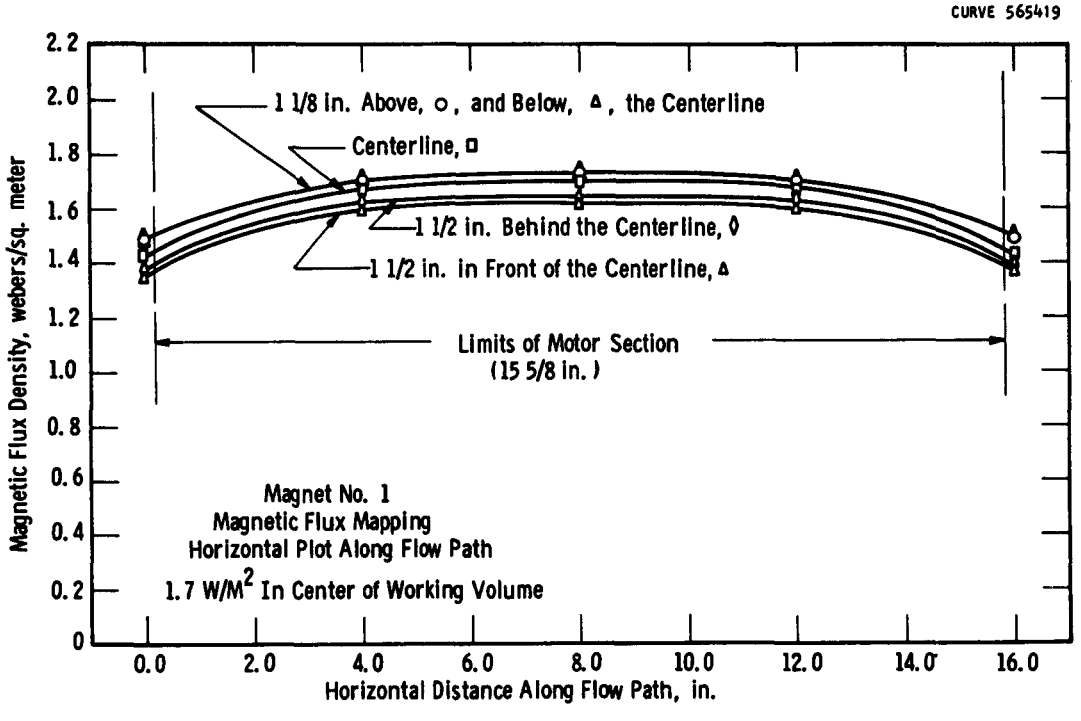
CURVE 565419
Magnetic Flux Density, webers/sq. meter
2.2
2.0
1.8
1.6
1.4
1.2
1.0
0.8
0.6
0.4
0.2
0
1 1/8 in. Above, o, and Below, Δ, the Centerline
Centerline, □
1 1/2 in. Behind the Centerline, ◊
1 1/2 in. in Front of the Centerline, Δ
Limits of Motor Section
(15 5/8 in.)
Magnet No. 1
Magnetic Flux Mapping
Horizontal Plot Along Flow Path
1.7 W/M2 In Center of Working Volume
0.0
2.0
4.0
6.0
8.0
10.0
12.0
14.0
16.0
Horizontal Distance Along Flow Path, in.

FIGURE 11

CURVE 565421

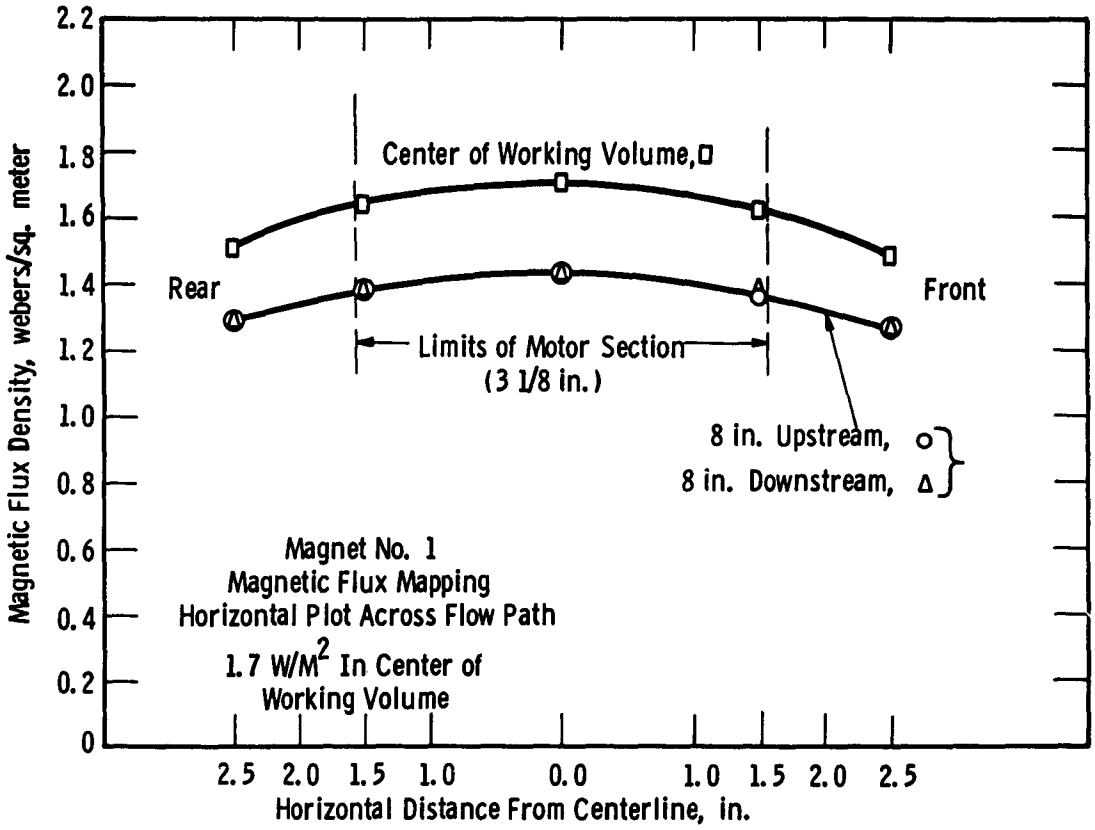

FIGURE 12

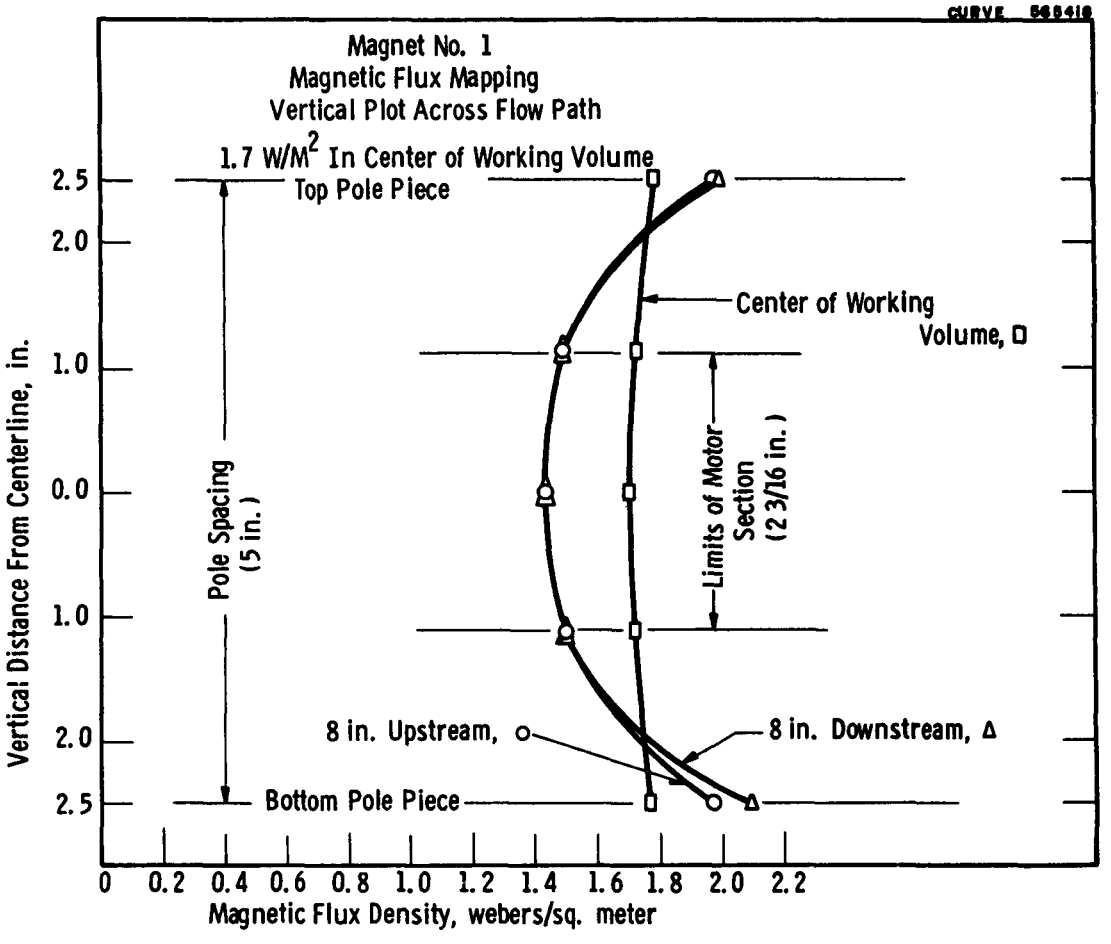
CURVE 868418
Magnet No. 1
Magnetic Flux Mapping
Vertical Plot Across Flow Path
1.7 W/M2 In Center of Working Volume
Top Pole Piece
Center of Working Volume, □
Pole Spacing (5 in.)
Limits of Motor Section (2 3/16 in.)
8 in. Upstream, ○
8 in. Downstream, Δ
Bottom Pole Piece
Vertical Distance From Centerline, in.
2.5
2.0
1.0
0.0
1.0
2.0
2.5
0 0.2 0.4 0.6 0.8 1.0 1.2 1.4 1.6 1.8 2.0 2.2
Magnetic Flux Density, webers/sq. meter

FIGURE 13

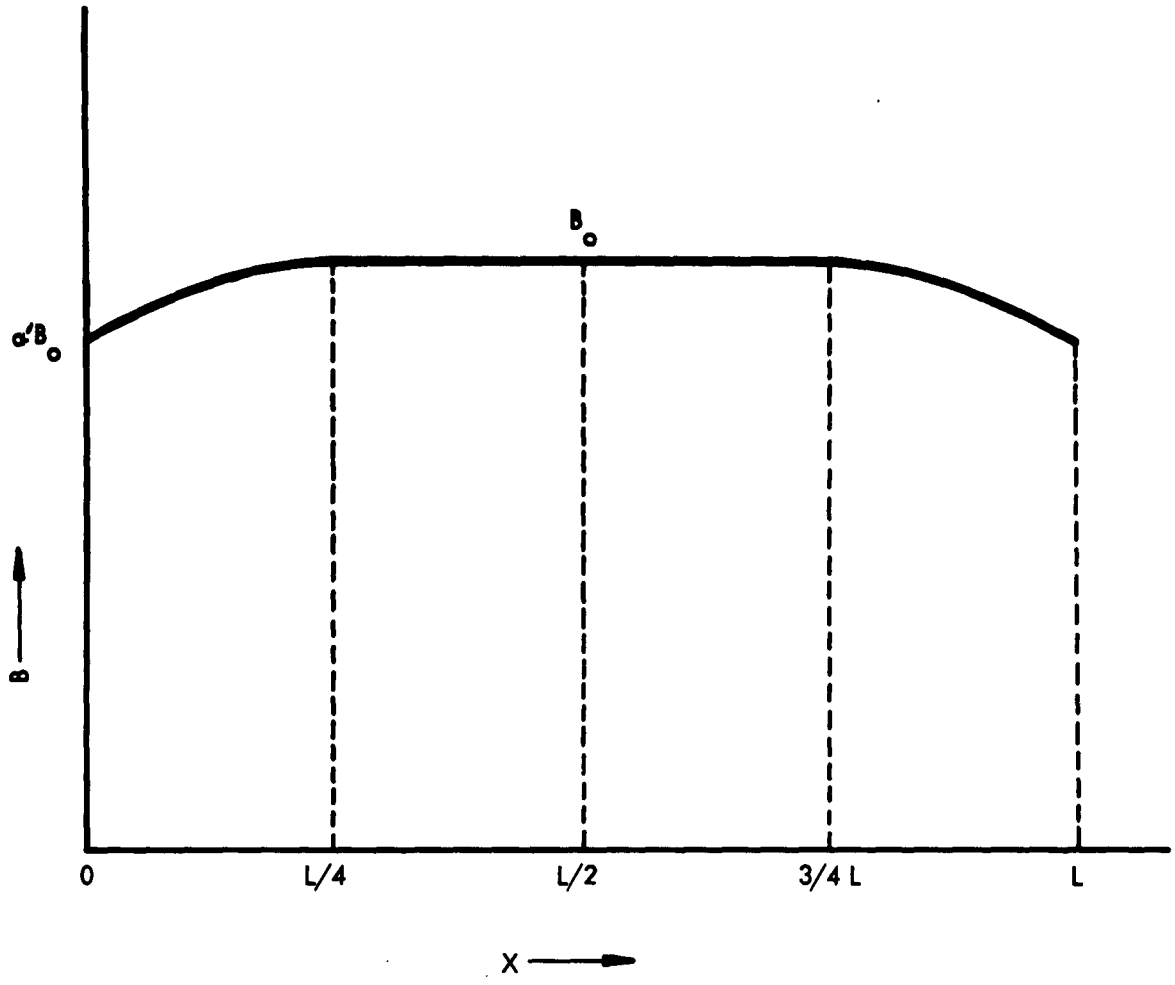

MODEL OF FLUX DENSITY (B) VARIATION WITH DUCT LENGTH (X)

FIGURE 14

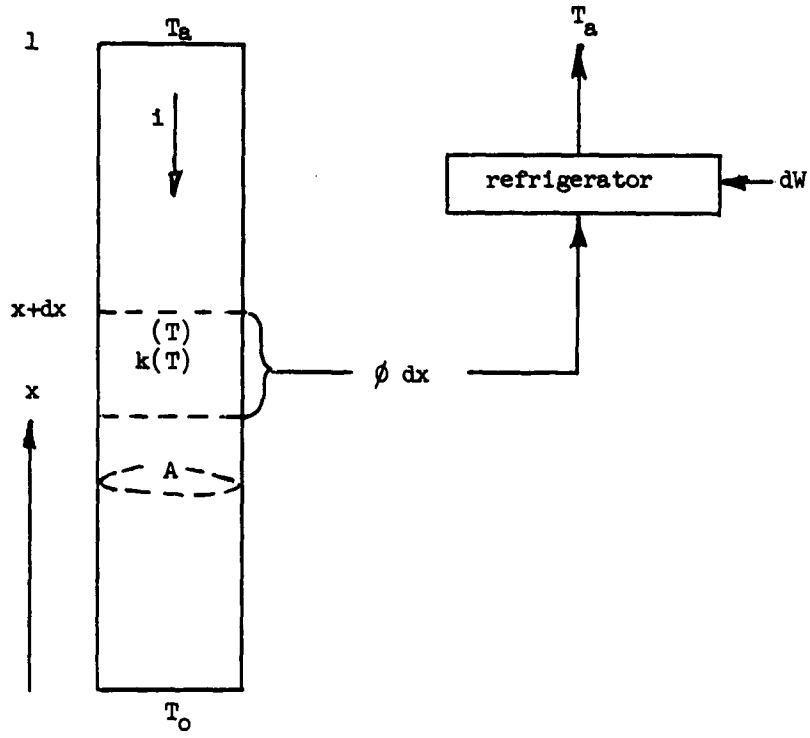

Fig. 15. Cryogenic electrical lead with optimum cooling

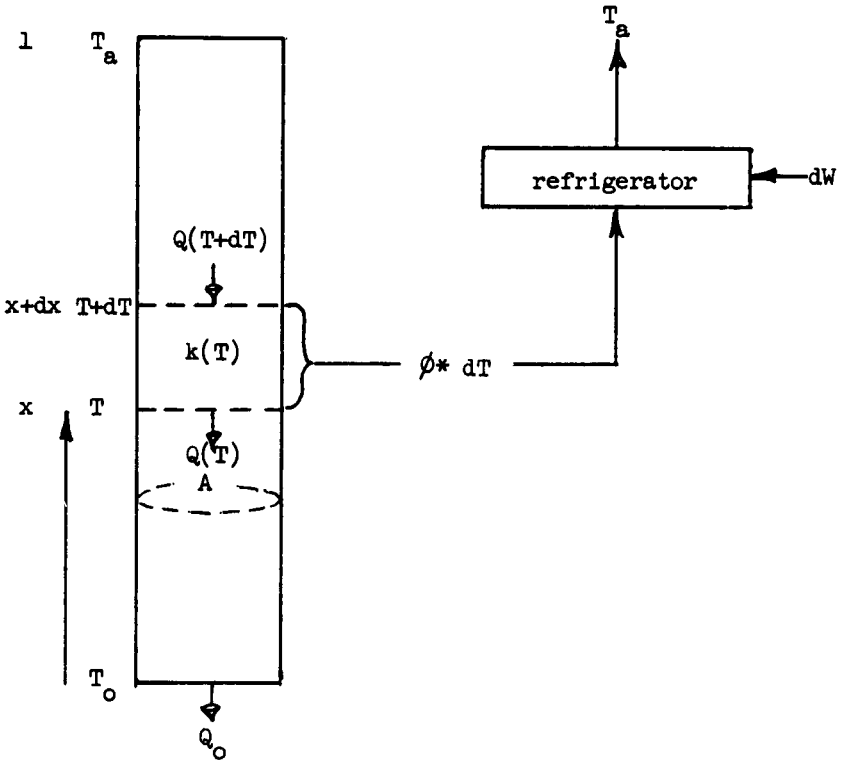

Fig. 16. Cryogenic conduction path with optimum cooling

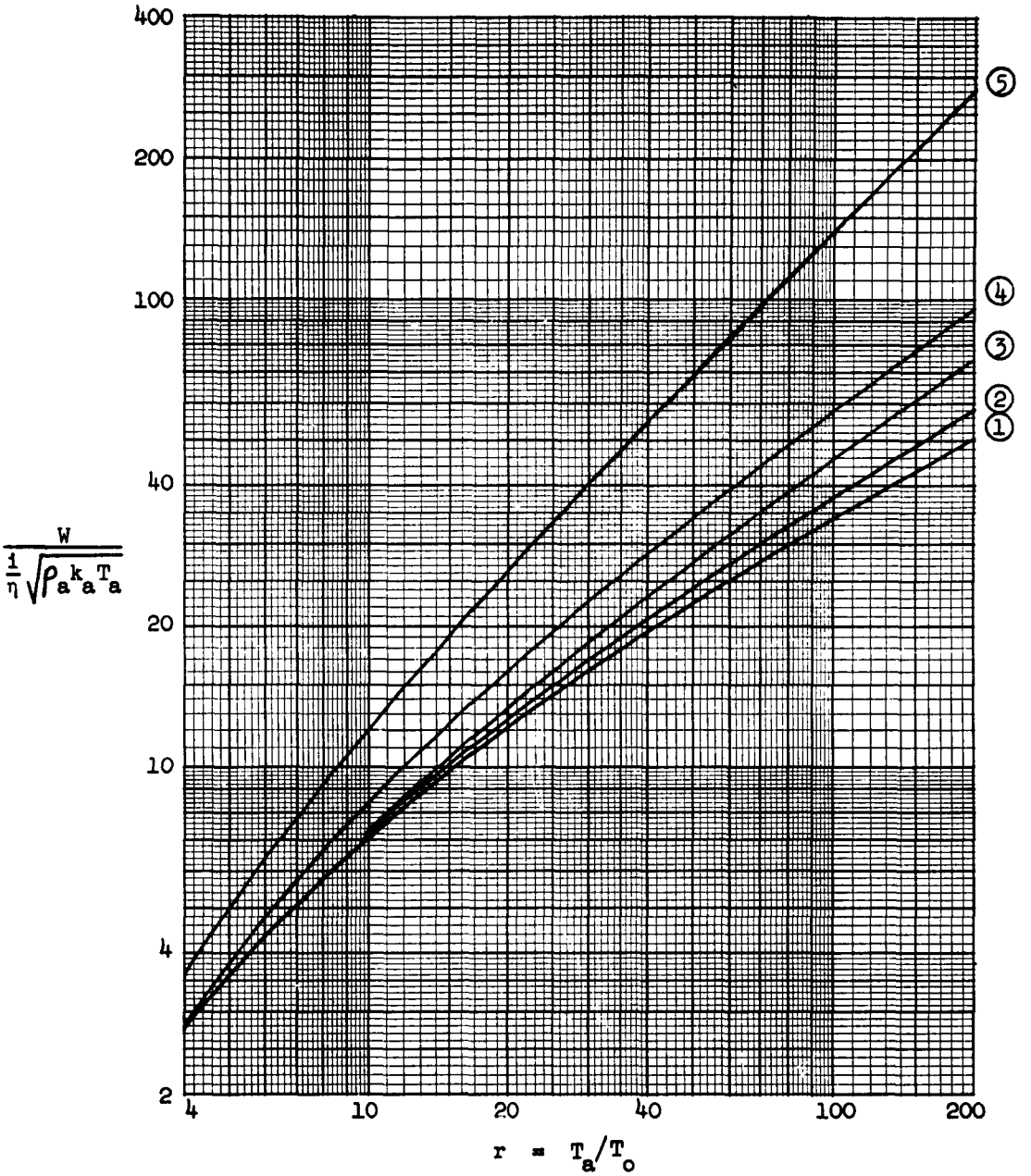

Fig. 17. Refrigeration work, W, for cooling a cryogenic electrical lead with resistivity constant resistivity, ρ, and η and k

1. optimum cooling
2. vapor cooling, $f = f_{optimum}$
3. vapor cooling, $f = 1$
4. vapor cooling, $f = 0.5$
5. cooling only at T_o

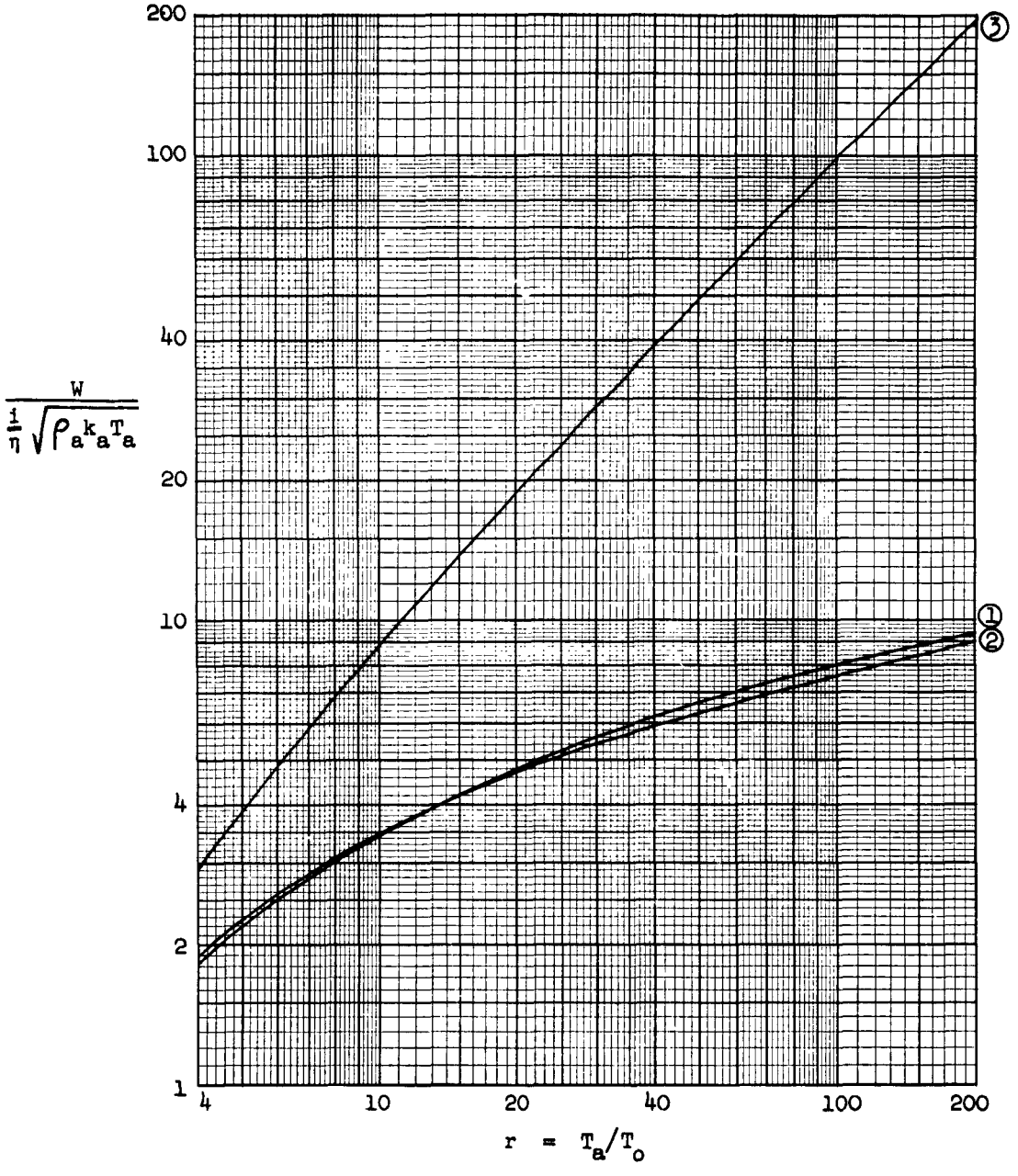

Fig. 18. Refrigeration work, W, for cooling a cryogenic electrical lead with resistivity $\rho = \rho_a(T/T_a)$, and η and k constant

1. optimum cooling
2. vapor cooling, f = 1
3. cooling only at T_o

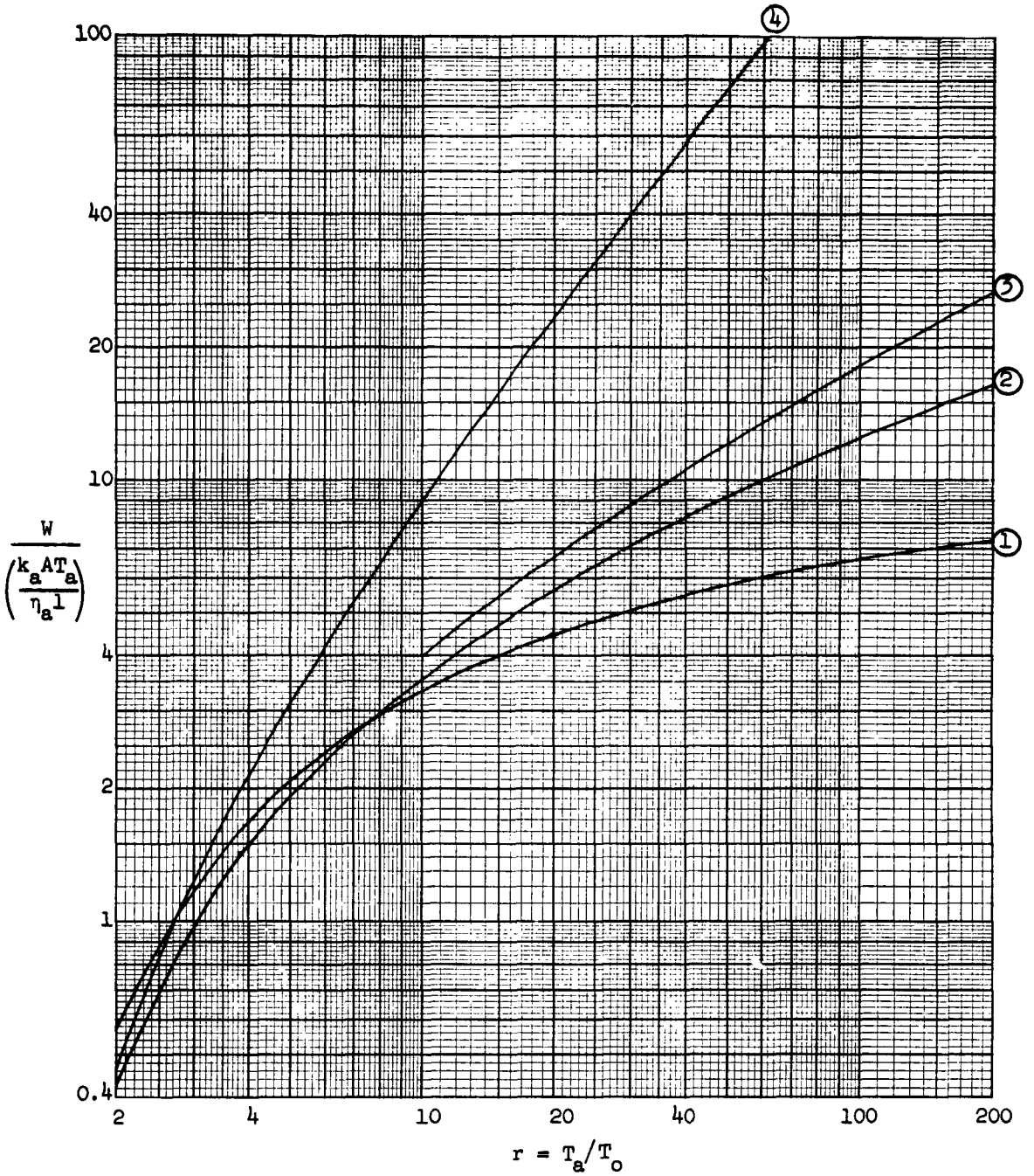

Fig. 19. Refrigeration work, W, for cooling a cryogenic conduction path with conductivity, $k = k_a(T/T_a)$ and ratio of refrigerator COP to Carnot COP, $\eta = \eta_a(T/T_a)^{0.3}$.

1. optimum cooling
2. vapor cooling, f = 1
3. optimum two stage cooling
4. cooling only at T_o

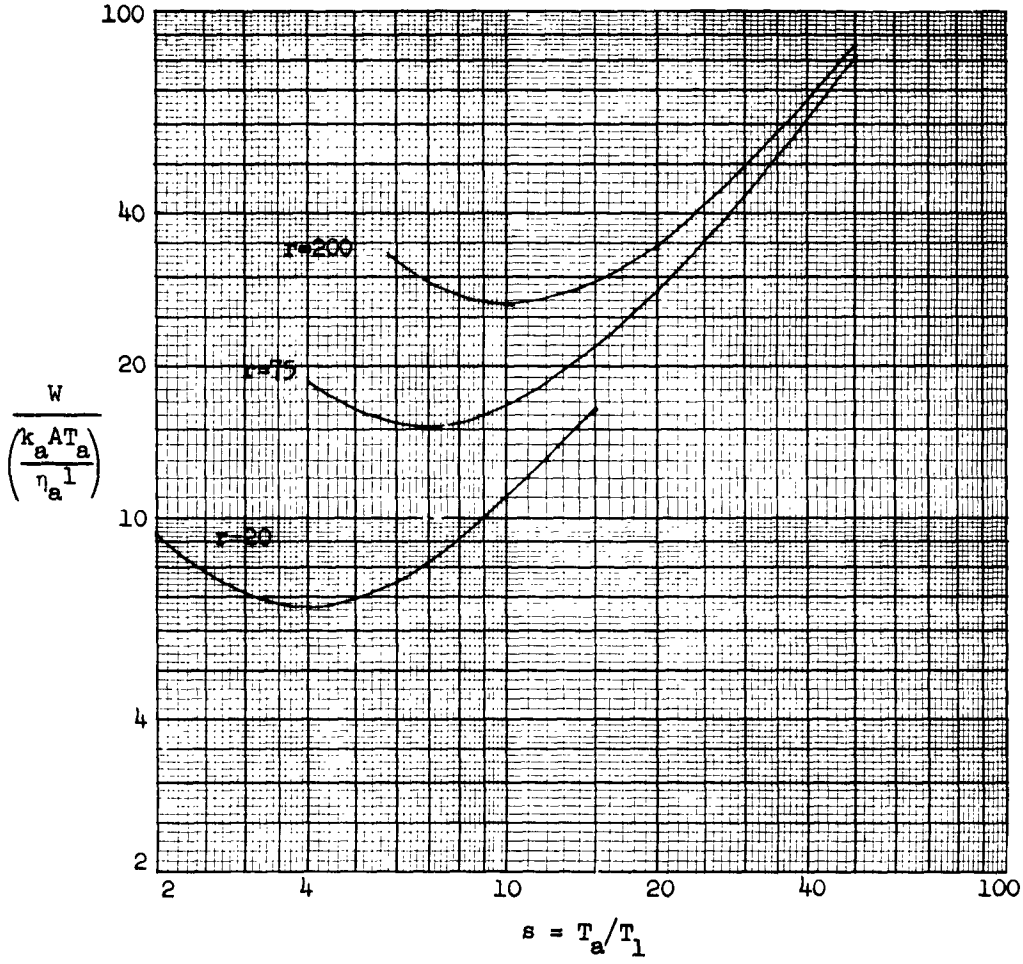

Fig. 20. Refrigeration work, W, for two stage cooling at T_l and T_o with conductivity, $k = k_a(T/T_a)$ and ratio of refrigerator COP to Carnot COP, $\eta = \eta_a(T/T_a)^{0.3}$, showing variations with s.

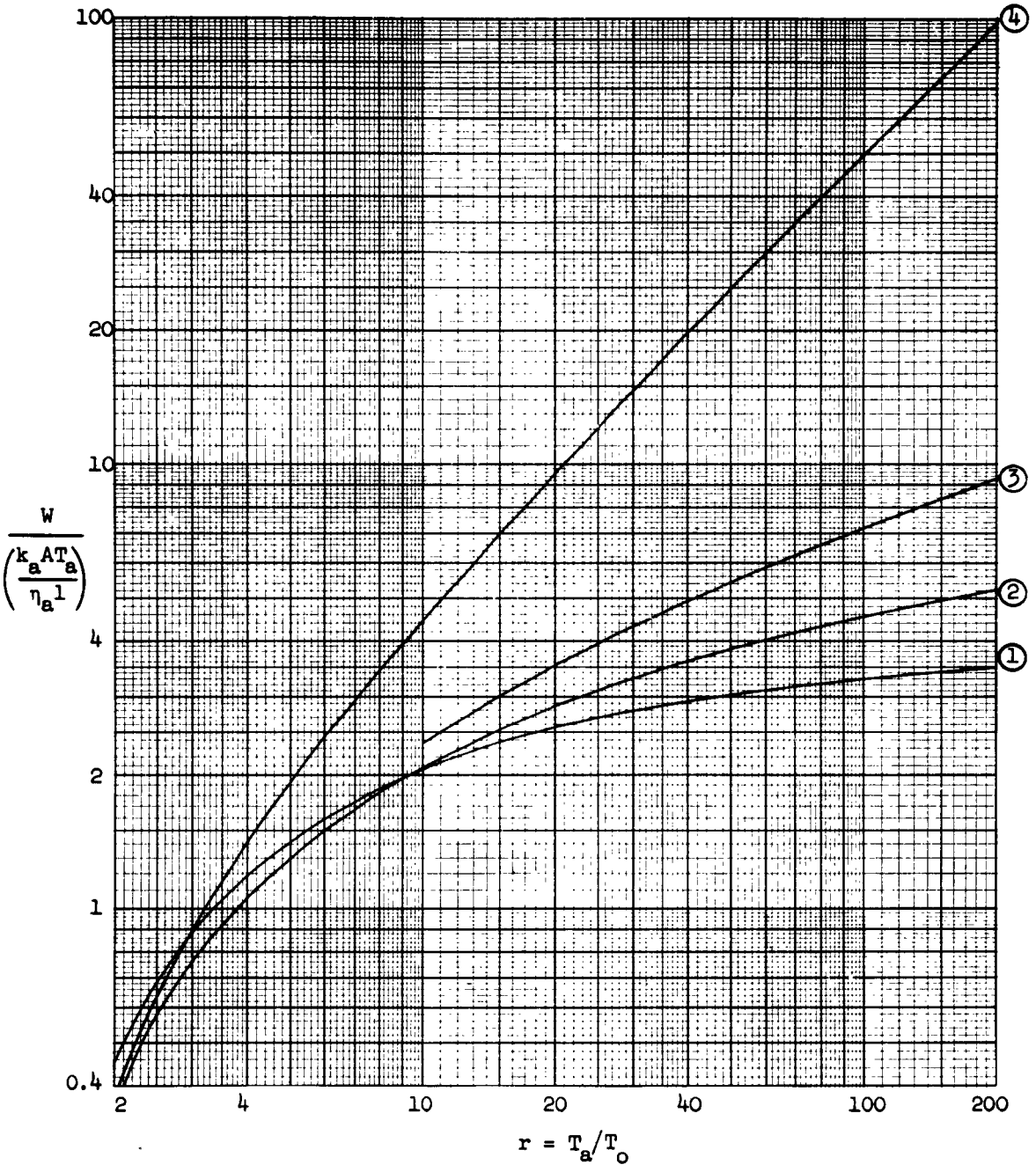

Fig. 21. Refrigeration work, W, for cooling a cryogenic conduction path with conductivity, $k = k_a(T/T_a)$ and constant η.

1. optimum cooling
2. vapor cooling, f= 1
3. optimum two stage cooling
4. cooling only at T_o

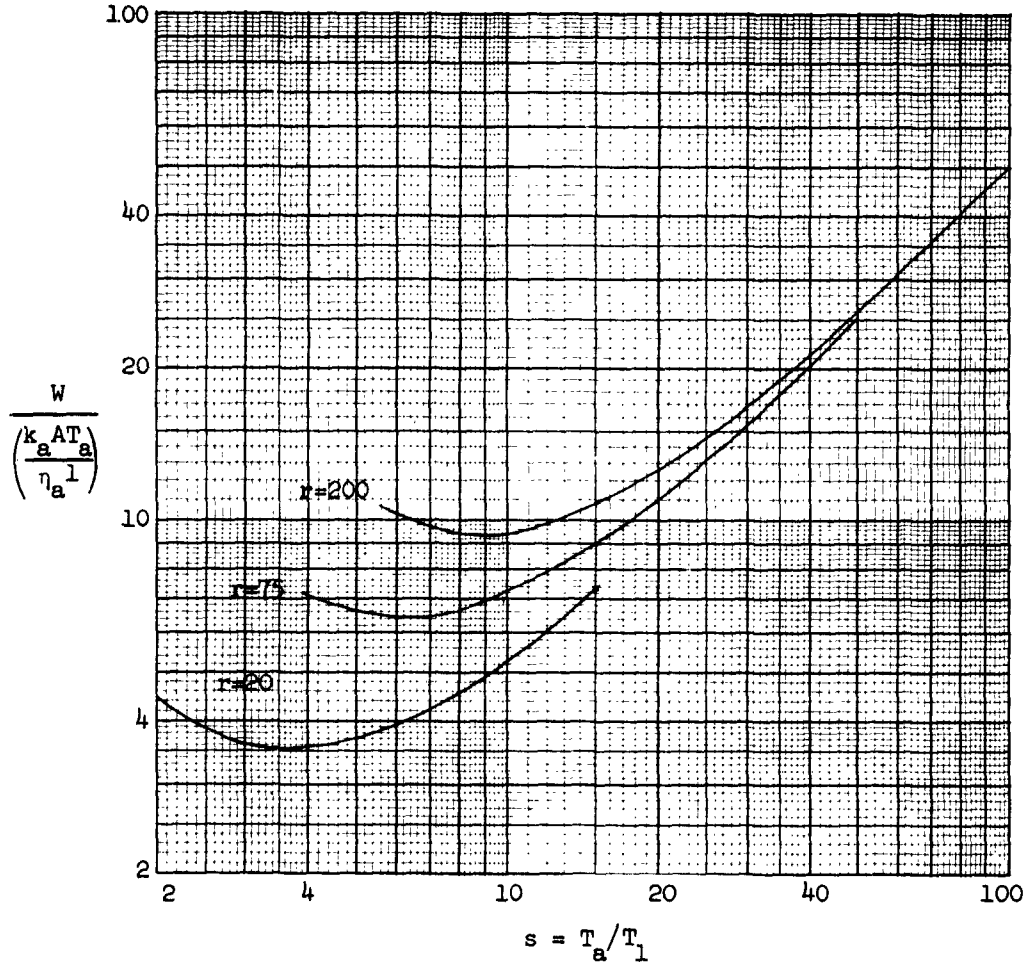

Fig. 22. Refrigeration work, W, for two stage cooling at T_1 and T_o, with conductivity, $k = k_a(T/T_a)$ and constant η, showing variations with s.

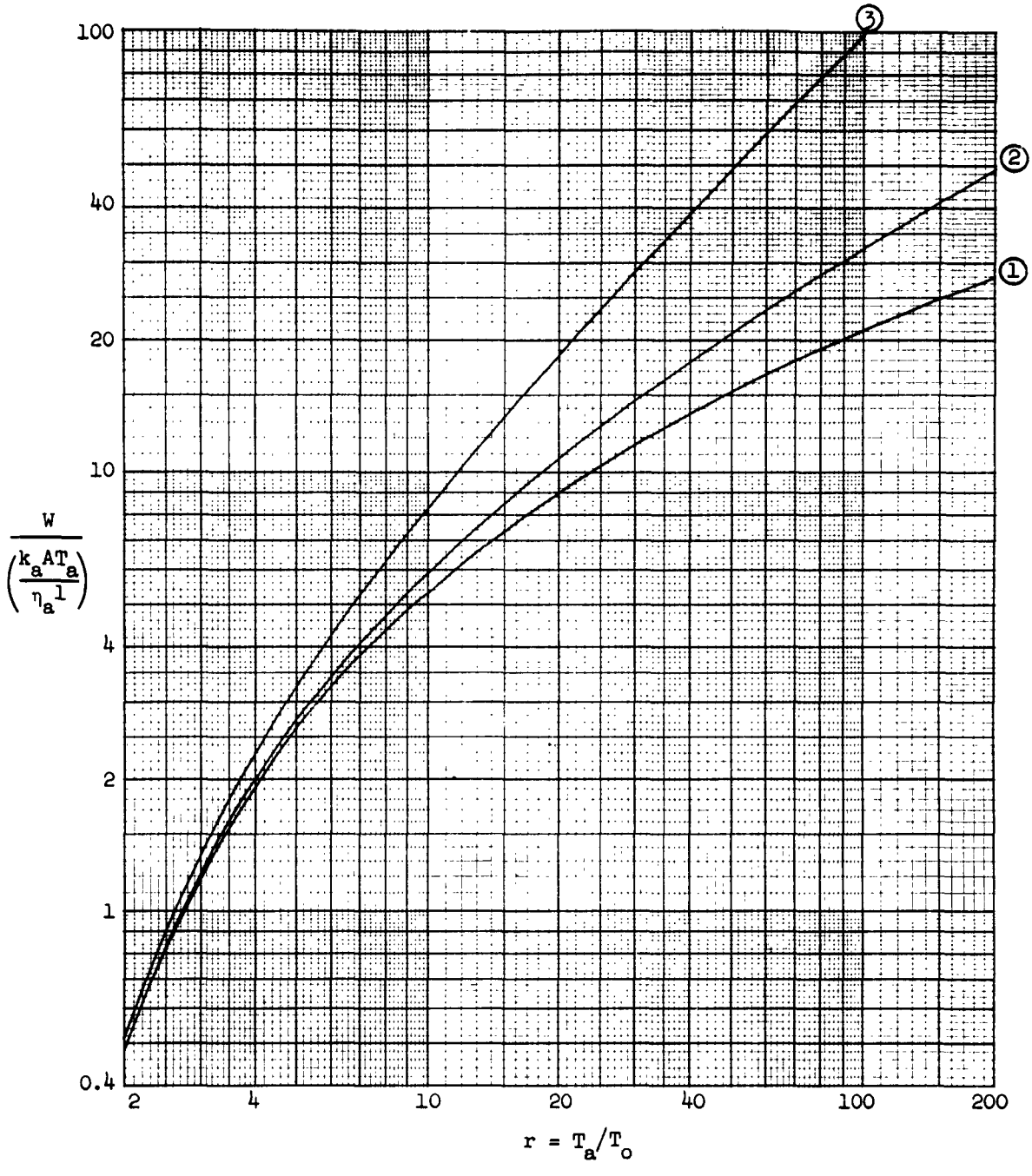

Fig. 23. Refrigeration work, W, for cooling a cryogenic conduction path with conductivity, k, and η constant.

1. optimum cooling (also vapor cooling, $f = f_{optimum} = 1$)
2. optimum two stage cooling
3. cooling at T_o only

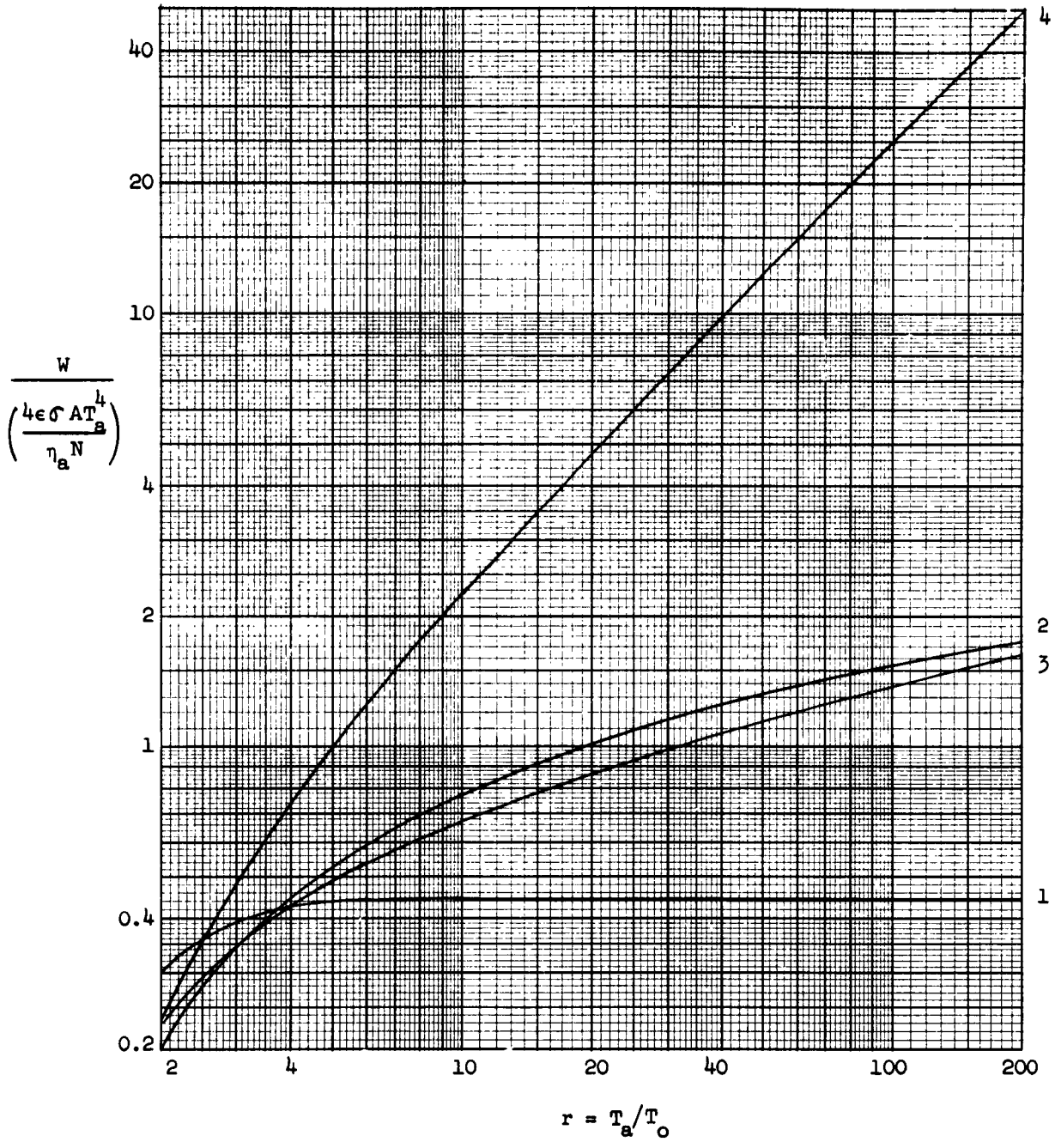

Fig. 24. Refrigeration work, W, for cooling a multiply shielded (N shields) cryogenic radiation path with constant emissivity, ϵ, and constant η.

1. optimum cooling
2. vapor cooling, f = 1
3. optimum two stage cooling
4. cooling only at T_o

APPENDIX E

DESIGN AND CONSTRUCTION OF A LARGE SUPERCONDUCTING MAGNET FOR MAGNETOHYDRODYNAMIC POWER AND PROPULSION IN SPACE

By

W. A. Stewart
D. T. Beecher
R. E. Kothmann
H. W. Szymanowski

Presented at

AIAA ELECTRIC PROPULSION CONFERENCE
Broadmoor Hotel, Colorado Springs, Colorado
March 11 - 13, 1963

APPENDIX F

Copies	
1	ASAPT Aeronautical Systems Division Wright Patterson AFB, Ohio
1	ASAPR Aeronautical Systems Division Wright Patterson AFB, Ohio
5	ASRPP-2 Aeronautical Systems Division Wright Patterson AFB, Ohio
1	Mr. John A. Satkowski Office of Naval Research Room 2509 Tempo 3 16th and Connecticut Ave. Washington 25, D. C.
1	Dr. H. Powell Jenkins, Jr. Head, Propulsion Applied Research Group (4506) U. S. Naval Ordnance Test Station China Lake, California
1	Mr. B. J. Wilson Naval Research Laboratory Room 322 4th & Chesapeake St., S. W. Washington 25, D. C.
10	ASTIA (TIPDR) Arlington Hall Stn. Arlington 12, Va.
1	SSD (SSTRE), Major W. Iller AF Unit Post Office Los Angeles 45, California
1	AFCRL (CRZAP), Dr. N. Rosenberg L G Hanscom Fld. Bedford, Mass.

Copies	
1	AFOSR (SRHPM) Dr. M. Slawsky Building T-D Washington 25, D. C.
1	Dr. John H. Huth Materials Sciences Office Advanced Research Projects Agency Washington 25, D. C.
1	U. S. Atomic Energy Commission Division of Reactor Development Direct Conversion Branch Washington 25, D. C.
1	NASA Lewis Research Center Library 21000 Brookpark Road Cleveland 35, Ohio
1	Mr. Walter Scott Chief, Space Power Tech Program National Aeronautics & Space Administration Washington 25, D. C.
1	NASA Research Center Electric Propulsion Office Attn: Mr. Albert E. Anglin 21000 Brookpark Road Cleveland 35, Ohio
1	Dr. J. E. McCune Aeronautical Research Associates of Princeton Princeton, New Jersey
1	Mr. T. Brogan AVCO-Everett Research Lab 2385 Revere Beach Parkway Everett, Massachusetts

Copies

1 Dr. J. Cole
Department of Aeronautics
California Institute of Technology
Pasadena, California

1 Westinghouse Electric Corporation
Research and Development
Attn: R. L. Hundstad
Beulah Road, Churchill Boro
Pittsburgh 35, Pennsylvania

1 Dr. M. Talaat
Martin Marietta Corporation
Nuclear Division
Baltimore 3, Maryland

1 Prof. H. H. Woodson
Electrical Engineering Department
Massachusetts Institute of Technology
Cambridge 39, Massachusetts

1 1 Dr. Vernon H. Blackman
MHD Research Incorporated
1535 Monrovia Street
Newport Beach, California

1 Dr. M. C. Gourdine
Chief Scientist
Curtiss-Wright Corporation
Wright Aeronautical Division
Wood Ridge, New Jersey

Copies

1 Dr. Robert Eustis
Thermosciences Division
Stanford University
Stanford, California

1 Mr. Stan Markowski
Pratt and Whitney Aircraft
400 Main Street
East Hartford 8, Connecticut

1 Dr. Richard Schamberg
Rand Corporation
1700 S. Main Street
Santa Monica, California

1 Dr. Sam Naiditch
President
Unified Science Associates
826 Arroyo Parkway
Pasadena, California

I. INTRODUCTION

Superconductors that carry very large currents in high magnetic fields have been achieved in the last two years. Quickly following the finding by Kunzler and his associates, Reference 1, that Nb_3Sn cored wires carried more than 10^5 amperes per square centimeter, other investigators began developing Nb-Zr wire and applying both to magnet construction. Now we manufacture solenoids that have flux densities of well over 50,000 gauss, Reference 2. What follows describes one magnet development and sketches the engineering problems and their solution for large, high field magnets. The design is to serve a plasma acceleration experiment.

Magnetohydrodynamic space propulsion or power generation systems requires electromagnets, which are normally very heavy and require a great deal of power. Suppose that exclusive of a magnet such a system had a weight W per kilowatt of power either produced or used in plasma acceleration. The power for a conventional magnet is studied in Appendix A.

$$Pe = \frac{4\rho_e l}{\lambda}\left(\frac{\pi B}{\mu}\right)^2\left(\frac{A}{a^2}\right)^{-0.46} \qquad \text{Eq. (1)}$$

And, the power in say an MHD generator for constant velocity u and conductivity is: Reference 3.

$$P = \sigma B^2 u^2 \eta_e(1-\eta_e)4a^2 l = 4a^2 u \rho_g \Delta h \qquad \text{Eq. (2)}$$

When Pe has to be supplied by output P and the weight of the magnet is added to the system weight WP, the weight power ratio can be found making use of Equations (1) and (2) to eliminate dimensions:

$$\frac{\text{Weight}}{\text{Net Power}} = \frac{W + \dfrac{2\rho_{cu} Al}{P}}{1 - \dfrac{P_e}{P}} = \frac{W + \dfrac{\rho_{Cu}(A/a^2)}{2\sigma B^2 u^2 \eta_e (1-\eta_e)}}{1 - \dfrac{4\pi^2 \rho_e (\rho_g \Delta h)(A/a^2)^{-0.46}}{\mu^2 \lambda \sigma u \eta_e (1-\eta_e) P}} \qquad \text{Eq. (3)}$$

Typical values might be σ, 10 mhos/m; B, 50,000 gauss; u, 10^3 m/sec; η_e, 0.8; ρ_e, 2×10^{-8} ohm m; $(\rho_g \Delta h)$, 4×10^4 joules/m^3; λ, 1; and say W of 10 lb/kw, and P, 12,000 kw. Then:

$$\frac{\text{Weight}}{\text{Net Power}} = \frac{10 + 0.25(A/a^2)}{1 - (A/a^2)^{-0.46}} \quad \text{(lb/kw)} \qquad \text{Eq. (4)}$$

Optimum A/a^2 is near 10 so 20% of total weight is in the magnet and 35% of P goes to the magnet. A very similar consideration applies to plasma propulsion. This very simplified estimate ignores magnet joule heat rejection. At P equal 1 megawatt, no net power could be obtained.

But, with the use of superconductors, high j leads to reduced conductor weight; no need for iron; elimination of Pe except for a modest amount of refrigeration power; and an ability to develop strong fields which shorten length l to reduce viscous and heat transfer irreversibilities or decrease electrical plasma dissipation fraction $1-\eta_e$.

II. SUPERCONDUCTOR PROPERTIES

Although many metals are superconductors, at temperatures below 20°K, recent attention has been focused on such intermetallic compounds typified by Nb_3Sn, V_3Si and V_3Ga and interstitial alloys typified by body-centered cubic systems around Nb in the periodic table, especially Nb-Zr. Unlike ideal superconductors which have critical fields of the order of 10,000 gauss and less, these materials exhibit mixed state behavior where flux does begin to penetrate wire portions that become normal conductors at fields above the thermodynamic critical field, but zero electrical resistance persists to a much higher field. Critical current density and fields are shown in Figure 1 which is taken from data given by Kunzler, Reference 4, for Nb_3Sn and Hulm, Reference 5, for Nb-25% Zr. Magnets up to 200,000 gauss appear to be possible using Nb_3Sn and up to 90,000 gauss using Nb-Zr. Variation of critical field with temperature follows approximately $H_c = H_o \left[1 - \left(\frac{T}{T_c}\right)^2\right]$ where critical temperature T_c for Nb_3Sn is 18°K and 11°K for Nb-25% Zr. The curves of Figure 1 shift up and right for lower temperature than 4.2°K; down and left for higher temperature. Wire performance in coils using maximum fields on the center inner winding of solenoids for data, shows reduced critical currents from those in short samples in all experiments to date. This degradation in Nb-Zr is least for 50% Zr, Reference 5, but short sample currents are also less than for lower Zr content. Optimum j occurs with 25 to 33% Zr. The degradation appears to result from a proximity effect of the near range individual conductor fields on each other and the resultant current distribution in wire. Current density also increases with cold work reduction in wire making. Because it is ductile we have used Nb-25% Zr wire, which has been hard drawn from 0.50 inch diameter rod to 0.010 inch diameter wire. Niobium-tin wire is brittle, making coil fabrication difficult. While the metallurgical structure gives the mixed state superconductor properties, it also gives high normal state superconductor resistivities which lead to one of the major engineering problems, coil protection.

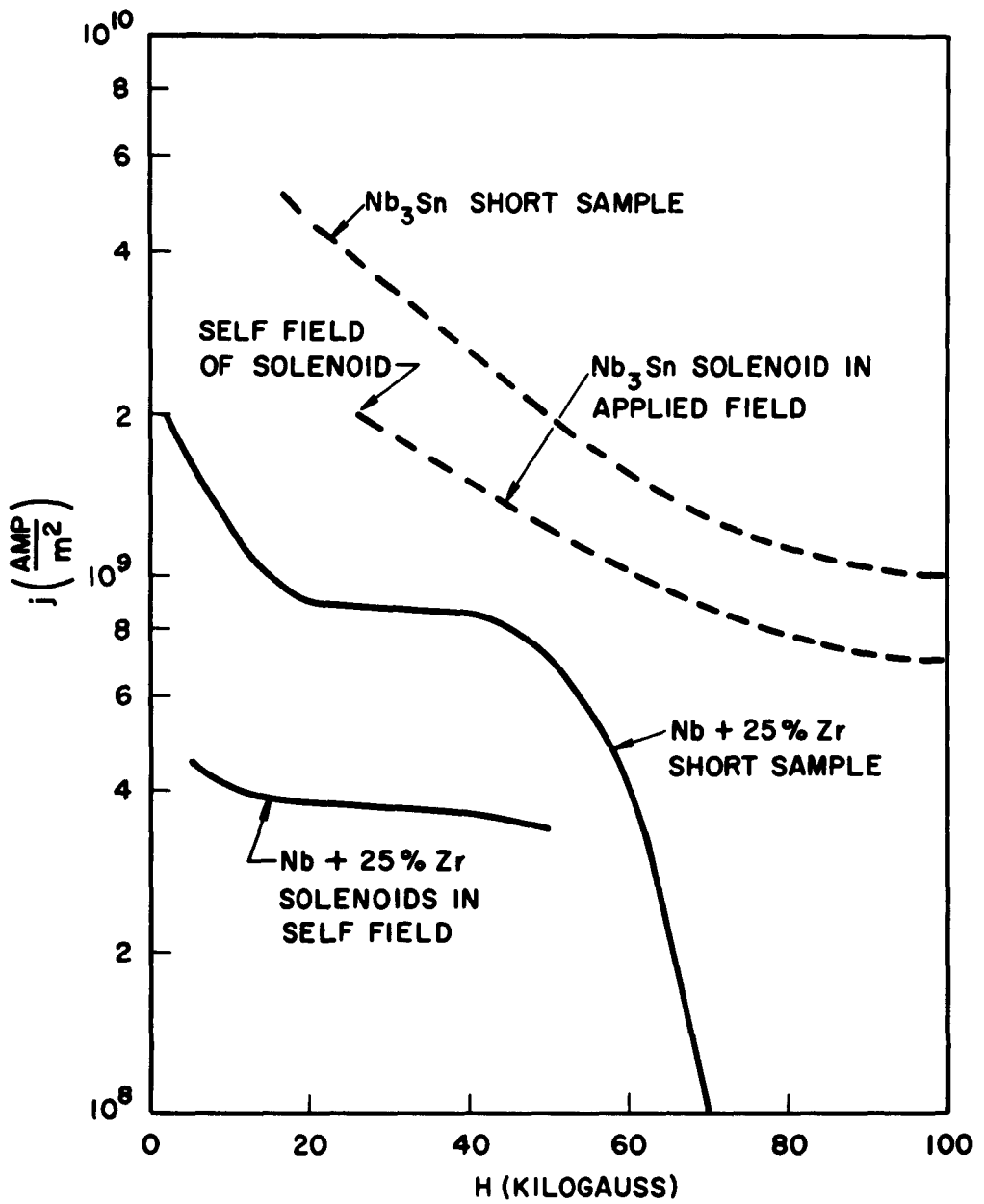

Figure 1 - Critical Current Density in 0.006 in. Nb_3 with 0.011 in. Diameter Nb Sheath and .010 in. Diameter Nb-25% Zr Wire at 4.2°K

III. MAGNET DESIGN

MAGNET SHAPE AND FIELD

Magnets for application to linear MHD devices, must produce somewhat uniform cross fields in a volume which is roughly square and, to avoid irreversible end effects, with a length to width ratio greater than unity. The coil shape shown in Figure 2 was used because it minimizes weight, can produce useful fields near the superconductor critical field, has relatively good uniformity of field, and it can be and has been fabricated.

The formulas in Appendix A, for case 5, give $\pi B_o/\mu j a \lambda$ equal 1.56 for a of 2.2, β_2 of 1.1 and β for a midplane split equal 0.05. This infinite conductor result can be increased by 7% to account for finite length and end conductors. The correction was calculated for a similar shape using right angle bends and rectangular sections. Then with λ equal 0.5, a equal 2.2 inches and j of 2.76×10^8 amp/m^2 for 14 amps in 0.010 inch wire, a field of 5.14 webers/m^2 would be developed.

If a simple, split solenoid pair whose shape has been optimized were used to obtain the same field over an effective length of 10 inches, its inside diameter would have to be 7.58 inches and 2.3 times the weight of wire would be used, because of the large split. Greater duct length to width ratios would increase the weight ratio even more. Worse yet would be field non-uniformity which for example would also cause a maximum field on superconductors to be 1.37 times center field, limiting MHD fields to 73% of critical field.

Coil winding techniques were investigated and one selected which after development produced the shape in Figure 2, which is essentially like a race track rolled on to a cylinder.

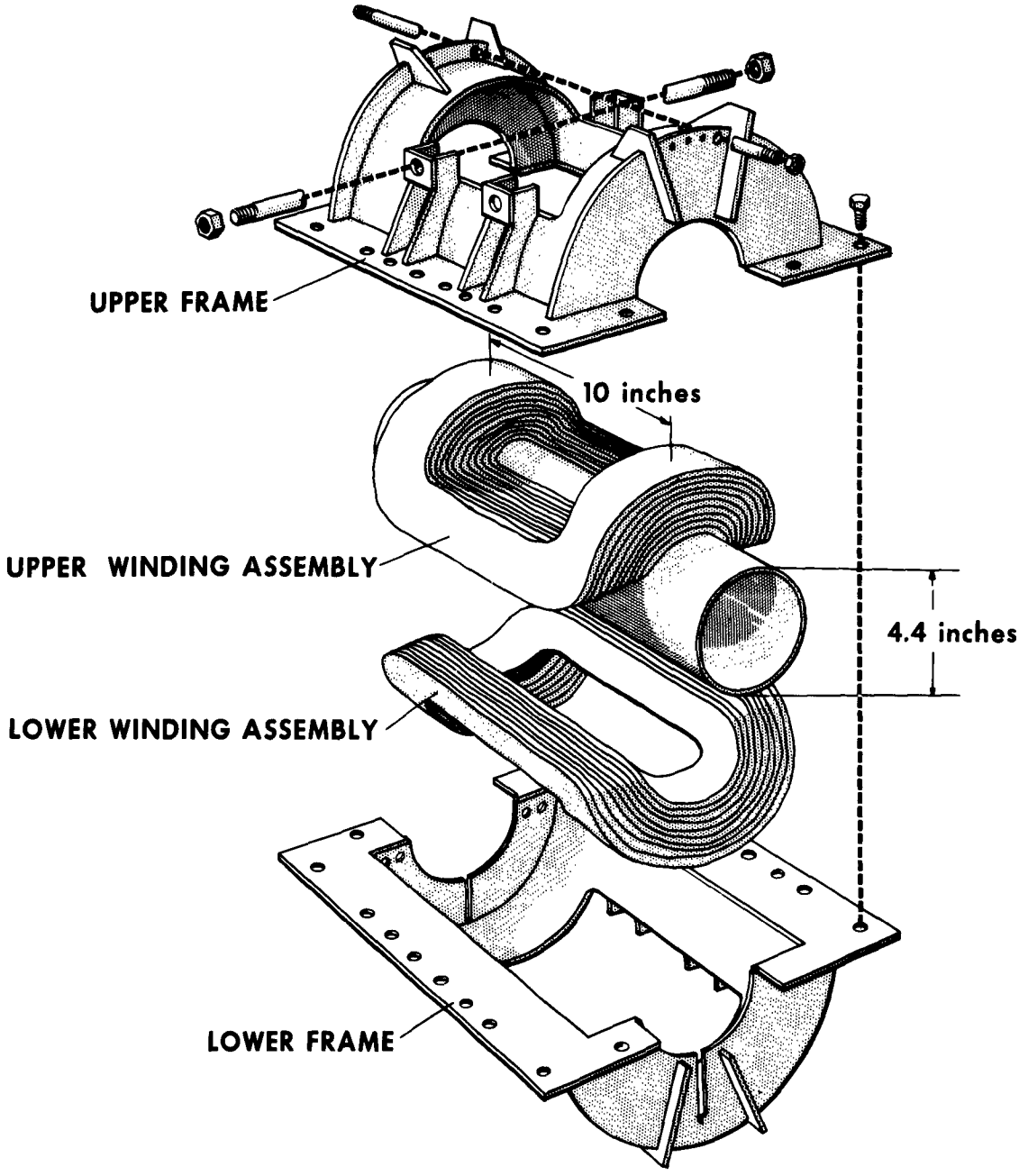

Figure 2. Superconducting Magnet Winding and Coil Support

Magnetic energy, T or $\frac{1}{2} Li^2$, for the design has been calculated from Equation (B-2) in Appendix B for equivalent rectangular conductor bundles ($\alpha = 2$, $\beta = 1$). In view of the work by Arnold, Reference 6, the result obtained using a 10 inch effective length should be quite accurate. There are about 87,000 joules when B_o is 5 webers/m^2 and therefore, L is 940 henries. Dissipating this large amount of energy is accompanied by a magnet protection problem should the conductors enter the normal state.

COIL PROTECTION

Though it is possible to operate superconducting magnet systems reliably, but by some accident, e.g. loss of refrigeration, the conductors enter the normal state, then in spite of dissipation of large amounts of magnetic energy, coils must be protected from destruction of the continuity of the superconductor. A simply wound coil having a portion resistive has the circuit shown in Figure 3(a). If externally supplied, by a battery and control resistor, still these are not significant circuit elements in a transient. Thermal energy increases temperature in normal portions and diffuses into superconducting regions causing propagation and growth of R which is proportional to the size of the normal region and, as resistivity changes slightly, its average temperature. Discussion of thermal propagation appears in Appendix C. For constant resistivity and turn inductances the transient is summarized below:

$$L\frac{di}{d\tau} + f(\tau)R_o i = 0,\ i(o) = i_o,\ f(\tau > \tau_o) = 1 \qquad \text{Eq. (5)}$$

$$\left.\begin{aligned} \frac{i}{i_o} &= e^{\frac{-R_o}{L}\int_o^{\tau} f\, d\tau},\ 0<\tau<\tau_o \\ \frac{i}{i_o} &= e^{\frac{-R_o}{L}\left[(\tau-\tau_o)+\int_o^{\tau_o} f d\tau\right]},\ \tau>\tau_o \end{aligned}\right\} \qquad \text{Eq. (6)}$$

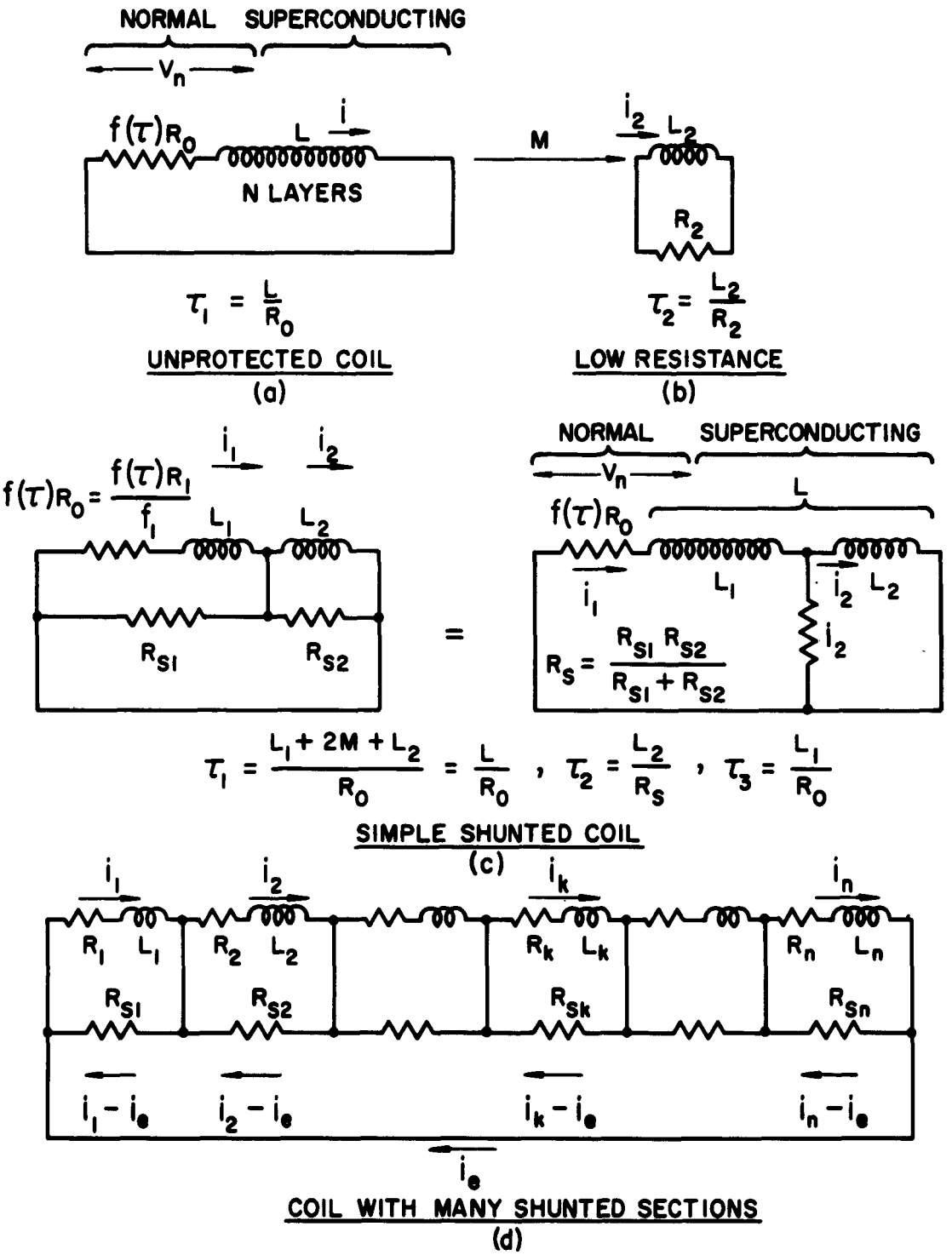

Figure 3 - Superconducting Coil Circuits During Normal Transients

$$\frac{2V_n}{fN} = 2\left[\frac{R_o}{N} i + \frac{Ld_i}{Nd\tau}\right] = \frac{2i_o R_o}{N}(1-f)\, e^{\frac{-Ro}{L}\int_o^\tau f d\tau}, \qquad \text{Eq. (7)}$$

$$0 < \tau < \tau_o$$

Largest voltage gradients occur between ends of pairs of the N layers wound back and forth in a coil. That layer to layer voltage for the normal region is given by Equation (7) which shows that it is largest when two whole layers are normal, and the fraction f is small so that voltage is twice i_o times layer normal resistance. Inductive gradient in the superconducting regions must be smaller since the factor 1-f is replaced by f in Equation (7) and when f is large, the exponential is small. An entirely normal coil has no voltage gradients by this simple theory. Should insulation breakdown and arcing occur, local heating anneals wire and destroys or weakens superconducting properties. Maximum voltage $2 i_o R_o/N$ can be alternately written as $2j\rho_e \lambda$ (layer volume) / (wire cross-section area). Clearly the protection problem arises from extremely high supercurrent densities, rather high normal resistivity and small wire diameter, for practical layer volumes. The MHD magnet design would have a possible 18,000 volts layer end to layer end were no protective techniques used.

A way that coil current and therefore high voltage may be reduced is by coupling magnetically from a short time constant (L/fR_o) normal superconductor system to a secondary which has a significantly longer time constant (L_2/R_2) because it has the low resistivity of copper or aluminum at cryogenic temperatures. The secondary of Figure 3(b) now alters the problem of Equation (5) to:

$$\left.\begin{aligned} L\frac{di}{d\tau} + f(\tau)R_o i + M\frac{di_2}{d\tau} &= 0,\ i(o) = i_o \\ M\frac{di}{d\tau} + L_2\frac{di_2}{d\tau} + i_2 R_2 &= 0,\ i_2(o) = 0 \end{aligned}\right\} \qquad \text{Eq. (8)}$$

Suppose that this system is closely coupled ($k^2 = M^2/L\,L_2 = 1$) and that as an approximation $f(\tau) = \tau/\tau_o$, then solution of Equation (8) gives:

$$\frac{2V_n}{fN} = \frac{2R_o}{N}(1-f)\,i = \frac{2i_o R_o}{N}\,\frac{(1-\tau/\tau_o)e^{-\tau/\tau_2}}{\left[1+\frac{\tau_2}{\tau_1}\,\frac{\tau}{\tau_o}\right]\left(1-\frac{\tau_1\tau_o}{\tau_2^2}\right)}\,,\ \tau<\tau_o \qquad \text{Eq. (9)}$$

Clearly from Equation (9) for a secondary to be effective τ_2 should be much greater than τ_1 and $\sqrt{\tau_1\tau_o}$. Then voltages are reduced quickly in a characteristics time $\tau_1\tau_o/\tau_2$ by a factor of $1 + f\frac{\tau_2}{\tau_1}$. However if there is not close coupling, a solution of Equation (8) by a series in time gives:

$$\frac{2V_n}{fN} = \frac{2i_o R_o}{N}\left[1 - \frac{\tau^2}{2\tau_i\tau_o(1-k^2)} + \ldots\right] \qquad \text{Eq. (10)}$$

When τ_2 is truly very large so that additional terms in Equation (10) are unimportant, then voltages may not be reduced nearly instantaneously in time $\tau_1\tau_o/\tau_2$, but decay in $\sqrt{2\tau_1\tau_o(1-k^2)}$. In either case, final slow decay occurs with a τ_2 time constant. Similarly when a fraction f_o of a coil goes normal suddenly, a reduction of Equation (7) by $1 + f_o\tau_2/\tau_1$ occurs instantaneously for close coupling. When k^2 is not one, reduction occurs with a time constant $(1-k^2)\,\tau_1/f_o$.

Another means of protection is resistance shunting of several coil sections. A coil with just two shunted sections where one is normal is shown in Figure 3(c). The governing equations are:

$$\left.\begin{aligned} L_1\frac{di_1}{d\tau} + M\frac{di_2}{d\tau} + f(\tau)R_o i_1 + R_s(i_1 - i_2) = 0,\ i_1(o) = i_o \\ M\frac{di_1}{d\tau} + L_2\frac{di_2}{d\tau} + R_s(i_2 - i_1) = 0,\quad i_2(o) = i_o \end{aligned}\right\} \qquad \text{Eq. (11)}$$

For close coupling and $f(\tau) = \tau/\tau_o$, the solution is:

$$\frac{2V_n}{fN} = \frac{2i_o R_o}{N}\left[1 - \frac{\tau/\tau_o}{f_1(1 + L_2/L_1)}\right]\frac{e^{-\tau/\tau_2}}{\left[1 + \frac{\tau_2}{\tau_1}\ \frac{\tau}{\tau_o}\right]\left(1 - \frac{\tau_1\tau_o}{\tau_2^2}\right)}\ ,\ \tau < f_1\tau_o \qquad \text{Eq. 12}$$

A comparison of Equations (12) and (9) shows that shunted behavior is very nearly like that for normal secondaries where now the secondary is composed of L_2 and R_s. Since the time constant τ_2 may be made arbitrarily large, the characteristic time for current and voltage decay to the slow transient is important. Here the time constant is $\sqrt{2\tau_3\tau_o(1 - k^2)}$ for $f = \tau/\tau_o$ and $\tau_3(1 - k^2)/f_o$ for instantaneously appearing resistance $f_o R_o$. The last results were obtained from series solution of Equation (12).

The usefulness of shunting sections of a coil is the rapid current decay in sections having normal wire, accompanied by rapid current increase, above i_o, in the most closely coupled superconducting sections. Analysis of the voltage across the terminals of the "k" section of Figure 3(d) shows:

$$\sum_{i=1}^{n} M_{k,i}\frac{di_i}{d\tau} + i_k R_k = (i_e - i_k)R_{sk} = \left(\frac{\sum_{i=1}^{n} i_i R_{s_i}}{\sum_{i=1}^{n} R_{s_i}} - i_k\right) R_{sk} \qquad \text{Eq. (13)}$$

In the limit, as n approaches an infinitely large number Equation (13) becomes:

$$\int_o^n M(k,\lambda)\frac{\partial i}{\partial \tau}(\lambda,\tau)d\lambda - \frac{\int_o^n i(\lambda,\tau)R_s(\lambda)d\lambda}{\int_o^n R_s(\lambda)d\lambda} + i(k,\tau)\left[R(k) + R_s(k)\right] = 0 \qquad \text{Eq. (14)}$$

Since the integrals are continuous, while R(j) may be discontinuous at a division of normal and superconducting sections, for example between the k and k + 1 sections, the current ratio from Equation (14) must be:

$$\frac{i_{(k+1)}}{i_{(k)}} = \frac{R(k) + R_s(k)}{R_s(k+1)} \qquad \text{Eq. (15)}$$

For low resistance shunts the ratio may be very large except that it may be assumed that section k + 1 must itself become normal for currents greater than i_c (critical current). The limiting process leading to Equations (14) and (15) implies close coupling as for a finite size solenoid with infinitesimal sections, which cannot be realized in practice. But if in the system of Figure 3(c) there is not close coupling, series solution of Equation (11) gives:

$$\frac{i_2}{i_o} = 1 + \frac{f_1 R_o k}{\sqrt{L_1 L_2 (1-k^2)}} \tau + \ldots \qquad \text{Eq. (16)}$$

From Equation (16) where $f_1 R_o$ appears instantaneously because current exceeds i_c, then the second section becomes normal in time $\left(\frac{i_c - i_o}{i_o}\right) \frac{\sqrt{L_1 L_2 (1-k^2)}}{f_1 R_o k}$. In an n section coil where all sections are the same and coupling effects are limited to one normal and one superconducting pair (where k is largest) a representative time for going normal is: $\left(\frac{i_c - i_o}{i_o}\right) \tau_1 \left(\frac{1-k^2}{k}\right)$. What has been described amounts to a fast, non-thermal propagation of a normal front. Behind the wave, sections have dissipated energy in the characteristic time found from Equation (16). Temperature rise is therefore of the order of:

$$\Delta T \approx \frac{i_o (i_c - i_o) \sqrt{L_1 L_2}}{C M_1} \left(\frac{1 - k^2}{k}\right) \qquad \text{Eq. (17)}$$

It is conceivable that when i_1 decays sufficiently, the section may still be at a low enough temperature that it may become superconducting again. However it would be just at the critical condition and any magnetic coupling would increase current and return it to the normal state.

The coil described in this paper is protected by 96 shunts and 46 interleaved copper secondaries. Were the coil not shunted, even though rather close coupling with

secondaries would be achieved (k = 0.975) and with copper occupying 10% as much space as superconductor, the reduction in maximum voltage shown in Equation (9) would not be significant for very small $f = \tau / \tau_o$. However, by subdividing the coil with shunts so that one secondary couples effectively with one normal section of 96, reduction may be attained. The shunting permits the current of one section to couple independently with any normal secondary or superconducting section. For two layers wholly normal in a section and with $\tau_{\text{secondary}}/\tau_{\text{normal section}} = 20$ for copper at 20°K, at most 2500 volts layer to layer could occur even without section to section coupling. The way in which thermal propagation of a normal front occurs in a section is complicated by cooperative heating in secondaries. A section's τ_o is conservatively estimated as 10^{-2} seconds (see Appendix C). Layer to layer voltage becomes a problem only when τ/τ_o becomes nearly two divided by the layers in a section. Then if there is not close coupling the time constant of Equation (10), for this design, need only be like $1/4\,\tau_o$. Since τ_1 is much less than τ_o, coupling need not be good. Then the reduction predicted by Equation (9) is attainable before large voltages appear. When two layers become normal suddenly, there is the time $(1-k^2)\,\tau_1/f_o$ (equal 8×10^{-6} seconds) for which reduction of voltage does not occur. However, capacitive energy storage in the dielectric between layers, prevents voltage rise for of the order of 10^{-5} seconds, so protection is achieved under this severe condition too.

The shunt action, provided adjacent sections could remain superconducting, would produce a 250 times reduction of maximum layer to layer voltage by Equation (12) or (15). Since in the design for maximum field they cannot remain superconducting, the useful effect of shunts, by themselves, is to propagate the normal region in $.19 \times 10^{-6}$ seconds per average section. In the design, shunted section time constants initially are longer than secondary time constants so that the propagation is not hindered by copper secondaries, at least for comparable coupling. Temperature rise in this time is of the order of 10°K by Equation (17), insuring that sections remain normal. If each

section was made completely normal by current increase, no voltage problem would exist and copper secondaries would be redundant except to slow final field decay. However, the secondaries do provide protection should only a fraction of each coil become normal, and the preceding discussion of secondaries again applies.

Another means of protection which has not been used is that where the superconductor is clad or plated with copper and, therefore, has a much reduced voltage problem by Equation (7). In effect, this copper is equivalent to a system of shunts for current continuity and secondaries for magnetic energy conservation. However, one further problem does exist. It is the final distribution of thermal energy in a coil. Were thermal propagation of normalcy slow, high temperatures would occur in the first superconductor to become normal, especially in large coils. The shunt system overcomes this by the extreme rapidity with which it spreads the normalcy. Then only in extremely high energy, large magnets does the resulting uniform distribution of thermal energy cause temperatures high enough to destroy the superconductor characteristic.

While the foregoing contains many approximations, such as the linear thermal propagation or sudden transition approximation and the assumption of constant properties, the conclusions and descriptions remain valid. A computer program including nonlinear thermal transfer, changing critical current with field and temperature, exact coupling coefficients and circuit analysis yields us detailed behavior and exact solutions.

SUPPORT OF MAGNETIC FORCES

In the system of conductors shown in Figure 2, the net result of $\underline{j} \times \underline{B}$ body forces, is to tend to enlarge the coil, to separate the sides by a force of 68,500 lb. found by Equation (D-2 of Appendix D), where $\alpha = 2$, $\beta = 1$, and to separate ends by a force of

77,000 pounds. Average stress on the coil form sides is quite accurately found from Appendix D, Equation (D-1) to be 1360 psi and varies less than 17% over the height of the side. The maximum compressive stress between halves is only a little more, 1640 psi. For still larger sizes and fields, stress increases. With the fully potted coil structure used, epoxy insulation will not be damaged by these stresses.

The magnet described here is unlike a simple solenoid where the coil supports itself with a stable conductor bundle pinch and hoop stress jrB (for a free wire turn of radius, r, with an axial field B at the wire) constraining coil enlargement. Rather the extra constraining coil form structure shown in Figure 2 is used.

Plate loading is reduced using end and side ribs which also act as beams to communicate load to axial and cross tension bolts. Side and end flanges are bolted to connect the beams. The side flanges also act as beams to carry side loading to circular end plates which acts as connecting tension members. End loading is also carried by the side coil form and by the flanges in superimposed tension. All members are stainless steel designed for 50,000 psi maximum stress at 4.2°K, except where there is redundant sharing of load. For example both side flanges plus coil form and longitudinal axial bolts can support the end loading by themselves.

ELECTRICAL CONNECTIONS

Over 200,000 feet of wire was used in the coils. Although up to 18,000 foot lengths of Westinghouse produced wire were supplied, the average single conductor length after coil fabrication was much less. Superconducting junctions were made by pressing twisted wire ends together between the bottom of a milled slot in a stainless steel bolt and a foot tightened by a nut on the bolt. These junctions were tested up to 20,000

gauss fields and found to have nearly the same critical current as the wire. Junctions are clamped over insulated fingers on a copper conduction cooling strip. In order to divide the coil into eight sections for external supply of current into individual sections and also to furnish different currents to the sections, seven three wire superconducting joints are used. The third wire, a superconducting lead, is carried through vacuum seals into wells on liquid helium tanks where connection is made to copper wire. The nine current joints are simply copper blocks clamping the superconductor.

Shunts are conventional 2 watt wire wound resistors, which, because resistance wire transmits heat well to high specific heat plastic, can absorb 100 joules of energy without failure. During a normal transient they can carry 14 amperes in 10 ohms for .05 sec., a time that is longer than that expected for shunt currents to flow. They connect at junction blocks where either superconducting joints or continuous conductors are brought out of the coil.

Figures 5 and 6 show the wire carrier used and the superconducting junctions.

IV. CRYOGENIC SYSTEM

GENERAL CONSIDERATIONS

Superconductors need to be maintained at the normal saturation temperature of helium, 4.2°K. Lower temperatures increase refrigeration requirements markedly without allowing much increase in critical currents. Higher temperatures, up to a maximum of 11°K, result in progressively smaller current densities. Refrigeration work to remove Q units of heat at temperature T and reject at T_r is:

$$W = \frac{1}{\eta} \frac{T_r - T}{T} Q \qquad \text{Eq. (18)}$$

Here η is the ratio of the coefficient of performance obtained to that of a Carnot cycle. For example for a helium cycle η is between 7 and 20% while rejecting at an Earth ambient of 300°K. For the lower value, Q/W is 0.001; that is, 1000 watts of power are required to remove a 1 watt heat flux into the cold region. The need for minimizing heat transfer, especially to the lower temperatures is well demonstrated by this consideration whether it be for the experimental development described here or for magnet cryogenics in space.

Heat transfer occurs by radiation from warm walls to the magnet, by conduction in residual gas unless vacuum pressures less than 10^{-5} mm mercury are used to make this heat flux negligible, by conduction in magnet mass and reaction supports and conduction and joule heating in electrical current and instrumentation lead conductors. Whether the object is to minimize weight and power of a space system refrigerator or to conserve liquid helium in experiments, refrigeration to remove as much heat as possible at temperatures above 4.2°K has the advantages implied in Equation (18). Since thermal conductivity in supports and radiation fluxes decrease rapidly with temperature, staged refrigeration is especially practical. Although it does not result in an optimum temperature distribution of refrigeration, vapor cooling, using enthalpy changes in the vapor

as well as evaporation is a good and simple technique. It may be applied to both conduction and radiation transfers through vapor cooling of supports, radiation shields, electrical leads, etc. For example, for constant η and properties k and c_p, Equation (E-5) of Appendix E together with a liquification process following Equation (18) gives refrigeration power for vapor cooling a heat path as:

$$P_{r\ \text{Vapor Cooling}} = \frac{1}{\eta}\frac{kA}{c_p x_o} \ln\left[1 + \frac{c_p(T_a - T)}{h_{fg}}\right]\left[c_p \int_{T_s}^{T_a} \left(\frac{T_a - T}{T}\right) dT + h_{fg}\left(\frac{T_a - T_s}{T_s}\right)\right] \quad \text{Eq. (19)}$$

Without vapor cooling the result would be:

$$P_{r\ \text{No Vapor Cooling}} = \frac{1}{\eta}\frac{kA}{x_o}\frac{(T_a - T_s)^2}{T_s} \quad \text{Eq. (20)}$$

Refrigeration power without vapor cooling would be four times that with vapor cooling considering transfer between 4.2°K and 300°K with helium. A similar consideration in the case of cooling electrical leads yields vapor cooling improvement by a factor of about three in a comparison of optimum cases.

THE MAGNET DEWAR

Figure 4 shows a schematic of the dewar design. The vacuum vessel is stainless steel made in two sections. A 3.9 inch I.D. by 18.6 inch long center tube about the MHD duct space, a head end plate and a lead-in neck comprise one part. The other is a 20.5 inch diameter outer cylinder and rear end plate which has "O" ring seals at a head end flange and at the rear end of the center tube. This arrangement allows relatively easy assembly.

A second plate at the rear end and a thin stainless steel cylinder form a part of the support structure, acting also as intermediate radiation shields and low emissivity surfaces.

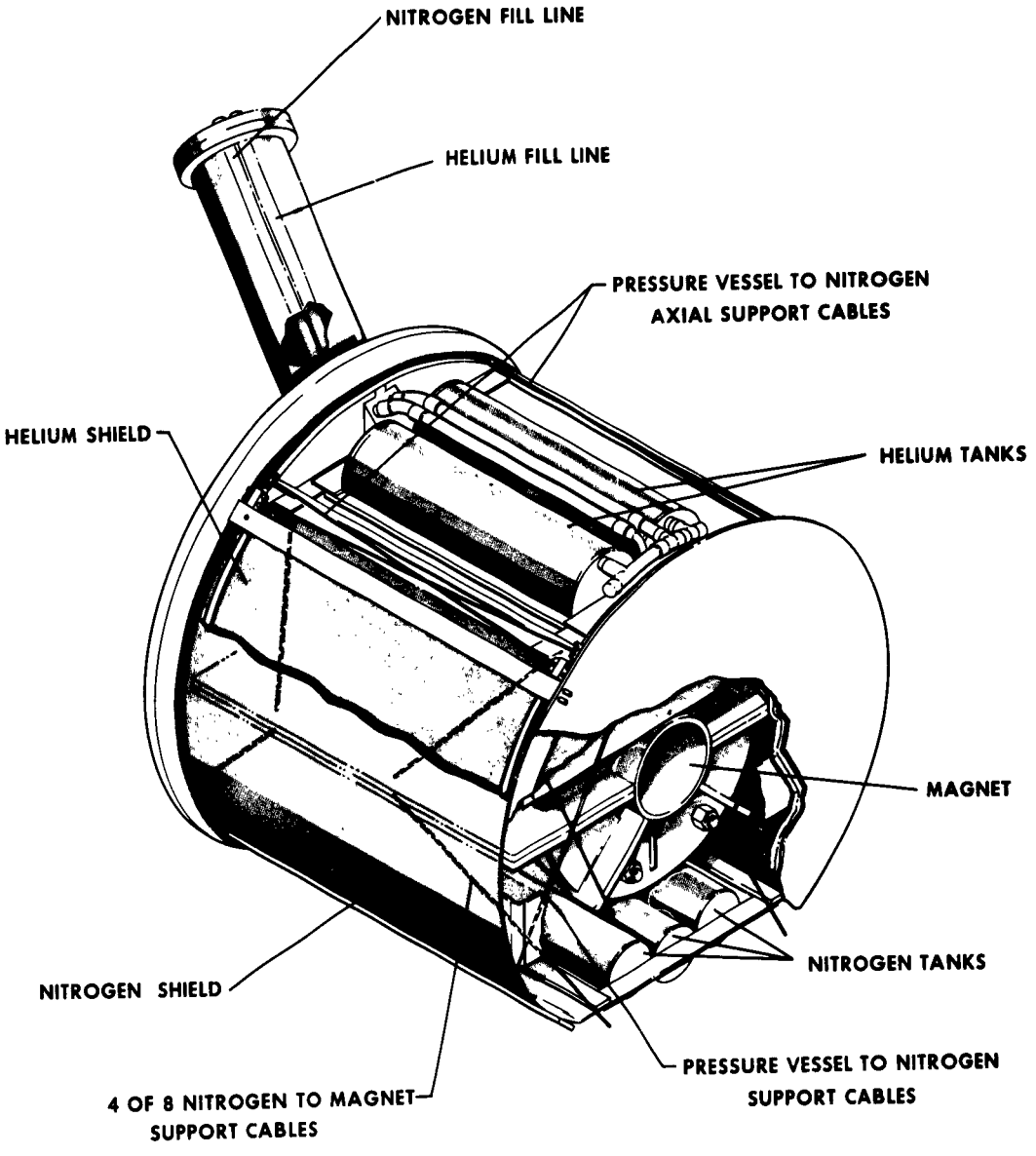

Figure 4 - Dewar and Suspension System

Four 0.10 inch diameter stainless steel cables at each end support and center the nitrogen system. Eight additional cables prevent axial displacement.

The nitrogen system has two copper end radiation shields with heavy outer rings to which the support cables are fastened. A stainless steel inner cylindrical shield is plated with copper strips arranged to conduct heat to the end shields but to offer a high resistance path for induced eddy currents which may deform it. An outer shield is a thin copper sheet. Heat is conducted to three interconnected cylindrical tanks at the bottom which hold 2.9 liters of liquid nitrogen. A single 0.010 inch wall stainless steel fill and vent tube connects with the top of the neck. Inside it is a small teflon tube used for filling. Eight adjustable support cables run diagonally from the nitrogen temperature ring to the coil form flanges.

Liquid helium is stored in two tanks holding 3.65 liters which are mounted on top of the coil form. Stainless steel sheet, plated with copper in strips, surrounds the magnet. They conduct radiated heat to the helium reservoirs at right angles to electric fields which could induce eddy currents during magnet normal transients. These shields are needed since many of the magnet surfaces offer high emissivities. Thin wall tubes run parallel from the neck to the head end nitrogen ring where they are heat shunted to nitrogen temperature. From there, one serves as a fill line which connects with a vapor cooling heat exchanger, while the other vents the two tanks at the rear end.

Helium and nitrogen temperature shield surfaces were gold plated to minimize oxidation and deterioration of emissivities. Nitrogen shielding of radiation and conduction paths effects the staging discussed above. Vapor cooling of electrical leads and tubing was calculated as optimum using equation (E-3 of Appendix E) with appropriate convection heat transfer theory. In this connection, it was noted that the effective h was increased by using heavily insulated lead-in wires since teflon thermal conductivity is not so low

that the additional resistance to heat flow by insulation offsets the gain in convection transfer area. Nine current leads are provided to the magnet and since all would not be carrying the planned current, their length to area ratio was chosen to give smallest heat input to helium liquid at either full or no current, i.e. x_o/A in Equation (E-4 of Appendix E) large rather than optimum by Equation (E-6). Table I summarizes the calculated heat transfer in the dewar for the superconducting magnet.

MAGNET COOLING AND COOL DOWN

The winding is kept cold by conduction from insulated tabs on pure copper secondaries to boiling helium in blind tube wells communicating with the helium tanks. Joint and superconductor lead carriers are similarly kept cold. A helium fill line of stainless steel connects to two vapor heat exchangers, also cooling secondaries, so that efficient vapor cool-down from nitrogen temperature is effected as described in Appendix F. The 200 pound magnet assembly would require 174 liters of boiling helium. However, using Equation (F-1) and (F-4) gives a calculated requirement of 14.2 liters for this design, exclusive of transfer losses. The boiling tubes and vapor heat exchanger may be seen in Figures 5 and 6.

During electrical charging, voltage for $L\, di/d\tau$ also causes dissipation of heat in secondaries and shunts. In shunts for example, total energy to charge to i_o in time τ', at a constant rate is $\left(\frac{2L}{\tau' R_s}\right)\left(\frac{1}{2} L i_o^2\right)$. A long charging time is used to minimize dissipation. Heat transfer calculations have been used to determine that the design will not warm superconductors appreciably during charging. Also, shunts have been chosen so that sections have nearly the same currents during charging.

Table I - Heat Transfer in Dewar

Heat Transfer by	Formula	Properties	Heat Flux to Nitrogen Watts	Heat Flux to Helium Watts
Radiation	$\frac{\sigma \text{ Area } \epsilon_1 \epsilon_2}{\epsilon_1 + \epsilon_2 - \epsilon_1 \epsilon_2} (T_2^4 - T_1^4)$	ϵ for stainless steel $300^\circ K$, 0.05 to 0.08 ϵ for Au on stainless steel $77^\circ K$, 0.03; $4.2^\circ K$, 0.02 ϵ for Au on copper $77^\circ K$, 0.02; $4.2^\circ K$, 0.02; $4.2^\circ K$, 0.02	9.6	0.026
Conduction in Support Cables	$\Sigma \frac{A}{x_o} \int_{T_1}^{T_2} k dT$	for stainless steel $\int_{4^\circ K}^{77^\circ K} k dT = 3$ watt/cm. $\int_{77^\circ K}^{300^\circ K} k dT = 26$ watt/cm.	0.78	0.064
Conduction in Unshielded Fill Tube	$\frac{A}{x_o} \int_{T_1}^{T_2} k dt$	Same	0.005	0.001
Conduction in Low Pressure Gas	$\frac{A}{2} \left(\frac{\gamma+1}{\gamma-1}\right) \sqrt{\frac{R_{He}}{2\pi T}} \, p \, (T_2 - T_1) \Big/ \left(\frac{1}{\alpha_1} + \frac{1}{\alpha_1}\right)$	for helium, 0.01, μHg pressure, $T_2 = 77^\circ K$, $T_1 = 4.2^\circ K$, $\gamma = 1.67$, $\alpha_2 = 0.6$, $\alpha_1 = 1$	--	0.105
Vapor Cooled Electrical Lead	Equations (E-2) and (E-3) (2 wires have 14 amp; 7 have 0 amps) $\dot{m}_{total} = Q_{total}/h_{fg}$	$h = 8 \times 10^{-3}$ watts/cm$^2{}^\circ K$ k (average copper) = 4.2 watts/cm$^\circ K$. $\rho_e = 0.76 \times 10^{-6}$ ohm cm.	--	0.192
Total			10.345	0.397

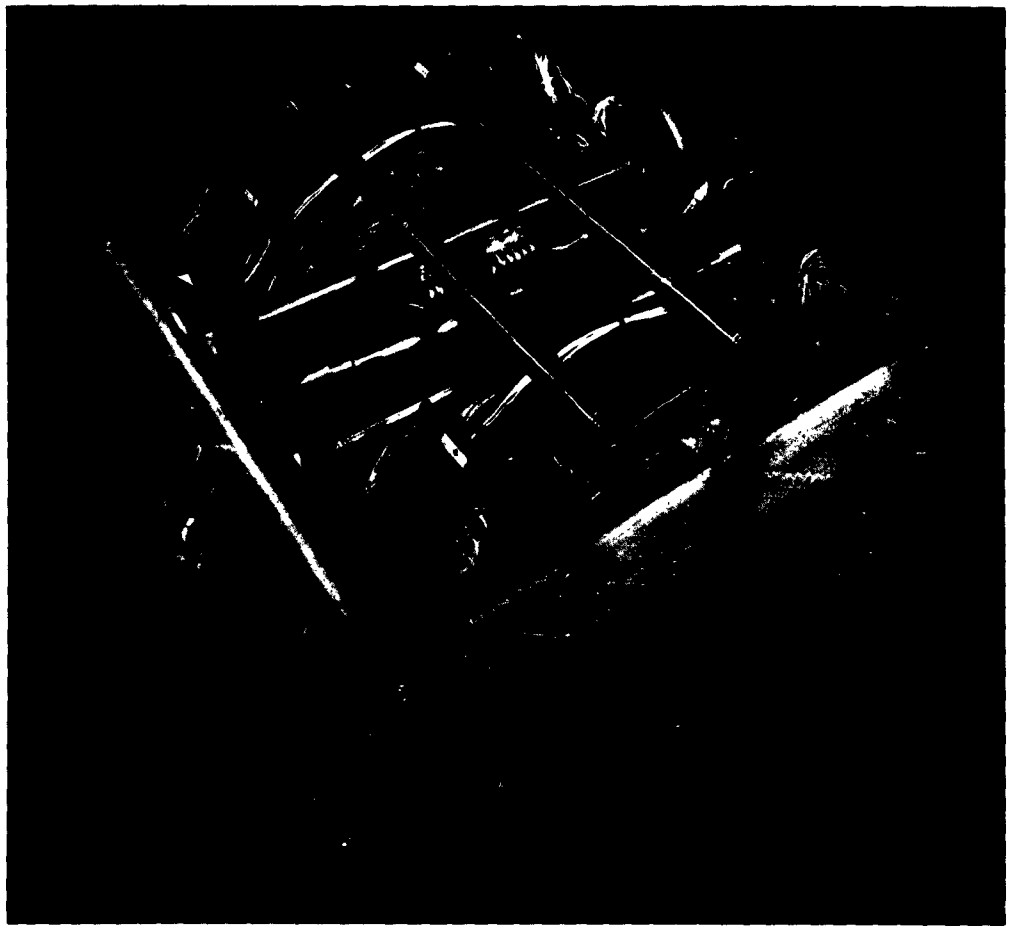

Figure 5 - Superconducting Magnet Bottom View

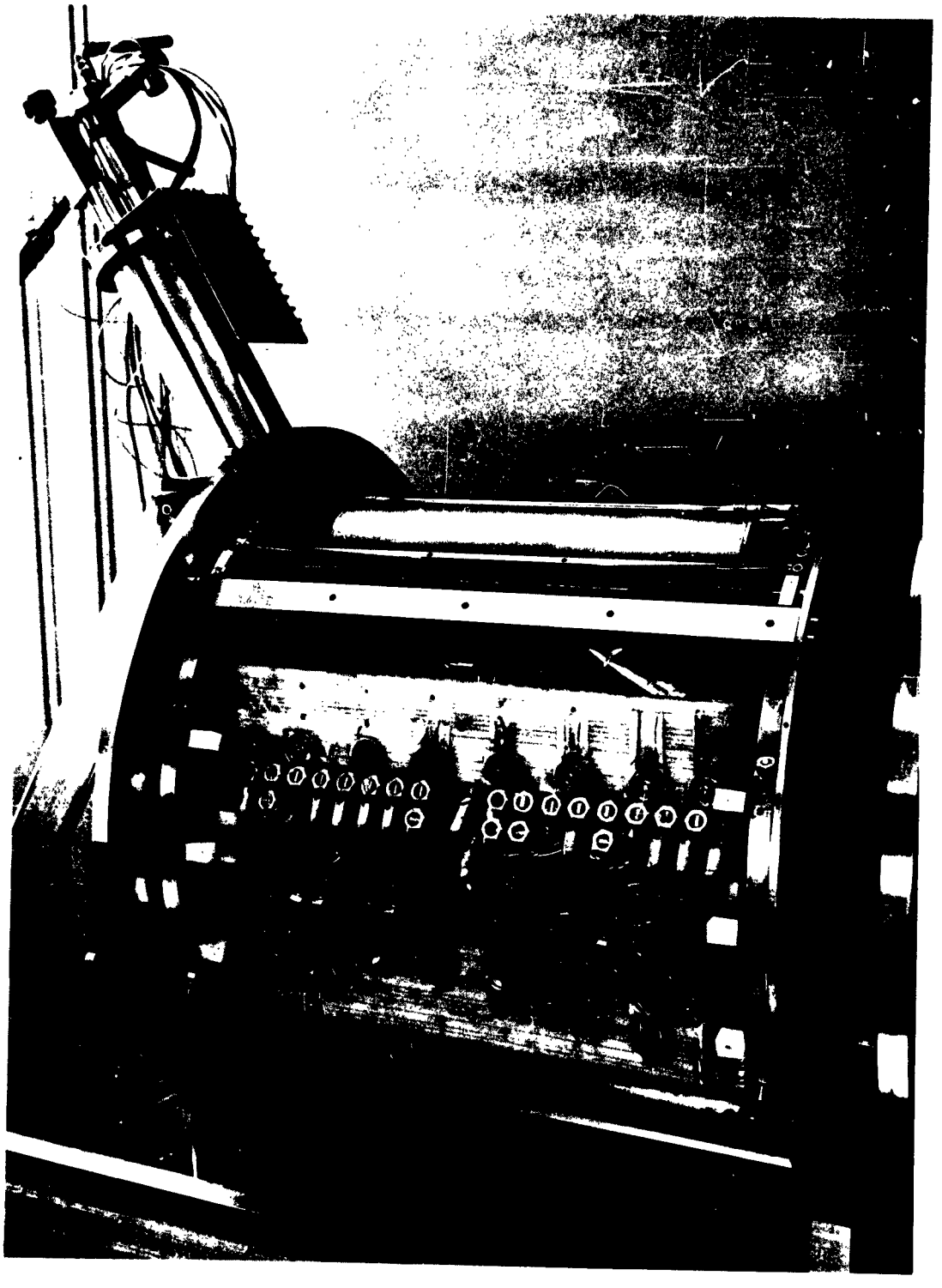

Figure 6 - Superconducting Magnet Assembly

V. INSTRUMENTATION

In addition to use of the nine current leads, to the magnet, five voltage leads are provided to monitor transient section voltages. Copper-constantan thermocouples are installed to measure nitrogen tank, magnet support and helium vapor exhaust temperature. Monitoring the latter two enables setting charging rates to obtain efficient vapor cool down. A nitrogen level gauge and helium level gauge are used to give continuous readings of tank fluid level. These level gauges are described in Appendix G.

APPENDIX A

Fields

The flux density normal to the axis of symmetry between two infinite parallel conductor bundles is twice the sum of contributions by current elements in one. (See Figure 7).

$$B_o = \frac{\mu}{\pi} \iint_A \lambda j \left(\frac{x}{x^2 + y^2}\right) dA \qquad \text{Eq. (A-1)}$$

The electrical power consumed by the pair in resistive magnets is:

$$Pe = 2\rho_e L \iint_A \lambda j^2 \, dA \qquad \text{Eq. (A-2)}$$

A current distribution that minimizes Pe is found by a variational method where, given B_o, Equation (A-1) is then a constraint.

$$j_{opt.} = j_o \, a \left(\frac{x}{x^2 + y^2}\right) \qquad \text{Eq. (A-3)}$$

$$Pe = 2\rho_e \, l \cdot (\pi B_o/\mu)^2 \, \frac{\iint_A \lambda j^2 \, dA}{\left[\iint_A \lambda j \left(\frac{x}{x^2 + y^2}\right) dA\right]^2} \qquad \text{Eq. (A-4)}$$

When j is constant or optimum from Equation (A-3) inspection of the alternative form of Pe in Equation (A-4) shows that only the integral in the denominator of Equation (A-4), which is $\pi B_o/\mu$, may be maximized to minimize Pe, as long as area, A, is considered to be fixed or constrained. The variational procedure maximizing $\pi B_o/\mu$, with A constant, gives an optimum limit in the integration on y. The best shape conductor bundle both for optimum j distribution and for constant j, is a circle touching the axis. A simpler shape is a rectangular one where again a variational method yields the optimum relation of dimensions. Note that the above procedure finds minimum power for area

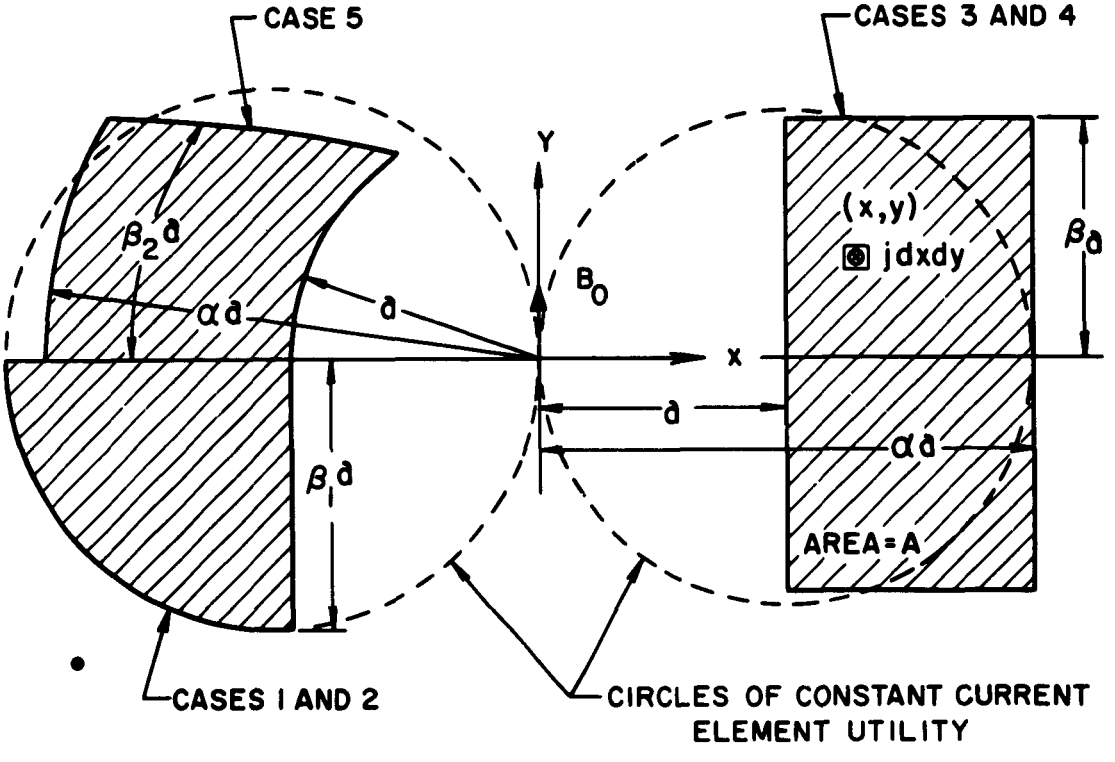

Figure 7 - Section of Parallel Conductor MHD Magnets

and flux density given, or minimum area and hence weight of conductor for power or j and flux density given in superconducting or normal magnets. Results obtained from the formulas above for cases of interest are given in Table A-I. Figure 8 shows results for dimensionless power of these cases.

Table A-I

Case	Winding Cross-Section	i	$\frac{B_o}{\mu i_o a \lambda}$	$\frac{Pe}{\frac{2\rho_e l}{\lambda}\frac{\pi B_o^2}{\mu}}$
1	Segment of circle $1<(\frac{x}{a})<\beta_1^2+1;\ (\frac{y}{a})^2<(\beta_1^2+1)(\frac{x}{a})-(\frac{x}{a})^2$ $A/a^2=\frac{1}{2}\beta_1(\beta_1^2-1)+\frac{1}{2}(\beta_1^2+1)^2\tan^{-1}\beta_1$	$i_o a(\frac{x}{x^2+y^2})$	$\frac{\beta_1}{\beta_1^2+1}-\tan^{-1}\beta_1-2\sum_{n=1}^{\infty}\frac{2^{2n}(2^{2n}-1)}{(2n+1)!}b_n(\tan^{-1}\beta_1)^{2n+1}=f_1$	$\frac{1}{f_1}$
2		i_o	$\beta_1+(\beta_1^2-1)\tan^{-1}\beta_1=f_2$	$\frac{(A/a^2)}{f_2^2}$
3	Rectangular, for optimum: $(\frac{2\alpha-1}{\alpha})(\frac{\beta\alpha}{\beta^2+\alpha^2}+\tan^{-1}\frac{\beta}{\alpha})=(\frac{\beta}{1+\beta^2}+\tan^{-1}\beta)$ $A/a^2=2\beta(\alpha-1)$	$i_o a(\frac{x}{x^2+y^2})$	$\cot^{-1}\frac{\beta}{\alpha}-\cot^{-1}\beta-\left[(\frac{\beta}{\alpha})-\frac{1}{3^2}(\frac{\beta}{\alpha})^3+\frac{1}{5^2}(\frac{\beta}{\alpha})^5-\ldots\right]$ $+\left[\beta-\frac{\beta^3}{3^2}+\frac{\beta^5}{5^2}-\ldots\right]=f_3$	$\frac{1}{f_3}$
4	Rectangular, for optimum: $(\alpha-1)\tan^{-1}\frac{\beta}{\alpha}=\frac{\beta}{2}\ln(\frac{\beta^2+\alpha^2}{\beta^2+1})$ $A/a^2=2\beta(\alpha-1)$	i_o	$\beta\ln(\frac{\beta^2+\alpha^2}{\beta^2+1})+2\alpha\tan^{-1}\frac{\beta}{\alpha}-2\tan^{-1}\beta=f_4$	$\frac{(A/a^2)}{f_4^2}$
5	Annular Segment $1<r/a<\alpha;\ \beta<\frac{\beta_2 a}{r}$ $A/a^2=2\beta_2(\alpha-1)$	i_o	$2\beta_2\left[\frac{\alpha}{\beta_2}\sin(\frac{\beta_2}{\alpha})-\frac{1}{\beta_2}\sin\beta_2+\ln\alpha\right.$ $\left.-\left(\frac{\beta_2^2}{2.2!}-\frac{\beta_2^4}{4.4!}+\ldots\right)+\left(\frac{(\beta_2/\alpha)^2}{2.2!}-\frac{(\beta_2/\alpha)^4}{4.4!}+\ldots\right)\right]=f_5$	$\frac{(A/a^2)}{f_5^2}$

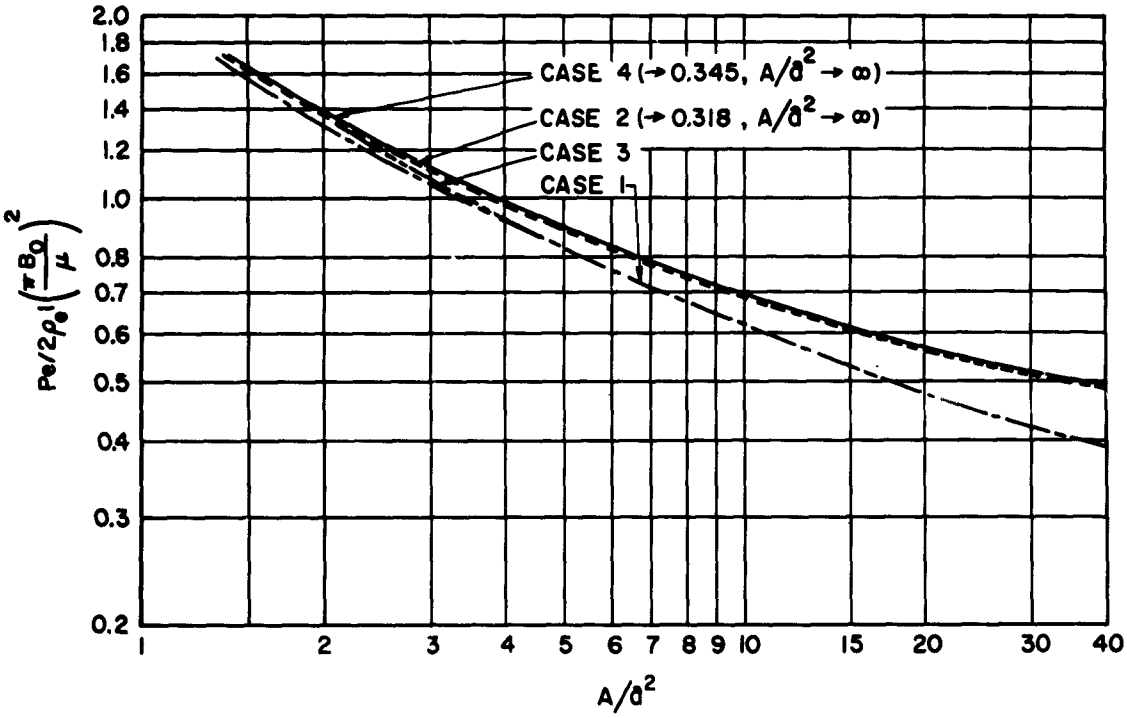

Figure 8 - Minimum Power in Optimized Air Core Electromagnets for MHD

APPENDIX B

MAGNETIC ENERGY

The vector potential for parallel infinite rectangular conductors as shown in Figure 7, Case 4, due to the sum of all current elements j dx' dy' is:

$$A_x = A_y = O,\ A_z = \frac{\mu i_o}{4\pi} \int_{\text{conductor area}} \ln\left[(x-x')^2 + (y-y')^2\right] dx'\,dy'$$

$$= \frac{\mu i}{4\pi}\begin{bmatrix}\phi(x-\alpha a, y-\beta a)-\phi(x-a,\ y-\beta a)-\phi(x-\alpha a,\ y+\beta a)+\phi(x-a,\ y+\beta a)\\ +\phi(x+\alpha a, y-\beta a)-\phi(x+a, y-\beta a)-\phi(x+\alpha a, y+\beta a)+\phi(x+a, y+\beta a)\end{bmatrix} \quad \text{(B-1)}$$

where $\phi(u, v) = uv \ln(u^2+v^2) + v^2 \tan^{-1}\frac{u}{v} + u^2 \operatorname{ctn}^{-1}\frac{u}{v}$

Magnetic energy per unit length has been found using (B-1) in the integration:

$$\frac{T}{l} = \frac{1}{2l}\iiint_{\text{coil volume}} \mathbf{j}\cdot\mathbf{A}\, dVol = 2j_o \int_0^{\beta a}\int_a^{\alpha a} A_z(x, y)\, dx\, dy$$

$$\frac{T}{l} = \frac{2\mu j^2 a^4}{3\pi}\Bigg[-\left(\frac{\alpha-1}{2}\right)^4 \ln\left(\frac{\alpha-1}{2}\right)^2 + \frac{1}{2}\alpha^4 \ln\alpha^2 - \left(\frac{\alpha+1}{2}\right)^4 \ln\left(\frac{\alpha+1}{2}\right)^2$$
$$-\beta^4 \ln\beta^2 - \frac{1}{2}(1-6\beta^2+\beta^4)\ln(1+\beta^2)$$
$$+\left[\left(\frac{\alpha-1}{2}\right)^4 - 6\left(\frac{\alpha-1}{2}\right)^2\beta^2+\beta^4\right]\ln\left[\left(\frac{\alpha-1}{2}\right)^2+\beta^2\right]$$
$$-\frac{1}{2}(\alpha^4 - 6\alpha^2\beta^2+\beta^4)\ln(\alpha^2+\beta^2)$$
$$+\left[\left(\frac{\alpha+1}{2}\right)^4 - 6\left(\frac{\alpha+1}{2}\right)^2\beta^2+\beta^4\right]\ln\left[\left(\frac{\alpha+1}{2}\right)^2+\beta^2\right]$$
$$-8\left(\frac{\alpha-1}{2}\right)\beta\left[\left(\frac{\alpha-1}{2}\right)^2 - \beta^2\right]\tan^{-1}\beta/\left(\frac{\alpha-1}{2}\right)$$
$$+4\alpha\beta(\alpha^2-\beta^2)\tan^{-1}\beta/\alpha$$
$$-8\left(\frac{\alpha+1}{2}\right)\beta\left[\left(\frac{\alpha+1}{2}\right)^2 - \beta^2\right]\tan^{-1}\beta/\left(\frac{\alpha+1}{2}\right)$$
$$+4\beta(1-\beta^2)\tan^{-1}\beta - 4\pi\left(\frac{\alpha-1}{2}\right)\beta^3\Bigg] \quad \text{(B-2)}$$

This result agrees with that by Dwight, Reference 7.

APPENDIX C

PROPAGATION OF A NORMAL FRONT IN A SUPERCONDUCTING SYSTEM

Steady state thermal propagation of a normal front along a superconductor may be obtained by considering an infinite wire, cooled by a liquid at temperature, T_o, with an overall heat transfer coefficient, h. The region $x > o$ is in the normal state. For a coordinate system moving with the interface velocity, v, the heat transfer problem is:

$$\left.\begin{aligned} &\frac{d}{dx}\left(kA\frac{dT_n}{dx}\right) - \rho cvA\frac{dT_n}{dx} - hs\,(T_n - T_o) + \frac{i^2\rho_e}{A} = 0, \quad x>0 \\ &\frac{d}{dx}\left(kA\frac{dT_s}{dx}\right) - cvA\frac{dT_s}{dx} - hs\,(T_s - T_o) = 0, \quad x<0 \\ &T_s(0) = T_n(0) = T_c;\; T_s(-\infty) = T_o;\; \frac{dT_n}{dx}(\infty) = 0;\; k\frac{dT_s}{dx}(0) = k\frac{dT_n}{dx}(0) \end{aligned}\right\} \quad \text{Eq. (C-1)}$$

$$v = \frac{i}{\rho cA}\sqrt{\frac{k\rho_e}{T_c - T_o}}\left[\frac{1 - \dfrac{2hsA(T_c - T_o)}{i^2\rho_e}}{\sqrt{1 - \dfrac{hsA(T_c - T_o)}{i^2\rho_e}}}\right] \quad \text{Eq. (C-2)}$$

This result is the same as that given by Broom and Rhoderick, Reference 8. When cooling is not present at the wire surface ($h = o$), the bracket in Equation (C-2) reduces to unity. Using Equation (C-2) and average thermal properties obtained by combining winding layers, insulation, and secondary material, the smallest propagation velocity, that perpendicular to the layers, is calculated to be 375 cm/sec for the magnet described here. Much higher velocities along the wire, as might be predicted by Equation (C-2), cannot be obtained because diffusion to helium, causing development of film boiling, or in coils, diffusion to high specific heat plastic insulation increases effective ρc in Equation (C-2).

Velocity along layers would be somewhat greater than across layers because of higher effective k. The result shows that for $2hsA\,(T_c - T_o) > i^2\rho_e$, propagation will not occur.

Riemersma, Reference 5, experimentally investigated propagation in small solenoids. The results in Figure 9 show thermal propagation in the A coil until f equal 0.25, when external cooling and complete energy dissipation stopped propagation. A similar coil, B, with turn to turn shunting propagated normalcy fifteen times faster by the coupling process described earlier. The coil B had 1207 turns of 0.010 inch Nb-Zr wire wound into a 0.19 inch I.D., 0.5 inch O.D., 1 inch long coil. The L_1 per turn was 2.13×10^{-8} henries; R_1 per turn, 0.113 ohms; k, 0.727 turn to turn, and average i_c (through the coil and during the transient) was assumed 10% higher than i_o. We then predict the time for the coil to become normal, $\frac{i_c - i_o}{i_o} \frac{L_1}{R_1} n \left(\frac{1-k^2}{k}\right)$, to be 15 microseconds. This result is plotted in Figure 9, where it may be seen that there is good agreement, especially in the rate when 30% to 70% of the coil is normal. A more accurate prediction could be obtained using critical current, field and coil current decay relations to eliminate the approximation of constant $i_c - i_o/i_o$ in the theory. Also, improved correlation would be obtained by considering slower transients in all neighboring turns and layers. The comparative experiments certainly demonstrate that induction propagation exists and that rates of the order of 25,000 cm/sec may be predicted with reasonable accuracy.

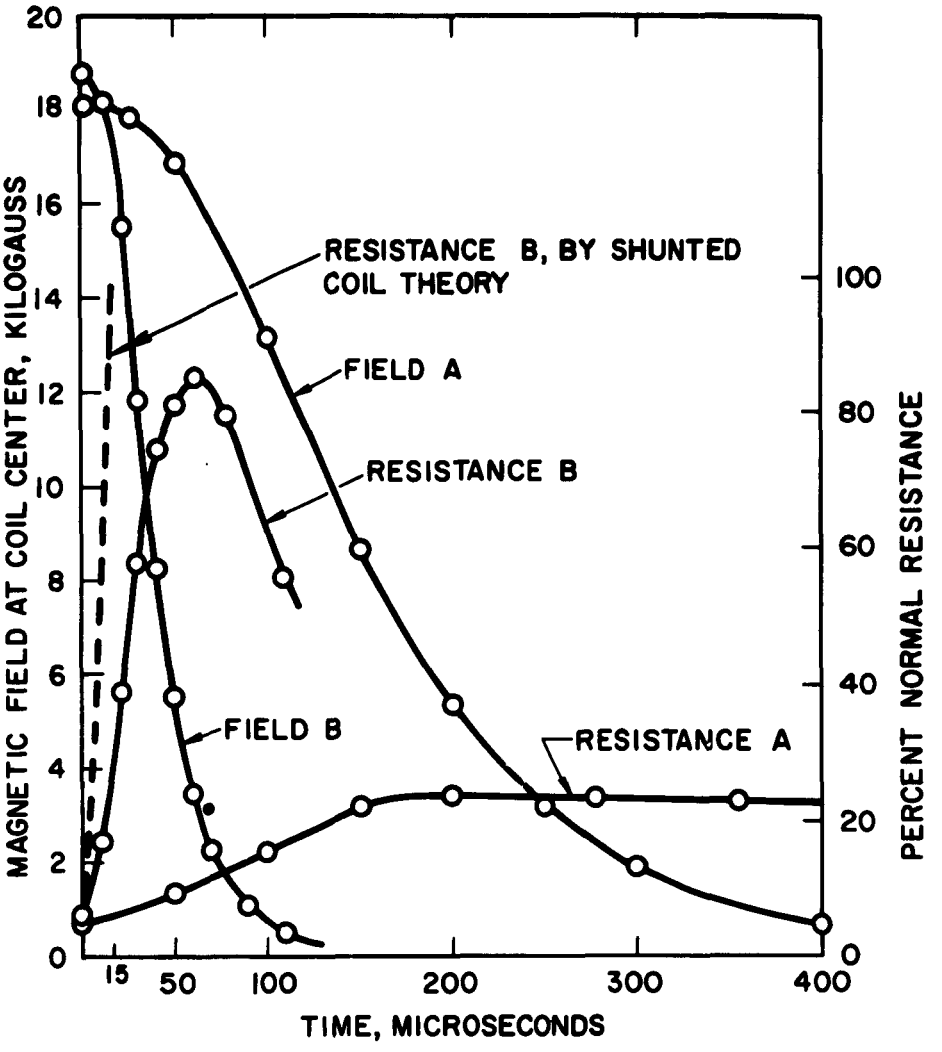

COIL A: 1380 TURNS, 670 GAUSS/AMP, EPOXY INSULATION.

COIL B: 1207 TURNS, 585 GAUSS/AMP, SHUNTED BY CONDUCTIVE INSULATION (0.01 OHM CM.)

COILS ARE 0.5 IN. O.D. x 0.19 IN. I.D. x 1.0 IN. LONG, 0.010 IN. WIRE, 0.0005 IN. THICK INSULATION.

Figure 9 - Decay of Magnet Field and Increase of Resistance Upon Entry to Normal State of Shunted and Unshunted Test Coils

APPENDIX D

MAGNETIC STRESS AND FORCE

Stress resulting from $\underline{j} \times \underline{B}$ body force per unit volume is easily found considering that $\underline{B} = \nabla \times \underline{A}$ and that in Figure 7, Case 4, boundaries $x = a$ and $y = \beta a$ have zero stress.

$$\left.\begin{aligned} \sigma_x(x,y) &= -j_o \int_a^x B_y(x,y)dx = j_o \left[A_z(x,y) - A_z(a,y)\right] \\ \sigma_y(x,y) &= -j_o \int_y^{\beta a} B_x(x,y)dy = j_o \left[A_z(x,y) - A_z(x,\beta a)\right] \end{aligned}\right\} \quad \text{Eq. (D-1)}$$

Net force F separating conductors may be found either by integrating compressive stress at the outer edge or using the principle that the variation in total magnetic energy, T, during a relative displacement of conductors at constant current, is equal the work by mechanical forces done by the current system. See for example Dwight, Reference 9. Keeping coil sections constant, especially $(\alpha-1)a$.

$$\begin{aligned} \frac{F}{T} = \frac{d(T/l)}{2da} = \frac{2\mu j^2 a^3}{3\pi} \Bigg(& 3\alpha\beta \ln\left[\frac{\alpha^2+\beta^2}{\left(\frac{\alpha+1}{2}\right)^2+\beta^2}\right] + \alpha^3 \ln\left[\frac{\alpha^2}{\alpha^2+\beta^2}\right] \\ & + 3\beta^2 \ln\left[\frac{1+\beta^2}{\left(\frac{\alpha+1}{2}\right)^2+\beta^2}\right] + 2\left(\frac{\alpha+1}{2}\right)^3 \ln\left[\frac{\left(\frac{\alpha+1}{2}\right)^2+\beta^2}{\left(\frac{\alpha+1}{2}\right)^2}\right] \\ & - \ln\left[1+\beta^2\right] + 2\beta\left[(3\alpha^2-\beta^2)\tan^{-1}\beta/\alpha \right. \\ & \left. + (3-\beta^2)\tan^{-1}\beta - 2\left(3\left(\frac{\alpha+1}{2}\right)^2-\beta^2\right)\tan^{-1}\beta/\left(\frac{\alpha+1}{2}\right)\right] \Bigg) \end{aligned} \quad \text{Eq. (D-2)}$$

Similarly end force is found as:

$$F_e = \frac{1}{2}\frac{dT}{dl} = \frac{1}{2}\frac{T}{l} \quad \text{Eq. (D-3)}$$

APPENDIX E

VAPOR COOLING OF THERMAL CONDUCTION PATHS AND ELECTRICAL LEADS

Heat transfer in a thermal and electrical conductor cooled by a mass flow m from a boiling fluid at one end of the conductor is summarized below:

$$\left.\begin{aligned} &\frac{d}{dx}\left(kA\frac{dT}{dx}\right) - hs\,(T - T_v) + \frac{i^2\rho_e}{A} = 0 \\ &\dot{m}\,c_p\frac{dT_v}{dx} - hs\,(T - T_v) = 0 \\ &T(0) = T_v(0) = T_o,\quad T(x_o) = T_a \end{aligned}\right\} \text{Eq. (E-1)}$$

For constant properties:

$$\left.\begin{aligned} &T - T_o = (T_a - T_o)\frac{\phi_{2(x)}}{\phi_2(x_o)} + \frac{i^2\rho_e}{\dot{m}c_pA}\left[\phi_1(x_o)\frac{\phi_2(x)}{\phi_2(x_o)} - \phi_1(x)\right], \\ &\phi_1(x) = \left(\frac{G+F}{E+F}\right)\left(\frac{e^{Ex}-1}{E}\right) + \left(\frac{G-E}{E+F}\right)\left(\frac{e^{-Fx}-1}{F}\right) - x, \\ &\phi_2(x) = \left(\frac{G+F}{E+F}\right)e^{Ex} - \left(\frac{G-E}{E+F}\right)e^{-Fx} - 1, \end{aligned}\right\} \text{Eq. (E-2)}$$

$$E = \frac{hs}{2\dot{m}c_p}\left(\sqrt{1 + \frac{(2\dot{m}c_p)^2}{hskA}} - 1\right),\quad F = \frac{hs}{2\dot{m}c_p}\left(\sqrt{1 + \frac{(2\dot{m}c_p)^2}{hskA}} + 1\right),\quad G = \frac{\dot{m}c_p}{kA}$$

The heat which is conducted to boiling fluid is

$$Q_o = \frac{\dot{m}c_p(T_a - T_o) + \frac{i^2\rho_e}{A}\,\phi_1(x_o)}{\phi_2(x_o)} \qquad \text{Eq. (E-3)}$$

When h is considered infinite, $T = T_v$, the result becomes from Equation (E-3):

$$Q_o = \frac{\dot{m}c_p(T_a - T_o) - \frac{i^2\rho_e}{A}x_o}{e^{\frac{\dot{m}c_p x_o}{kA}} - 1} + \frac{i^2\rho_e K}{\dot{m}c_p} \qquad \text{Eq. (E-4)}$$

If Q_o is the only heat flux vaporizing liquid then it is also $\dot{m}h_{fg}$. Then where i is zero:

$$\dot{m} = \frac{kA}{c_p x_o} \ln\left(1 + \frac{c_p(T_a - T_o)}{h_{fg}}\right) \qquad \text{Eq. (E-5)}$$

Minimizing Q_o in Equation (E-4) with respect to x_o/A for an electrical lead, considering $\dot{m}c_p x_o/kA$ larger than one gives:

$$\left(\frac{x_o}{A}\right)_{\text{optimum lead}} = \frac{k}{\dot{m}c_p} + \frac{\dot{m}c_p(T_a - T_o)}{i^2\rho_e} \qquad \text{Eq. (E-6)}$$

The minimum value of $\dot{m}c_p x_o/kA$ results when $\dot{m}$ is just Q_o/h_{fg}. And using Equations (E-4) and (E-6) is $1 + \frac{c_p(T_a - T_o)}{h_{fg}}$, which is considerably greater than one for helium to nitrogen or room temperature. Thus the optimization is rather meaningless since the heat flux Q_o is practically $i^2\rho_e k/\dot{m}c_p$ for a range of values of x_o/A, if $\dot{m}$ results independently from a number heat flux sources other than leads.

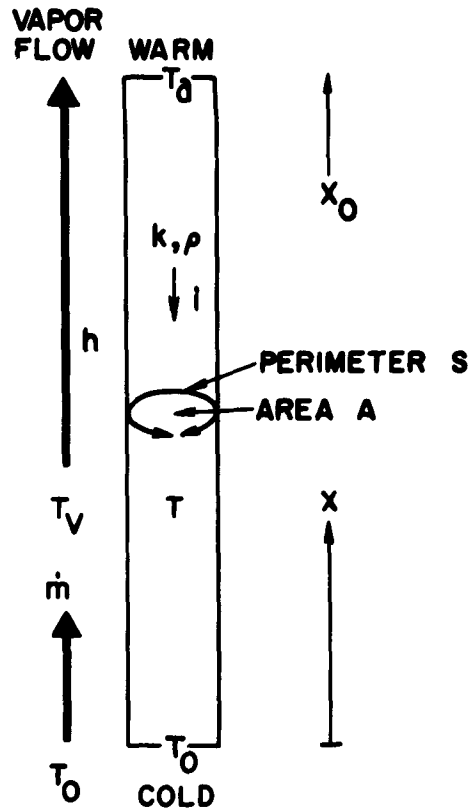

Figure 10 - Vapor Cooling of Conduction Paths and Electrical Leads

APPENDIX F

VAPOR COOL-DOWN

Cooling a mass M with boiling helium from a temperature T_1 to T_o requires a mass m of helium:

$$m_{boiling} = \frac{M}{h_{fg}} \int_{T_o}^{T_1} c\,dT \qquad \text{Eq. (F-1)}$$

But if vapor is also used to cool an isothermal mass by passing through an isothermal heat exchanger at temperature T, a smaller amount of helium is needed.

$$m_{vapor\ cool} = M \int_{T_o}^{T_1} \frac{c\,dT}{ec_p T + (h_{fg} - ec_p T_o)} \qquad \text{Eq. (F-2)}$$

$$\frac{T_{vapor\ out} - T_o}{T - T_o} = e = 1 - e^{-\frac{hA_{wall}}{mc_p}} \qquad \text{Eq. (F-3)}$$

For helium, $h_{fg} - ec_p T_o$, is approximately zero. Most metals have specific heats which vary as $c = c_o (T/T_o)^n$, $2<n<3$.

$$\frac{m_{vapor\ cool}}{m_{boiling}} = \frac{h_{fg}}{ec_p T_1} \left(\frac{n+1}{n} \right) \qquad \text{Eq. (F-4)}$$

For heat exchange efficiency of 0.75, cooling metal from nitrogen temperature, 77°K, to 4.2°K produces a ratio of 9 to 11 from (F-4) while a factor of 7 is obtained for plastics.

Consider that the body M is not isothermal but made up of differential masses $M\,dx/x_o$, that specific heat, c, is constant, that helium vapor flow starts at $x = o$, that there is

always equilibrium with the vapor and the masses do not conduct heat to each other. Then:

$$\frac{mc_p x_o}{Mc} \frac{\partial T}{\partial x} + \frac{\partial T}{\partial \tau} = 0,\ T(0,\tau) = T_0, T(x,o) = T_1 \qquad \text{Eq. (F-5)}$$

$$T = \mathcal{L}^{-1} \left\{ \frac{T_1}{p} - \frac{(T_1 - T_o)}{p} e^{-\frac{M_c}{mc_p} \frac{x}{x_o} p} \right\} \qquad \text{Eq. (F-6)}$$

This result shows that mass and vapor temperatures are a step function up from T_o to T_1 at $\frac{x}{x_o} = \frac{mc_p}{Mc}$. Thus all enthalpy of the vapor between T_o and T_1 is used until the last mass at x_o is cooled. A maximum possible reduction of m from that by Equation (F-1) is therefore $1 + c_p (T_1 - T_o)/h_{fg}$, or for helium to nitrogen temperature, 19.6. Isolating system parts and cooling down with a series path for vapor has some advantage. But isothermal mass cool down with vapor and vapor-mass equilibrium (e = 1) gives factors only 25% to 33% less because materials have large specific heats at high temperatures.

APPENDIX G

LEVEL GAGES

Convection heat transfer coefficients from a resistance element to vapor are much less than in boiling in liquid. Temperature rise causes a proportional resistivity change in vapor and a variation of resistance with level. A conductor of area A, perimeters s for convection and having temperature coefficient of resistivity α_r and effective heat conduction area A' when there is support structure, immersed in liquid at T_o from x_o to 1, but vapor at T_o up to x_o is described by:

$$\frac{d^2T}{dx^2} - \frac{hs}{kA'}(T - T_o) + \frac{i^2\rho_e}{kA'A}\left[1 + \alpha_r (T - T_o)\right] = 0 \qquad \text{Eq. (G-1)}$$

$$\frac{dT}{dx}(0) = 0,\ T = T_o,\ x_o < x < 1$$

$$T - T_o = \frac{\theta}{1 - \alpha_r \theta}\left[1 - \frac{\cosh \delta \frac{x}{l}}{\cosh \delta \frac{x_o}{T}}\right] \qquad \text{Eq. (G-2)}$$

$$\frac{\Delta R}{R} = \frac{1}{T}\int_o^{x_o} \alpha_r (T - T_o)\, dx = \frac{\alpha_r \theta}{1 - \alpha_r \theta}\left[1 - \frac{\tanh \delta \frac{x_o}{T}}{\delta \frac{x_o}{T}}\right]\frac{x_o}{T} \qquad \text{Eq. (G-3)}$$

where

$$\theta = \frac{i^2\rho_e}{hsA},\quad \delta = \sqrt{\frac{hsl^2}{A}\left(1 - \frac{\alpha_r i^2 \rho_e}{hsA}\right)}$$

Gage sensitivity $\alpha\theta$ is also α (gage power)/hS. Therefore it is important to have high α_r and small wire perimeter to minimize power. Ten feet of 0.00124 inch diameter copper wire wound on a mylar ribbed coil form serves as a nitrogen gage consuming 0.01 watts. The helium gage is a string of eight carbon, 1/10 watt, 27 ohm resistors consuming less than 0.001 watts. Sharpness parameter δ, is adequate for usefulness for both gages that are shown in Figure 11, although there is not linearity. The measuring circuit used is similar to that used by Maimoni, Reference 10, who gives a good discussion of resistance level gages.

Helium

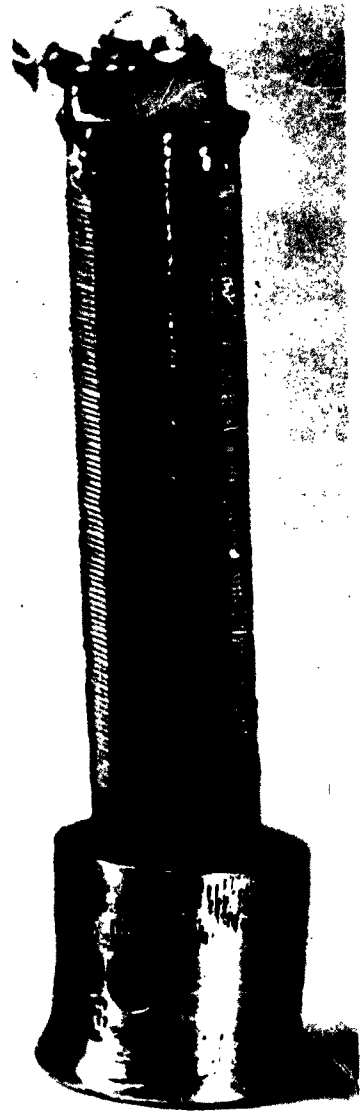

Nitrogen

Figure 11 - Helium and Nitrogen Level Gages

NOMENCLATURE

a	=	half width between magnet conductors
A	=	section area of magnet winding, thermal path, etc.
b_n	=	n'th Bernoulli number
B	=	magnetic flux density
c	=	specific heat of magnet, etc.
c_p	=	specific heat of vapor
e	=	heat exchanger effectiveness
f	=	fraction of coil that is normal (resistive)
F	=	force
h	=	convection heat transfer coefficient
h_{fg}	=	latent heat of vaporization
H	=	magnetic field intensity
i	=	current
j	=	current density
k	=	thermal conductivity or magnetic coupling coefficient
l	=	MHD duct, magnet or gage wire length
L	=	inductance
$\mathcal{L}^{-1}$	=	inverse Laplace transform operator
m	=	mass of coolant
M	=	mutual inductance or mass to be cooled
n	=	number of shunted coil sections
N	=	number of layers in coil
p	=	Laplace transform variable
P	=	generated power
Pe	=	electrical power

Q = heat removed at temperature T

r = radius

R = resistance

R_{He} = gas constant of helium

s = perimeter

T = absolute temperature

u = plasma velocity

v = velocity of normal front

V_n = voltage across normal fraction of coil

W = system weight to power ratio

x, y, z = coordinates

α = dimensionless distance to outside of magnet

α_r = temperature coefficient of resistance

α_1, α_2 = accommodation coefficients

β = dimensionless half height of magnet

γ = ratio of specific heats

ϵ = emissivity

η = ratio of coefficient of performance to Carnot cycle COP

η_e = electrical efficiency

λ = ratio conductor volume to total volume

μ = magnetic permeability of free space

ρ_e = electrical resistivity

ρ = density

σ = plasma conductivity or Stefan-Boltzmann constant

σ_x, σ_y = stress

τ = time

REFERENCES

1. Kunzler, J. E., Buehler, E., Hsu, F. S., and Wernick, J. H., "Superconductivity in Nb_3Sn at High Current Density in a Magnetic Field of 88 Kgauss," Phys. Rev. Letters 6, 89 (1961).

2. Hulm, J. K., Fraser, M. J., Riemersma, H., Venturino, A. J., and Wien, R. E., "A High-Field Niobium-Zirconium Superconducting Solenoid," High Magnetic Fields, (M.I.T. Press and John Wiley and Sons, Inc., New York, 1952), p. 332.

3. Way, S., DeCorso, S. M., Hundstad, R. L., Kemeny, G. A., Stewart, W., and Young, W. E., "Experiments with MHD Power Generation," Trans. ASME, Ser. A, 83, 397 (1961).

4. Kunzler, J. E., "Superconducting Materials and High Magnetic Fields," J. App. Phys. 33, 1042 (1962).

5. Hulm, J. K., Chandrasekhar, B. S., and Riemersma, H., "High Field Superconducting Magnets," 1962 Cryogenic Engineering Conference, U. of Calif.

6. Arnold, A. H. M., "The Inductance of Linear Conductors of Rectangular Section," Journ. Inst. of Elect. Eng., 70, 579 (1931-32).

7. Dwight, H. B., "Reactance Values for Rectangular Conductors," The Electric Journal, XVI, No. 6, 255 (1919).

8. Broom, R. F., and Rhoderick, E. H., "Thermal Propagation of a Normal Region in a Thin Superconducting Film and Its Application to a New Type of Bistable Element," British J. of Appl. Phys., 11, 292 (1960).

9. Dwight, H. B., Electrical Coils and Conductors (McGraw-Hill Book Company, Inc., New York, 1945), 1st. Ed., Chap. 33, p. 298.

10. Maimoni, A., "Hot Wire Liquid Level Indicator," Rev. Sci. Inst. 27, 1024 (1956).